Geosciences Research Program
Office of Basic Energy Sciences
Geosciences Models – Where are the Rocks?
Gaithersburg. Maryland
May 14-16, 2014

2012 Best Paper

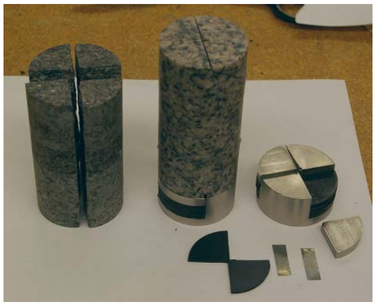

Nakagawa et al - Direct fracture shearing experiments

2013 Best Paper

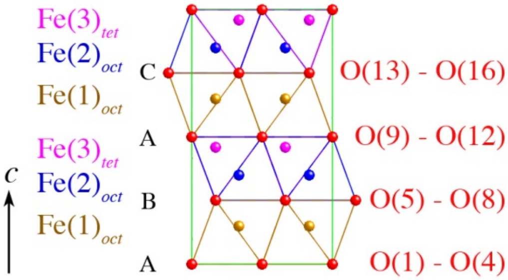

Gilbert et al - Hybrid Ferrihydrite Structure

2012 Best Paper

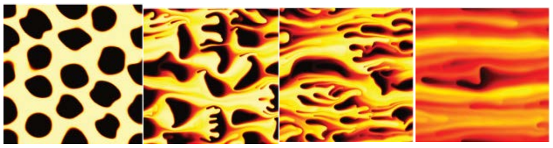

Juanes - Snapshots of the concentration field at increasing time steps from a numerical simulation of miscible viscous fingering.

2013 Best Paper

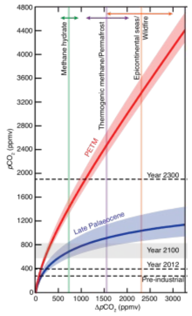

Schubert and Jahren - Carbon stable isotope fractionation

FORWARD

Geosciences Models – Where are the Rocks? is the twentieth in a series of Geosciences Research Program Symposia dating from 1995. These symposia are topically focused meetings for principal investigators in the program and provide opportunities for our investigators to give presentations on their Office of Basic Energy Sciences' supported research. In addition to the recognition the symposium gives to all of the investigators, we traditionally also recognize one outstanding contribution from a DOE Laboratory Project and one from a University Project. The outstanding contributions are selected by our session chairpersons. This year these include: Dr. Thomas Torgersen from NSF, Dr. Joanne Fredrich from BP, Prof. Michael Manga from University of California at Berkeley, Dr. Andrew Stack from Oak Ridge, Dr. Steve Laubach from the Texas Bureau of Economic Geology, Prof. Dan Rothman from MIT, Prof. Dave Cole from Ohio State University, Prof. Laura Pyrak-Nolte from Purdue University, Prof. Bill Casey from University of California at Davis, Prof. Steve Sutton from the University of Chicago, Prof. Bruce Watson from Rensselaer Polytechnic Institute, and Dr. Paul Fenter from Argonne National Laboratory. For their efforts on behalf of the investigators I thank them all. We are looking forward to an outstanding series of presentations.

Nicholas B. Woodward
Geosciences Research Program
Office of Basic Energy Sciences
U.S. Department of Energy

* * * * *

Table of Contents

Captions for cover illustrations:

Figure 1: 2012 best paper award winner: Seiji Nakagawa, Lawrence Berkeley National Laboratory – “Static and dynamic coupling of fractures and fluid: Laboratory investigations.”

Figure 2: 2012 best paper award winner: Ruben Juanes – MIT – “Fingering, Fracturing and Dissolution in Granular Media”

Figure 3: 2013 best paper award winner: Ben Gilbert, J. Erbs, R.L. Penn, V. Petkov and G. Waychunas, Lawrence Berkeley National Laboratory “A hybrid unit cell for Ferrihydrite”

Figure 4: 2013 best paper award winner: Brian Schubert and Hope Jahren, University of Hawaii, “Carbon stable isotope fractionation during C3 photosynthesis and its use in probing the terrestrial rock record.”

AGENDA

Wednesday Afternoon

12:00 Registration

1:00 **Introduction and Greetings**
Nicholas Woodward, Department of Energy

Session 1: **Multimedia: Multiscale, Multiphase, Multiprocess**
Chairs: Tom Torgersen and Steve Laubach

1:15 ***Grain-boundary transport in rocks and related kinetic phenomena***
E. Bruce Watson, Jay B. Thomas and Veronika Homolova
Dept. of Earth and Environmental Sciences, Rensselaer Polytechnic Institute

1:40 ***Evolution of pore structure and permeability under hydrothermal conditions***
Brian Evans, Yves Bernabé and Uli Mok
Dept. of Earth, Atmospheric and Planetary Sciences, Massachusetts Institute of Technology

2:05 ***Non-Darcian Flow, Imaging, and Coupled Constitutive Behavior of Heterogeneous Deforming Porous Media***
Hongkyu Yoon, Thomas Dewers, and Jason Heath
Geomechanics Department, Sandia National Laboratories

2:30 ***Geochemical self-organization and the evolution of permeability***
Tony Ladd, University of Florida

2:55 ***Fingering, fracturing and dissolution in granular media***
Ruben Juanes, Massachusetts Institute of Technology

3:20 ***Coffee***

3:45 ***High resolution dielectric properties of organic-rich reservoirs with implications for thermal maturation and the liberation of polar fluids***
Manika Prasad, John Scales and Rezwan Rhaman, Colorado School of Mines

4:10 ***Weathering Models: Dissolution and Porosity Development in Crystalline Rocks***
Susan L. Brantley, Gary Stinchcomb, X. Gu, M. Lebedeva, and K. Bazilevskaya
Pennsylvania State University

4:35 ***Branching of stream networks***
Daniel H. Rothman, Yossi Cohen, Hansjorg Seyböld, and Robert Yi
Lorenz Center, Dept. of Earth, Atmospheric, and Planetary Sciences, Massachusetts Institute of Technology

5:00 ***New Opportunities for Geoscience Research using the Multi-bend Achromat Storage Ring being Proposed for the Upgrade of the Advanced Photon Source***
Stephen R. Sutton, M.L. Rivers, P.E. Eng, M. Newville, A. Lanzirotti, and J. Stubbs
University of Chicago – GSECARS

5:30 – 7:30 P.M. Dinner on your own.

Wednesday Evening – Poster Chairs: Michael Manga and Andrew Stack

7:30 – 9:30 P.M. Poster Session 1: All Posters will be on display for the entire meeting.

Thursday Morning

7:30 ***Coffee***

Session 2: Analytical Geochemistry and Associated Geochemical Models

Chairs: William Casey and Daniel Rothman

8:00 ***Observing Molecular-Scale Dynamics at the Interface Between Rock-Forming Minerals and Aqueous Solutions***
Paul Fenter[1], Sang Soo Lee[1], Nouamane Laanait[1], and Neil C. Sturchio[2]
[1]Chemical Sciences and Engineering Division, Argonne National Laboratory
[2]Department of Earth and Environmental Sciences, University of Illinois at Chicago

8:25 ***Actinide Geochemistry and Geochronology with Real Rocks***
Steve Goldstein, Mick Murrell, Joanna Denton, Andy Nunn, and Kim Hinrichs
Los Alamos National Laboratory

8:50 ***Kinetic Isotope Fractionation in Laboratory and Natural Samples***
Frank Richter, Dept. of the Geophysical Sciences, University of Chicago

9:15 ***Geologic Complexity in Surface Complexation Models***
Dimitri A. Sverjensky, Johns Hopkins University

9:40 ***Geochemistry of Interfaces: From Surfaces to Interlayers to Clusters***
Jeffrey A. Greathouse[1], Louise J. Criscenti[1], Kevin Leung[2], Anastasia G. Ilgen[1], Lynn E. Katz[3], Heather C. Allen[4], Randall T. Cygan[1]
[1]Geochemistry Department, Sandia National Laboratories; [2]Surfaces and Interface Science Department, Sandia National Laboratories; [3]Department of Civil, Architectural and Environmental Engineering, University of Texas, Austin; [4]Chemistry Department, Ohio State University

10:05 ***Coffee***

10:30 ***Atomic- to Pore-Scale Probes and Predictions of Mineral Reactivity***
Andrew G. Stack[1], J.R.D. Godinho[1], L.M. Anovitz[1], G. Rother[1], A.A. Chialvo[1], D.J. Wesolowski[1], E. Mamontov[1], J.C. Burreguero[1], P.R.C. Kent[1], K.C. Littrell[1], J.N. Bracco[2], S.R. Higgins[2], J.E. Stubbs[3], P.J. Eng[3], M. Rivers[3], P. Fenter[4], S.S. Lee[4]
[1]Oak Ridge National Laboratories; [2]Wright State University; [3]University of Chicago; [4]Argonne National Laboratory

10:55 ***Measurements and Conceptual Models of the Reactivity of the World's Smallest Rocks*: *Bacteriogenic and Abiogenic Mineral Nanoparticle Aggregates***
Michael F. Hochella, Jr., J. Xu, M. Murayama, C. Roco, G. Singh, and N. Qafuku
[1]Department of Geosciences and ICTAS, Virginia Tech; [2]Pacific Northwest National Laboratory

11:20 ***Molecular Mechanisms of Interfacial Reactivity in Near Surface and Extreme Geochemical Environments***

Andrew R. Felmy, J.M. Zachara, A.M. Chaka, J. Loring, and S. Kerisit

11:45 ***Stable-isotope probe of nano-scale mineral-fluid redox interactions***
Abby Kavner
Dept. of Earth, Planetary and Space Sciences, University of California, Los Angeles

12:10 – 1:10 Lunch Provided

Thursday Afternoon

Session 3: Fractures, Faults and Diagenesis
Chairs: Steve Sutton and Joanne Fredrich

1:10 ***Non-Gassmann Pore-fill Substitution in Heterogeneous Rocks***
Gary Mavko, Nishank Saxena, Jack Dvorkin, and Amos Nur
Geophysics Department, Stanford University

1:35 ***Rock deformation at submicron scale***
Ronnie Borja, Martin Tjioe, and Kane C. Bennett
Department of Civil and Environmental Engineering, Stanford University

2:00 ***Rates of Fracture Array Growth and Sealing from a Model of Quartz Cementation and Implications for Fracture Size Scaling***
Stephen E. Laubach,[1] R.H. Lander,[2] Jon E. Olson,[3] and Peter Eichhubl[1]
[1]Bureau of Economic Geology, The University of Texas at Austin, [2]Geocosm and BEG, [3]Department of Petroleum and Geosystems Engineering, the University of Texas at Austin

2:25 ***Structural Heterogeneities and Paleo Fluid Flow in an Analogue Sandstone Reservoir***
Atilla Aydin and David D. Pollard, Stanford University

2:50 ***Coffee***

3:15 ***Fractures in Rock: Swarms, Scaling and Intersections***
Laura Pyrak-Nolte,[1,2,3] Eric Boomsa,[1] Siyi Shao,[1] and Brad Abell[1]
[1]Department of Physics, Purdue University; [2]Department of Earth and Atmospheric Science, Purdue University; [3]School of Civil Engineering, Purdue University

3:40 ***Geophysical Monitoring of Fluid Invasion***
Steve Pride, Greg Newman, Michael Commer, Don Vasco, Seiji Nakagawa, Stephen Breen, and Jim Berryman
Lawrence Berkeley National Laboratory

4:05 ***New Measurements of Elasticity in Earth Materials Guiding a New Theoretical Approach***
Paul Johnson, Los Alamos National Laboratory

4:30 ***Modeling shale anisotropy based on microstructure, fabric, pore and grain geometry – comparison of simulations with experiments***
Hans-Rudolf Wenk, Roman Vasin, and Waruntorn Kanitpanyacharoen
Department of Earth and Planetary Science, University of California, Berkeley

4:55 ***Rheological description of mantle rocks: Comprehensive in situ analysis of mantle minerals deforming at high pressure***

Nathanial A. Dixon[1], W.B. Durham[1], D.L. Kohlstedt[2], S. Mei[2], and J. Homburg[2]
[1]Massachusetts Institute of Technology, Cambridge, MA
[2]University of Minnesota, Minneapolis, MN

5:30 – 7:30 Dinner on your own

Thursday Evening

7:30 PM – 9:30 PM Poster Session 2:

Friday Morning

7:30 Coffee

Session 4: Nucleation and Redox Geochemistry
Chairs: David Cole and Bruce Watson

8:00 ***In search of processes driving clumped-isotope (dis)equilibrium in geoscience systems: New insights from data and theory***
Aradhna Tripati
University of California, Los Angeles

8:25 ***Quartz cements and basin evolution: Illinois Basin and Wisconsin Arch***
John W. Valley, Anthony D. Pollington, Ayumi Hyodo, and Reinhard Kozdon
Dept. of Geoscience, University of Wisconsin, Madison

8:50 ***Kinetic isotope fractionation during mineral growth and fluid phase transport***
Don J. Depaolo, J.N. Christensen, B.M. Kennedy, M.E. Conrad, and Ian Bourg
Lawrence Berkeley National Laboratory, Berkeley, CA

9:15 ***NMR spectroscopy of aqueous solutions to 2.0 GPa***
W.H. Casey[1,2], Brent Pautler[1], Chris Colla[2], Rene Johnson[1], Steve Harley[3], and Peter Klavins[4]
[1]Dept. of Chemistry, University of California, Davis; [2]Dept. of Earth and Planetary Sciences, University of California, Davis; [3]Lawrence Livermore National Laboratory; [4]Dept. of Physics, University of California, Davis

9:40 ***In situ transformation of amorphous calcium carbonate (ACC): Structural and compositional changes***
Richard J. Reeder and Brian L. Phillips, Stony Brook University

10:05 ***Coffee***

10:30 ***NMR and Computational Modeling of Clay-Organic Composites with H_2O and CO_2 Fluids***
R. James Kirkpatrick,[1] Geoffrey M. Bowers,[2] A. Ozgur Yazaydin,[3] Marimuthu Krishnan,[3] Moumita Saharay,[3] Brennan O. Ferguson,[2] David W. Hoyt,[4] Sarah D. Burton,[4] and Tamas Varga[4]

[1]College of Natural Science, Michigan State University; [2]Division of Chemistry, Alfred University; [3]Dept. of Chemistry, Michigan State University; [4]William R. Wiley Environmental Molecular Sciences Laboratory, Pacific Northwest National Laboratory

10:55 ***Investigation the Physical Basis of Biomineralization***
Patricia M. Dove[1,] James J. De Yoreo[2] and Anthony J. Giuffre[1], [1]Dept. of Geosciences, Virginia Tech;[2] Physical Sciences Division, Pacific Northwest National Laboratory

11:20 ***Unexpected crystal structures in biominerals***
Ross T. DeVol[1], Claire B. Salling[1], Adam Z. Blonsky[1], Christopher E. Killian[1], Lee Kabalah-Amitai[2], Boaz Pokroy[2], Assaf Gal[3], Steve Weiner[3], Lia Addadi[3], and Pupa U. P. A. Gilbert[1] [1]University of Wisconsin - Madison, USA , [2]Technion-Israel Institute of Technology, Haifa, Israel, [3]Weizmann Institute of Science, Rehovot, Israel

11:45 ***How should we interpret the carbon isotope composition of terrestrial rocks? Insight from controlled plant-growth experiments***
Hope Jahren,[1] and Brian A. Schubert[2]; [1]University of Hawaii, SOEST, Honolulu, HI; [2]School of Geosciences, University of Louisiana at Lafayette

12:10 – 1:10 Lunch

Friday Afternoon

Session 5: Use-Inspired Multiscale Research: Shales, CO_2 Sequestration and Hydrocarbons

Chairs: Laura Pyrak-Nolte and Paul Fenter

1:10 ***High Resolution X-ray CMT imaging of Supercritical CO_2 in Porous Media: Pore-scale Results in Support of Larger-Scale Implementation of CO_2 Storage***
A.L. Herring, L. Andersson, and Dorthe Wildenschild
School of Chemical, Biological and Environmental Engineering, Oregon State University

1:35 ***Subsurface Flow and Transport Tomography Using Streamlines***
Akhil Datta-Gupta, Texas Engineering Experimental Station

2:00 ***Thermodynamically Consistent Multiscale Models of Transport Phenomena in Porous Medium Systems***
Cass T. Miller and William G. Gray, University of North Carolina

2:25 ***Nanopore Confinement of Carbon-bearing Fluids Relevant to Subsurface Energy Systems***
David R. Cole, Alberto Striolo, David Tomasko, Siddharth Gautam, Salim Ok, Tingting Liu; [1]The Ohio State University, [2]University College London

2:50 ***Genesis, Storage, Producibility, and Natural Leakage of Shale Gas***
Arndt Schimmelmann and Maria Mastalerz, Indiana University, Bloomington, Indiana

3:15 ***Coffee***

3:40 ***Energy sources and sinks during the hydration of ultramafic rocks***
Alexis Templeton, University of Colorado

4:05 ***Role of iron chemistry in oxyhydroxide nucleation and olivine carbonation***

Ben Gilbert, B. Legg, M. Zhu, H. Zhang, G. D. Saldi, D. Duval, K. G. Knauss, G. A. Waychunas, J. F. Banfield, Lawrence Berkeley National Laboratory

4:30 ***Designing seals: integration of field observations, experimental analysis, and numerical modeling to constrain the long-term effectiveness of engineered storage systems***

Elizabeth Petrie[1], Steven Bauer[2], Santiago Flores[1,4], Stephen Radua[3], Peter Mozley[3], and James P. Evans[1]; [1]Dept. of Geology, Utah State University; [2]Geomechanics Department, Sandia National Laboratories; [3]Dept. of Earth and Environmental Science, New Mexico Tech;[4]Chesapeake Energy, Oklahoma City, OK

6:30 Optional Conference Dinner - THAT’S AMORE

POSTERS

Wednesday Evening

Wednesday Poster 1
Stress deformation on the redistribution of fluid flow paths in unconsolidated porous media
Kathleen Issen[1] and Zuleima Karpyn[2]
[1]Clarkson University, [2]Pennsylvania State University

Wednesday Poster 3
Stress deformation of unconsolidated porous media and its impact on pore geometry and phase trapping, V. A. Torrealba[1], Z. T. Karpyn[1], H. Yoon[2], K. A. Klise[2], D. Crandall[2], [1]Pennsylvania State University and [2]Sandia National Laboratory, Albuquerque

Wednesday Poster 5
Erosion and particle transport driven by fluid flow in heterogeneous granular medium
Arshad Kudrolli, Vikrant Yadav, and David Scheff, Clark University

Wednesday Poster 7
Permeability Evolution and the Mechanisms of Porosity Change
Wenlu Zhu and Meg Tivey
Department of Geology, University of Maryland
Department of Marine Chemistry and Geochemistry, Woods Hole Oceanographic Institute

Wednesday Poster 9
Geoscience Challenges for Extracting Energy Safely from the Earth: The Rocks Matter
Elizabeth Eide, National Academy of Sciences

Wednesday Poster 11
Pb and Cd Sorption to the Calcite-Water Interface: Structure and Process
Erika Callagon,[1] Kathryn L. Nagy,[1] Neil. C. Sturchio,[1] Sang Soo Lee,[2] Nouamane Laanait,[2] and Paul Fenter[2]
[1]Department of Earth and Environmental Sciences, University of Illinois at Chicago
[2]Chemical Sciences and Engineering Division, Argonne National Laboratory

Wednesday Poster 13
Controlling and Measuring Water Potentials and Water Film Thicknesses on Mineral Surfaces
T.K. Tokunaga[1], Y. Kim[1], J. Wan[1], T.W. Kim[1], S. Wang[1], A. Lanzirotti[2], M. Newville[2], S. Sutton[2], W. Rao[2], S. Wirrick[2], [1]LBNL and [2]University of Chicago

Wednesday Poster 15

Integrated X-ray, neutron and electron microscopic crystal chemical investigation of uranium contamination

David C. Elbert and David R. Veblen, the Johns Hopkins University

Wednesday Poster 17

Structure and Dynamics of Aqueous Solutions and Mineral-Solution Interfaces

David J. Wesolowski, Ariel A. Chialvo, L. Vlcek, M.S. Gruszkiewicz, P.T.Cummings, J.O. Sofo, J.D. Kubicki, A.C.T. van Duin, P.R.C. Kent, M.L. Machesky, P.A. Fenter, F. Bellucci, F. Geiger, E. Mamontov, and A.G. Stack, Oak Ridge National Laboratory

Wednesday Poster 19

First Principles Simulation of Interfacial Processes: Methods Development, Application and Analysis of Observations

John Weare and Eric Bylaska, University of California at San Diego and Pacific Northwest National Laboratory

Wednesday Poster 21

Computational Studies of Interfacial Processes in Carbonate Mineral Geochemistry

David A. Dixon[1], Sebastien Kerisit[2], and Anne Chaka[2]

[1]University of Alabama, [2]Pacific Northwest National Laboratory

Wednesday Poster 23

Insights into the Geochemistry of U Oxides: Theory and Experiment

Paul S. Bagus and Eugene S. Ilton, University of North Texas and Pacific Northwest National Laboratory

Wednesday Poster 25

Adsorption of Metals and Oxyanions to Mineral Surfaces

Lynn Katz[1], Kevin Leung[2], Heather Allen[3] and Louise Criscenti[2]

[1]University of Texas at Austin; [2]Sandia National Laboratories, [3]Ohio State University

Wednesday Poster 27

The Impact of Mg^{2+} solvation on aqueous complexes, mineral precipitation, and biogeochemistry

Louise Criscenti[1], Heather Allen[2], and Lynn Katz[3]

[1]Sandia National Laboratories; [2]Ohio State University; [3]University of Texas at Austin

Wednesday Poster 29

Geochemical Studies of Natural Geological and Environmental Materials using High-Energy X-ray Probes

Anthony Lanzirotti, Sutton, S. R., Rivers, M. L., Stubbs, J., Eng, P., and Wirick, S. University of Chicago and National Synchrotron Light Source, Brookhaven National Laboratory

Wednesday Poster 31

Development of a Tender-Energy Microprobe for Geosciences at NSLS and NSLS-II: First Measurements

Paul Northrup, Stony Brook University and National Synchrotron Light Source, Brookhaven National Laboratory

Wednesday Poster 33

Development of Tandem, Double-focusing, Electron Impact, Gas Source Mass Spectrometer for Measurement of Rare Doubly-Substituted Isotopologues in Geochemistry

Doug Rumble and Ed Young, Carnegie Institution of Washington and University of California at Los Angeles

Thursday Evening

Thursday Poster 2

Bulk and Interfacial Cation Behavior in OM-H_2O and Clay-OM-H_2O Composites: Molecular Scale Insights

Geoff Bowers, Alfred University

Thursday Poster 4

Comparison between modeled, measured, and predicted $\delta^{13}C$ and pCO_2 values from terrestrial sediments

Brian Schubert, University of Louisiana

Thursday Poster 6

Porosity/Permeability Evolution and Pore-Confined Fluid Properties in Natural and Synthetic Geologic Media

Lawrence M. Anovitz, G. Rother, M.S. Gruszkiewicz, S.L. Brantley, D.R. Cole, P.T. Cummings, C. McCabe, S. Hlushak, L. Vlcek, E. Mamontov, A.K. Kolesnikov, and N. Choudhury, Oak Ridge National Laboratory

Thursday Poster 8

Experimental and Computational Methods Used to Probe the Behavior of Fluids in Nanopores

Siddharth Gautam[1], David Cole[1], and Alberto Striolo[2]

[1]Ohio State University, [2]University of Oklahoma

Thursday Poster 10

Iron Oxide Redox Transformation Pathways: The Bulk Electrical Conduction Mechanism

Michelle Scherer and Kevin Rosso, University of Iowa and Pacific Northwest National Laboratory

Thursday Poster 12

Reactivity of Structural Iron in Natural Nontronite and Synthetic Fe-Phyllosilicate

Anastasia Ilgen and Jessica Kruichak, Sandia National Laboratories, Albuquerque, NM

Thursday Poster 14
Optimizing capillary trapping for storage of CO_2: Lattice Boltzmann simulations of the Brine-CO_2 system for reservoir conditions
Marcel Schaap, University of Arizona

Thursday Poster 16
The influence of water on the deformation behavior of mantle rocks
S. Mei[1], D. L. Kohlstedt[1], N. A. Dixon[2] and W. B. Durham[2]
[1]University of Minnesota, [2]Massachusetts Institute of Technology

Thursday Poster 18
Gas and melt migration in the crust and mantle: New clues from mafic veins
Mark Kurz, Woods Hole Oceanographic Institution

Thursday Poster 20
Three-Dimensional Inverse Modeling of Damped Elastic Wave Propagation in the Fourier Domain
Petr Petrov and Greg Newman, Lawrence Berkeley National Laboratory

Thursday Poster 22
Poroelastic Interactions between Seismic Waves and Fluid-Filled Fractures at Low (<1 kHz) Frequencies: Theory and Laboratory Measurements
Seiji Nakagawa, Lawrence Berkeley National Laboratory

Thursday Poster 24
Elastic Network Models and the Resonance Behavior of Berea Sandstone
Timothy W. Darling[1], Will Struble[1], James A. TenCate[2] and Paul A. Johnson[2]
[1]University of Nevada, Reno, NV 89557, [2]Los Alamos National Laboratory, Los Alamos NM 87545

Thursday Poster 26
Modified Invasion Percolation Model for Hydrofracture and other Applications
J. Quinn Norris, Donald L. Turcotte, and John B. Rundle, University of California at Davis

Thursday Poster 28
Nucleation and Fracture in Complex Geo – Systems
William Klein[1], J. B. Rundle[2], H. Gould[2] and T. Keyes[1], [1]Boston University and [2]University of California at Davis

Thursday Poster 30
Geofluid Dynamics of Faulted Sedimentary Basins
Grant Garven, Tufts University

Thursday Poster 32

Comparison of He isotopes in Tertiary basins of Southern California: evidence of fault-related mantle helium

Jim Boles, University of California, Santa Barbara

Thursday Poster 34

Frequency-dependent attenuation and elasticity in unconsolidated earth materials

Hernan Makse, John J. Valenza, and David L. Johnson, City University of New York

Thursday Poster 35

Particulate Suspension Flow in Fractures

Joel Koplik, City College of New York

ABSTRACTS

ORAL PRESENTATIONS

Grain-boundary transport in rocks and related kinetic phenomena

E. Bruce Watson, Jay B. Thomas and Veronika Homolova
Department of Earth and Environmental Sciences, Rensselaer Polytechnic Institute, Troy, NY

The textural and compositional evolution of rocks is strongly controlled by the solubility and transport of elements in grain boundaries. Since grain-boundary transport is commonly 10^4 to 10^6 times faster than diffusion through the lattices of most rock forming minerals, rapid transport of components through low volume grain boundaries may govern the kinetics of textural, geochemical and isotopic equilibration. There is a general consensus that addition of water will enhance grain-boundary transport, but there are no experimental studies that have systematically investigated the dependence on grain boundary 'moisture' content. Grain boundaries also act as important geochemical reservoirs because elements that are incompatible in the dominant matrix minerals of a rock are partitioned into intergranular regions. The geochemical evolution of rocks can be strongly affected by grain-boundary diffusion and partitioning processes, which may produce elemental and isotopic fractionations similar to processes that modify compositions in mineral/melt and mineral/fluid systems. During the last cycle we studied diffusion-induced fractionation of lithium isotopes in grain boundaries of polycrystalline olivine rocks (dunites), and the effect of water on transport of titanium in quartz grain boundaries (quartzites).

Lithium isotopic fractionation by grain boundary diffusion

Diffusion-induced fractionation of isotopes in grain boundaries has been suggested to occur in natural settings but has not been experimentally investigated. Lithium isotopes are ideal for studying isotopic diffusion induced fractionation because the mass difference between ^{6}Li and ^{7}Li is large and accordingly, any isotopic fractionation should be large and easy to measure. The experiments consisted of prefabricated, synthetic, polycrystalline olivine rocks that were placed against Li-rich sources (spodumene). The Li concentration profiles show that Li concentration decreases with increasing distance from the source. High precision Li isotopic measurements show that isotopic profiles corresponding to the Li concentration gradients consist of two parts. The part of the isotopic profiles more proximal to the Li source shows a substantial decrease in the ^{7}Li/^{6}Li ratio suggesting large diffusion induced isotopic fractionation in this part of the profile. The more distal parts of the profiles have a more or less constant ^{7}Li/^{6}Li ratio indicating that no isotopic fractionation occurred far from the source interface.

The role of water in grain-boundary transport of titanium in quartzites

Many recent studies have used the Ti-in-quartz thermobarometer to estimate P–T conditions of metamorphic and deformation events. Changes in P–T conditions will change the Ti content of quartz crystals in quartzites by transport and partitioning in quartz grain boundaries. We conducted experiments to study transport of Ti in quartz grain boundaries with variable water contents because there is little information on the behavior of Ti in grain boundaries. Diffusion couples were assembled by placing rutile (TiO_2) against quartzites with variable water contents. The quartzites were synthesized with water contents that ranged from dry (no water added) to 1150 ppmw H_2O. Infrared spectroscopic measurements of individual crystals in 'dry' quartzites show that they contain ~15 ppmw H_2O. Bulk measurements of 'dry' quartzites show that they contain ~140 ppmw H_2O. The difference of ~125 ppmw H_2O is attributed to water contained in the quartz grain boundaries [which was likely added to the dry experiments as adsorbed water on the starting quartz material]. Similarly, individual quartz crystals in the quartzite with ~1150 ppmw H_2O are nominally anhydrous, implying that the balance of the water was contained in the grain boundaries. Grain-boundary diffusion experiments were conducted at the same P–T conditions as synthesis experiments (1 GPa, 900°C). Cathodoluminescence (CL) images of diffusion couples show more extensive Ti uptake in intergranular regions of the quartzite with ~1150 ppmw H_2O (Fig. 1). Quartzites with ~140 ppmw H_2O have quartz crystals with high Ti (bright CL) intergranular regions that are ~6 μm wide near the rutile source. Quartzites with ~1150 ppmw H_2O have quartz crystals with high Ti intergranular regions that are ~13 μm wide near the rutile source. Bulk Ti measurements using LA-ICP-MS included high Ti intergranular regions and low Ti quartz cores into analytical volumes. Titanium measurements show that Ti transport and uptake is enhanced in the water-rich quartzites (Fig. 1). Kinetic and equilibrium phenomena affect the overall transport of Ti into the quartzite. Grain-boundary diffusion supplies Ti to the intergranular regions, and incorporation of Ti into quartz crystals adjacent to grain boundaries must be controlled by Ti-in-quartz solubility, lattice diffusion and grain-boundary migration 'capture'.

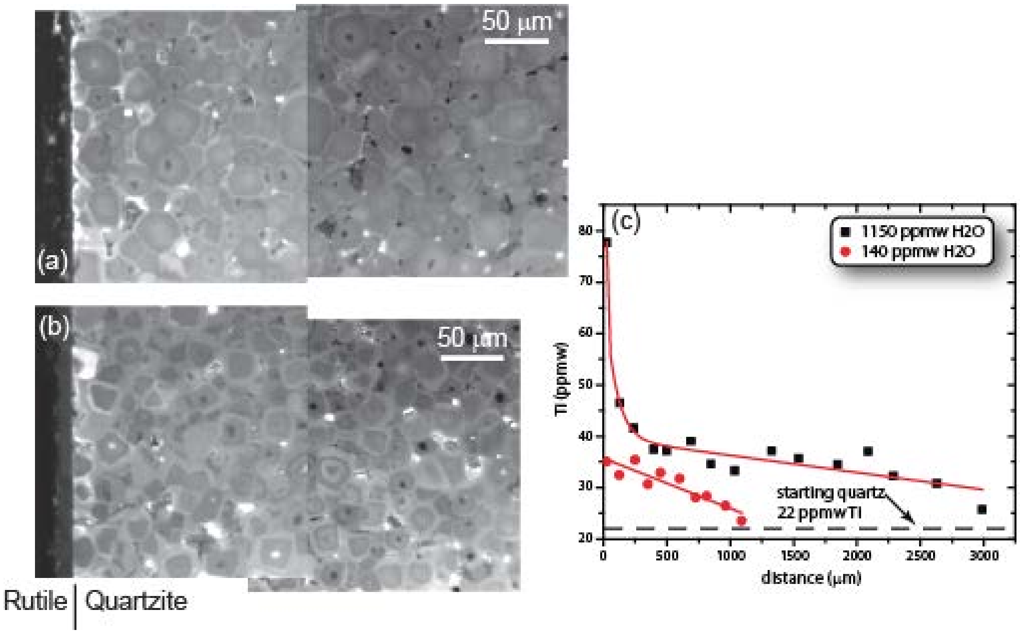

Figure 1. Cathodoluminescence (CL) images of rutile-quartzite diffusion couples. No water was added to the quartzite in (a), and 1150 ppmw H_2O was added to the quartzite in (b). The bright CL rims have higher Ti than the dark CL cores. Titanium uptake into quartz crystals is more extensive in the quartzite with 1150 ppmw H_2O. (c) Titanium concentration gradients measured in rutile-quartzite diffusion couples. Titanium concentrations decrease exponentially from high values near the rutile-quartzite interfaces followed by a linear decrease that approaches the starting quartz Ti concentration (dashed line). Titanium was measured using LA-ICP-MS with a 40 μm laser spot size intended to sample multiple grains and intergranular regions.

Publications Resulting From DOE Funds:

Thomas, J.B., Watson, E.B. (2014) Diffusion and partitioning of magnesium in quartz grain boundaries. Contributions to Mineralogy and Petrology (in review).

Homolova, V., Watson, E.B. (2013) Diffusive fractionation of lithium isotopes in polycrystalline olivine. Invited talk at the Goldschmidt Conference.

Watson, H.C., Watson, E.B. (2013) Grain Boundary Diffusion of Sulfur in MgO. Fall American Geophysical Union Fall meeting.

Evolution of Pore Structure and Permeability of Rocks under Hydrothermal Conditions

Brian Evans, Yves Bernabé, Uli Mok
Dept. Earth, Atmospheric, and Planetary Sciences,
Massachusetts Institute of Technology, 77 Mass. Ave., Cambridge, MA

The broad objective of this proposal is to study interrelationships among permeability, mechanical properties, and pore structure of rocks under hydrothermal conditions using laboratory experiments and computations. Recent laboratory work has included experiments on single asperities during pressure solution, the flow of two immiscible fluids in fractured rocks, and the effective pressure law in reservoir rocks. In this presentation we report on two current aspects of our computational work: The first is an investigation into pressure-solution deformation with two interacting mechanisms, interface dissolution and interface diffusion. The second is a network simulation of electrical conductivity in a granular rock filled with two immiscible fluids, one a non-conductor, the other conductive.

Low-temperature deformation of granular rocks saturated with aqueous fluids usually involves multiple, interacting physical mechanisms, which may include brittle cracking, precipitation from a fluid phase, and dissolution and diffusion along grain-boundaries, interphase-boundaries, and fluid/solid interfaces. To provide tractable solutions, constitutive relations are often constructed to describe situations where a particular mechanism is rate-limiting, or for idealized grain-packing geometry. Using a mechanical analysis of deformation involving fully coupled dissolution and diffusion processes [Lehner and Leroy, 2004], we extended earlier results for transient deformation along a single fluid-laden asperity to simulate creep of a three-dimensional, random pack of quartz spheres. The calculation uses a distinct element method [Cundall and Strack, 1979] and assumes that initial contact forces are purely normal to the boundary and given by the non-linear model of Digby [1981]. We performed simulations of long duration (> 1000 years) for both isostatic and oedometric compressions with the confining pressure or the uniaxial stress ranging from 40 to 120 MPa, and temperatures between 773 and 973°K. Overall volumetric strain of the aggregate displayed a complex time dependence, unlike any constitutive laws assuming a single rate-limiting mechanism. The sensitivity of log strain rate to log stress had values between 0.3 and 0.6, depending on loading conditions (i.e., isostatic or oedometric) and the value of the contact interface diffusivity. Similar power law exponents (<1) have been observed in experiments by Dysthe et al. [2003] and Visser et al. [2012]. In our simulations, decreases in strain rate were caused partially by increases in mean contact size and increases in contact coordination number, which approached 10. The mean contact force decreases markedly, while there is a considerable increase of the bulk modulus. When interpreted using a macroscopic constitutive law with a variable effective activation enthalpy and stress exponent, the activation enthalpy decreased with time suggesting that PS becomes diffusion controlled in the long time limit.

Effects of changes in pore connectivity and heterogeneity on transport properties: In collaboration with Prof. M. Li, Southwest Petroleum University, Chengdu, China, we continued our study of the effect of pore connectivity and pore size variability on the transport properties of rocks using network simulations to estimate the electrical conductivity changes as a function of brine saturation during drainage by a non-wetting and electrically non-conducting fluid (oil or gas). Our goal is to relate these changes to the geometrical and topological characteristics of the portion of the pore space saturated with brine and to test whether the formation factor model of *Bernabé et al.* [2011] can be successfully used to predict the resistivity index. We also started to investigate solute transport by simulating the motion of solute particles in a pipe network by randomly assigning transit times in individual pipes according to a probability distribution derived from Taylor dispersion and by randomly selecting the pipes into which the solute particles travels according to probabilities proportional to the pipe flow rates. These procedures amount to up scaling Taylor dispersion, i.e., the pore scale transport process, to the macroscopic scale (up to 10 m).

Publications

Bernabé, Y., M. Zamora, M. Li, A. Maineult, and Y. B. Tang (2011), Pore connectivity, permeability, and electrical formation factor: A new model and comparison to experimental data, *Journal of Geophysical Research-Solid Earth*, *116*, B11204 DOI:11210.11029/12011jb008543, doi:10.1029/2011jb008543.

Cundall, P. A., and O. D. L. Strack (1979), A discrete numerical model for granular assemblies, *Geotech.*, *29*, 47-65.

Digby, P. J. (1981), The effective elastic moduli of porous granular rocks, *J. Appl. Mech.*, *48*, 803-808.

Dysthe, D. K., F. Renard, J. Feder, B. Jamtveit, P. Meakin, and T. Jossang (2003), High-resolution measurements of pressure solution creep, *Physical Review E*, *68*(1).

Lehner, F. K., and Y. Leroy (2004), Sandstone compaction by intergranular pressure solution, in *Mechanics of Fluid-Saturated Rocks*, edited by Y. Guéguen and M. Boutéca, pp. 115-168, Elsevier Academic Press, New York.

Visser, H. J. M., C. J. Spiers, and S. J. T. Hangx (2012), Effects of interfacial energy on compaction creep by intergranular pressure solution: Theory versus experiments on a rock analog (NaNO3), *Journal of Geophysical Research*, *117*(B11), doi:10.1029/2012jb009590.

Non-Darcian Flow, Imaging, and Coupled Constitutive Behavior of Heterogeneous Deforming Porous Media

Hongkyu Yoon, Thomas Dewers, and Jason Heath
Geomechanics Department, Sandia National Laboratories, Albuquerque, NM

Single and multiphase flow and deformation of all porous media strongly depend on pore-scale processes and the underlying pore-scale dynamics that govern deformation, flow and transport are not understood quantitatively for low porosity and permeability earth materials. This project consists of three distinct tasks including mudstone multiphysics, percolation methods for multiphase flow, and testing plasticity paradigms. This talk focuses on Task 1, with the remaining tasks being discussed in the Workshop poster session. Specific objectives of Task 1 include 1) determining shale pore structures to characterize distributions of pore size, shape and connectivity, and pore-lining phases of microfacies at micron to nanometer scales, 2) examining clay aggregate deformation and the onset of anisotropy from nano- to micro-scale and document the transition from dominantly Darcy-to-non-Darcy flow as clay-bearing sediments consolidate, and 3) measuring mechanical response of mudstones at the micron level to scales more typical of rock mechanics testing and applying results to testing new techniques for computational modeling and upscaling.

Focused ion beam-scanning electron microscopy (FIB-SEM) is used to characterize shale pore structures at > 10 nm resolution, and we introduce a state-of-the art aberration corrected scanning transmission electron microscopy (AC-STEM) for visualizing 3D connectivity and structure of the <10-nm pore population (~ 1nm resolution). Moreover, energy dispersive X-ray spectrometry (EDS) is used to identify the distribution of chemical composition of pore-lining phases. Data obtained from topological and chemical analysis is being mapped together to reconstruct three-dimensional (3-D) pore structures with different phases. Reconstructed 3-D pore topologies are used as an input for gas transport simulations in shale gas rocks to improve our understanding of enhanced diffusion processes (e.g, Knudson diffusion, slippage) in nano-pores and impact of chemical, mineralogical, and textural characteristics on shale gas transport.

In-situ neutron diffraction experiments using custom-made titanium oedometers are performed to examine clay aggregate deformation and pore structures from nm to mm scales. In particular, water in pores less than ~10-nm (at or below typical FIB-SEM resolution) will deviate from those of bulk water, which can influence non-Darcy flow and mechanical response. The flow of gases in these pore networks may result in molecular sieving and resulting elemental fractionation. It was estimated that half of shale pore volume can reside in networks of pores of <10-nm size, which is relevant for shale/clay yield, failure, and matric potential effects. Our oedometer studies are intended to compliment and advance knowledge on coupled geomechanical and fluid flow properties of clays under non-hydrostatic stress (i.e., uniaxial strain) with pore pressure, as compared to other recent hydrostatic-only, in situ X-ray or neutron studies. The difference in intensity for the low and high pressure conditions are likely occurring from changes in pore structure with compactional pore volume loss. Data interpretation is underway for pore structure and sizes for the different levels of pore volume loss. In general, neutron scattering methods are a promising tool to reveal pore structure information across length scales of relevance (i.e. nanometers to microns), and the oedometer design is allowing observation of in-situ non-hydrostatic deformation of clay aggregates in partial-to-saturated fluid conditions.

We also report on updated data acquisition and control capabilities in Ssandia’s temperature controlled creep laboratory. Creep experiments are being used to examine influence of organic carbon and clay content on shale microstructural damage and creep mechanisms.

Geochemical Self-Organization and the Evolution of Permeability

Tony Ladd
University of Florida, Gainesville, Florida, 32611

Reactive infiltration instabilities occur in a wide range of geophysical and geotechnical systems. The simplest such instability occurs when fluid flows between two soluble plates, which is an idealized model of fractured limestone. Even when the initial aperture is uniform at the nanoscale, an instability in the reaction front develops leading to the formation of pronounced solutional channels or "wormholes". We have suggested that this instability may explain the onset of large underground caves systems, by allowing a much deeper penetration of reactant than is possible by uniform opening of the fracture.

Dissolution is a form of self-organization where patterns seem to develop in a similar way over a wide range of initial conditions. This is an interesting and important subject that offers the possibility of a theoretical understanding of geomorphologies formed by dissolution-precipitation reactions. We present numerical simulations to indicate the insensitivity of key statistical markers to the initial distribution of porosity.

Predictions of a linear stability analysis in porous and fractured rocks vary considerably depending on the underlying model assumptions. We have previously identified the appropriate non-dimensional group that distinguishes between the different cases. Numerical simulations of dissolution predict that a planar front breaks up into a number of competing fingers. The nature of the competition is again different in fractured and porous rocks. We are presently trying to understand the growth of individual fingers, which numerical simulations show to be steadily propagating in time, much like the better-known phenomena of viscous fingering. We will indicate the difficulties that have so far prevented us from finding an explicit solution to the finger size, shape and velocity.

1. P. Szymczak and A. J. C. Ladd. *Reactive infiltration instabilities in rocks. Dissolution of a porous matrix.* J. Fluid Mech., 738:591-630, 2014.
2. P. Szymczak and A. J. C. Ladd. *Interacting length scales in the reaction-infiltration instability* Geophys. Res. Lett., 40:3036-3041, 2013.
3. P. Szymczak and A. J. C. Ladd. *Reactive infiltration instabilities in rocks. Fracture dissolution* J. Fluid Mech., 702:239-264, 2012.
4. P. Szymczak and A. J. C. Ladd. *Instabilities in the dissolution of a porous matrix.* Geophys. Res. Lett., 38:L07403, 2011.
5. P. Szymczak and A. J. C. Ladd. *The initial stages of cave formation: Beyond the one-dimensional paradigm.* EPSL, 201:424-432, 2011

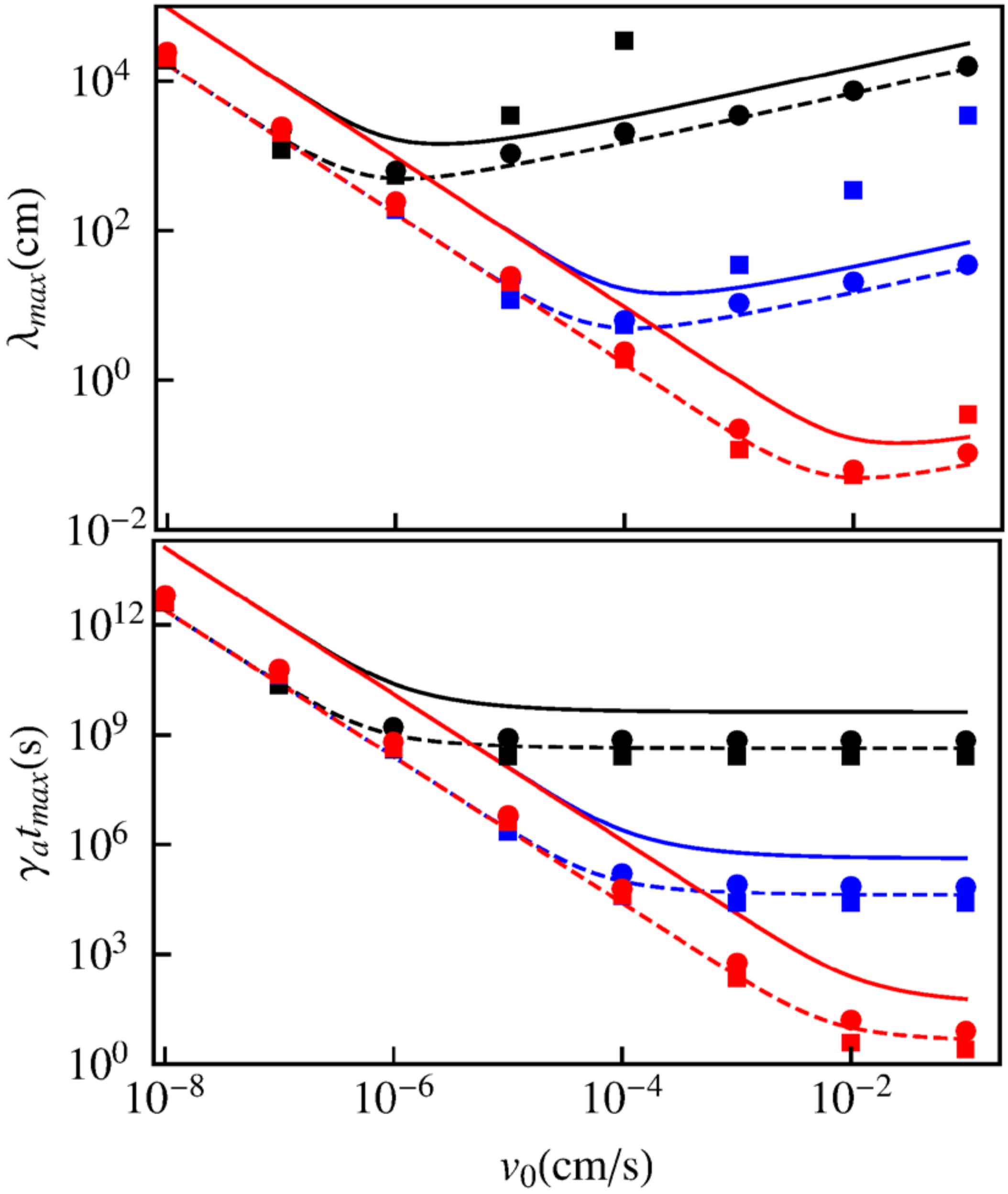

The figure illustrates the typical wavelength and growth rates for dissolutional instabilities in porous media at different flow velocities. The results span the range from natural subsurface flows to the much higher velocities achieved by acidization. The different colors correspond to different reaction timescales – 10^{-8} *s (black), characteristic of slow processes such as quartz dissolution;* 10^{-4} *s (blue) corresponding to calcite dissolution in natural conditions; and* 1 *s (red) typical of acidization. Our stability analysis shows there is a minimum in both the wavelength and growth rate as a function of flow rate, a consequence of the two length scales in a dissolving porous matrix.*

Fingering, fracturing and dissolution in granular media

Ruben Juanes
Massachusetts Institute of Technology

The displacement of one fluid by another in a porous medium give rise to a rich variety of hydrodynamic instabilities. Beyond their scientific value as fascinating models of pattern formation, unstable porous-media flows are essential to understanding many natural and man-made processes, including water infiltration in the vadose zone, carbon dioxide injection and storage in deep saline aquifers, and hydrocarbon recovery. Here, we review the pattern-selection mechanisms of a wide spectrum of porous-media flows that develop hydrodynamic instabilities, discuss their origin and the mathematical models that have been used to describe them. We point out many challenges that remain to be resolved in the context of multiphase flows, and suggest modeling approaches that may offer new quantitative understanding.

In particular, I will present experimental, theoretical and computational results for: (1) fluid spreading under partial wetting; (2) the impact of wettability on viscously unstable multiphase flow in porous media; (3) capillary fracturing in granular media; and (4) rock dissolution during convective mixing in porous media.

High resolution dielectric properties of organic-rich reservoirs with implications for thermal maturation and the liberation of polar fluids.

Manika Prasad, John Scales and Rezwan Rhaman
Colorado School of Mines

Porosity estimates in self-resourcing organic-rich reservoirs are critically dependent on our understanding of pore space in fine-grained constituents, organic matter and clay minerals. However, pore sizes and pore volumes change with electrochemical interactions between rock constituents and polar fluids liberated during organic maturation. Quantification of these changes will make rock property models and reserves estimates more reliable. Interactions between clay minerals and some functional groups of polar organic contaminants are governed by the surplus electric charge on the clay surface. We expect similar interactions in the subsurface between polar hydrocarbon byproducts of kerogen maturation and inorganic clay minerals. In this talk we will describe our recent work using high-resolution sub-millimeter dielectric characterization to map the polarizability of rocks and fluids. We are building a database of dielectric properties and plan to extend our work to electron spin resonance in order to measure density of free radicals.

Weathering Models: Dissolution and Porosity Development in Crystalline Rocks

S. L. Brantley, G. Stinchcomb, X. Gu, M. Lebedeva, K. Bazilevskaya
Pennsylvania State University, Earth and Environmental Systems Institute, Univ. Pk PA 16802

A fundamental goal of DOE-funded geochemical research is to develop numerical models of reactive transport to simulate natural water-rock systems. To test the underlying conceptual models and parameterize the numerical simulations requires analysis of systems that record rates of geochemical change over varying timescales. The most well studied examples of geochemical systems that have evolved over timescales varying from 10^3 to 10^6 years are found at earth's surface: depth profiles of regolith. However, at present our ability to create conceptual and numerical models of regolith formation is limited because we do not understand the coupling between chemical reaction and porosity evolution.

Our focus here is on one-dimensional models of weathering: depth profiles that document alteration of crystalline rocks or shale exposed at ridgetops. As protolith, these rocks have low porosity but are fractured. As the protolith becomes exposed to weathering fluids higher in the profile, they become fractured and altered. At depth, solute transport is dominated by diffusion but near the land surface, interactions with $H_2O + CO_2 + O_2$ open up porosity, eventually bringing in infiltrating fluids. Mineral reaction fronts in regolith record the largest changes in porosity. These fronts are documented in the element-depth profiles as i) *completely developed fronts* where the primary minerals have dissolved completely, and ii) *incompletely developed fronts* where the primary minerals are still present at the land surface because of slow mineral kinetics compared to erosion.

At long-exposed ridgetops such as in the Virginia Piedmont, diabase and granite regolith are characterized either as thin (diabase) or thick (granite) completely developed weathering profiles (3). We attribute the difference in the two crystalline rocks to the dominant modes of solute transport at the bedrock-saprolite interface: diffusion versus advection for diabase versus granite respectively. In contrast to these crystalline rocks, profiles developed on ridges on Rose Hill shale in Pennsylvania are mantled by thin regolith that is characterized by incompletely developed reaction fronts for the dominant primary minerals(2). These patterns are documented by neutron scattering of thin sections versus depth (Figure 1).

The observations from PA and VA may elucidate weathering profiles worldwide: for example, regolith developed on granite is usually thicker than on diabase, perhaps because of enhanced infiltration and advection for felsic as compared to mafic rock. Enhanced advection is attributed to three factors: i) the granite experiences deep fracturing and disaggregation during weathering, ii) the granite contains quartz which holds open the regolith porosity once regolith forms; iii) the granite does not form the same types of permeability-occluding clay layers that can form on diabase. Deep fracturing may occur in granite at least partly because the low-ferrous iron of the felsic rock allows downward-percolating fluids to retain dissolved oxygen to deeper depths than CO_2 as weathering proceeds. Thus, oxidizing fluids penetrate deep into the rock, causing biotite oxidation which in turn drives fracturing. In contrast, weathering fluids percolating downward through diabase are likely first depleted in O_2 and then CO_2 so that the deepest reactions result from carbonated solutions that mobilize ferrous iron without oxidation and fracturing. To complete numerical models of these systems requires understanding patterns in concentrations of O_2 and CO_2 in deep regolith pore space – measurements of these soil gases are ongoing.

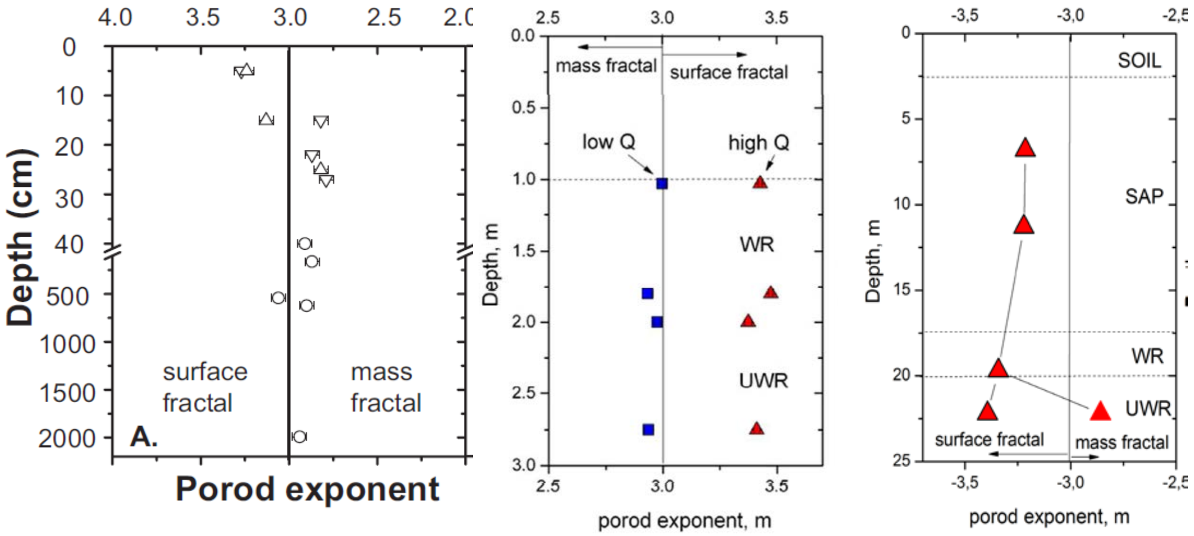

Figure 1. Plots summarizing neutron scattering through thin sections of weathered rock sampled versus depth on three lithologies. Unweathered fragments of diabase (MIDDLE) and granite (RIGHT) show that the internal pore-grain interfaces are mass + surface fractals whereas unweathered shale (LEFT, A) is a mass fractal. With onset of weathering and oxidation, the granite and shale transform to a surface fractal as fracturing promotes increasing solute transport in infiltrating fluids. In contrast, the diabase begins as a mass + surface fractal and does not transform into a surface fractal: solute transport in this rock is by diffusion. LEFT (A): Porod exponents in bedrock (deeper than 50 cm) and in weathered Rose Hill shale chips (upper 40 cm) weathered at a ridgetop in Pennsylvania and sampled from a borehole. Exponents reveal the fractal dimensions for the pore-grain interface as shown. MIDDLE: Fractals that comprise the pore-grain interface of weathering diabase collected in a borehole drilled at a Virginia ridgetop from unweathered rock (UWR) to weathered rock (WR) to saprolite (SAP) to SOIL as indicated. All samples are mass + surface fractals as shown. RIGHT: The interface inside granite UWR from a nearby ridgetop is also characterized as both a mass and surface fractal but micro-fracturing during weathering due to biotite oxidation transforms the rock to a surface fractal in the UWR. In general, the mass fractal inside the unweathered crystalline rocks describes the distribution of pores (~300 nm to ~ 5 µm) along grain boundaries and triple junctions. The surface fractal describes the distribution of smaller features (1-300 nm), i.e. the bumps at the grain/ pore interface.

References

(1) Bazilevskaya, E., Rother, G., Mildner, D., Pavich, M., Cole, D., Bhatt, M., Jin, L., Steefel, C., and Brantley, S. L., 2014, in review. How oxidation and dissolution in diabase and granite control porosity during weathering. *Soil Science Society of America Journal*.

(2) Brantley, S. L., Holleran, M. E., Jin, L., and Bazilevskaya, E., 2013. Probing deep weathering in the Shale Hills Critical Zone Observatory, Pennsylvania (U.S.A.): the hypothesis of nested chemical reaction fronts in the subsurface. *Earth Surface Processes and Landforms* **doi:10.1002/esp.3415**.

(3) Bazilevskaya, E., Lebedeva, M., Pavich, M., Rother, G., Parkinson, D. Y., Cole, D., and Brantley, S. L., 2013. Where fast weathering creates thin regolith and slow weathering creates thick regolith. *Earth Surface Processes and Landforms* **38**, 847-858, doi: 10.1002/esp.3369.

(4) Navarre-Sitchler, A. K., Cole, D., Rother, G., Jin, L., Buss, H. L., and Brantley, S. L., 2013. Porosity and surface area evolution during weathering of two igneous rocks. *Geochimica Cosmochimica Acta* **109**, 400-413, doi: 10.1016/j.gca.2013.02.

Branching of Stream Networks

Daniel H. Rothman, Yossi Cohen, Hansjörg Seybold, and Robert Yi
Lorenz Center, Department of Earth, Atmospheric, and Planetary Sciences
Massachusetts Institute of Technology

In humid environments, rainfall infiltrates the ground and recharges the groundwater supply. When the water re-emerges at the surface, shear stresses can be sufficient for erosive incision of channels. As these channels grow, they often *branch* or *bifurcate*. We have studied this process theoretically and observationally. By representing streams as growing paths in a diffusing field, we predict the characteristic bifurcation angle $\alpha=2\pi/5=72^{\circ}$ [1,2]. Our observations of nearly 5000 bifurcated streams growing in a groundwater field on the Florida Panhandle yield a mean bifurcation angle of $71.9^{\circ}\pm0.8^{\circ}$, confirming our theory.

The Florida network is unusual in that stream growth is unequivocally driven by groundwater seepage in a reasonably homogeneous environment. To investigate the extent to which seepage flows drive river networks more generally, we have measured the bifurcation angles of all stream junctions present in the NHDPlus Version 2 database of drainage networks in the continental United States. The result is shown in Figure 1a. We hypothesize that the resulting pattern should be associated with the influence of groundwater flow into streams. We have therefore created a corresponding map (Figure 1b) of the *aridity index* $A=P/\mathrm{PET}$, where P is the precipitation rate and PET is potential evapotranspiration. PET measures the rate at which water would be evaporated if it were present. Thus wherever $A>1$, groundwater is recharged. Visually, one sees that larger angles are correlated with higher values of the aridity index A. We quantify this correlation by computing the average bifurcation angle as a function of A, shown in Figure 1c. We obtain a remarkable result: when A is greater than about 2, the mean bifurcation angle reaches a maximum at about 72°. There is also a sharp transition to smaller bifurcation angles in arid regions, where $A<1$. A surprising immediate implication of these results is that groundwater seepage has a profound impact on the growth of river networks wherever groundwater is recharged, which corresponds to roughly half the area of the continental United States.

We hypothesize that the transition from humid to dry climates in Figures 1a and 1b represents also a transition from network growth dominated by diffusive subsurface flow to growth dominated by advective overland flow. In arid climates, channels are likely incised by overland flow during major storms. Figure 1c suggests that this advective limit is characterized by a bifurcation angle of about 45°.

After summarizing the above results, we return to the purely diffusive case of the Florida network and briefly discuss three recent lines of inquiry. First, we note that the principle of local symmetry can be adopted from fracture theory to predict the direction in which streams grow. Second, we consider the three-dimensional shape of the valleys that contain the streams, and characterize their diffusive limit mathematically. Finally we discuss early results that attempt to derive erosion rates from cosmogenic isotopes measured at the Florida site.

New Opportunities for Geoscience Research using the Multi-bend Achromat Storage Ring Being Proposed for the Upgrade of the Advanced Photon Source

Sutton S. R., Rivers M. L., Eng P. E., Newville M., Lanzirotti A., and Stubbs J.
University of Chicago and GSECARS

The Advanced Photon Source (APS) is planning a new storage ring magnet lattice design – the multi-bend achromat (MBA) – that promises a revolutionary increase in brightness several orders of magnitude beyond that of the current APS. The new MBA lattice technology will provide three key improvements over the current APS design: the ability to focus all of the X-rays down to nanometer-size spots, dramatic increases in coherent flux, and orders of magnitude increase in brightness per X-ray pulse for time-resolved experiments. These new capabilities will open up new scientific opportunities in geoscience research.

Solving important geoscience questions requires characterization of samples at all scales, from the molecular level through field scale. Enhanced characterization of highly heterogeneous natural materials, made possible by the new MBA capabilities, will particularly advance the understanding of geologic processes at the nano- and meso-scales. This presentation will outline some of the key technical aspects of the MBA upgrade and provide some examples of geoscience applications where the advanced capabilities will extend knowledge of the properties of natural earth materials and related processes.

The essential feature of the MBA upgrade is the replacement of each of the large synchrotron bending magnets, devices in the accelerator used to curve the electron beam to produce a closed loop, with multiple, smaller bending magnets. The result is a dramatic reduction in the horizontal emittance of the electron beam which in turn greatly increases the brightness of the X-ray sources.

Geoscience applications that will particularly benefit from these advances will be any that can take advantage of higher flux in smaller beams. Notable are scanning probe applications involving microbe-mineral-fluid interactions, such as those that control the speciation, migration and toxicity of contaminants, and those that are important in nutrient and metal cycling in the oceans. Higher flux in smaller spots also translates into more rapid chemical and mineralogical mapping of larger samples at higher spatial resolution. Such improvements will advance searches for geological sources of strategic elements and improve processing methodologies, for example. Greater analytical speed will also allow the characterization of more rapid geochemical reactions and better definition of intermediate states.

An exciting opportunity is the ability to obtain detailed chemical state information at the highest spatial resolutions (~ tens of nms) using resonant inelastic X-ray scattering (RIXS) measurements at fixed incident energy with crystal analyzers or high-resolution energy-dispersive detectors (currently under development) and zone plates or KB mirrors for focusing. Such analyses are currently limited by small-scale instabilities associated with energy-scanning methods.

The coherence of the X-ray beams is a property that the geoscience community has yet to exploit to any great extent but has enormous potential. One example is the application of coherent diffraction imaging which allows a detailed structural analysis of minute samples without the use of focusing optics which can degrade resolution. The MBA upgrade to the APS will increase the coherent flux by a factor of 100 and hence dramatically increase the capability of coherent X-ray imaging.

Observing Molecular-Scale Dynamics at the Interface between Rock-Forming Minerals and Aqueous Solutions

Paul Fenter[1], Sang Soo Lee[1], Nouamane Laanait[1], and Neil C. Sturchio[2]
[1]*Chemical Sciences and Engineering Division, Argonne National Laboratory*
[2]*Department of Earth and Environmental Sciences, University of Illinois at Chicago*

Mineral-water interfaces are the primary reaction sites in low-temperature geochemical systems. Our understanding of these systems has improved markedly over the past two decades, specifically due to the ability to make direct in-situ observations. In particular, the development and application of high resolution X-ray based tools have provided fundamentally new insights into the molecular-scale structure and reactivity of interfaces, including the mineral surface structure, the organization of interfacial hydration layers, and the speciation and coordination of adsorbed ions. Here, we describe new opportunities to observe and understand dynamics at these interfaces using variations of X-ray reflectivity. Time-resolved measurements of changes in adsorbed ion distributions at the muscovite-water interface (one of the most abundant rock-forming minerals) provide new insights into adsorption kinetics and the energetic landscape experienced by the adsorbing ion, including ion binding energies as well as the barriers between adsorbed states. Real-time measurements of calcite surface topography reveal how it responds subtly to changes in solution saturation index, including both reversible and irreversible changes. Finally, observations of calcite-water interfaces with high-brilliance X-ray reflection interface microscopy (XRIM) show surprising changes in topography induced by the XRIM beam, revealing the role of water hydrolysis products on altering the stability of these interfaces, with possible implications for geochemical reactions occurring in high radiation fields.

Actinide Geochemistry and Geochronology with Real Rocks

Steve Goldstein, Mike Murrell, Joanna Denton, Andy Nunn, Ron Amato, and Kim Hinrichs
Los Alamos National Laboratory

Uranium-series geochemistry and geochronology techniques have a wide range of applications in a number of fields including hydrology, paleoclimatology, paleooceanography, and volcanology. Our project aims to use well established bulk measurement techniques such as MC-TIMS and MC-ICPMS along with new high spatial resolution LA-MC-ICPMS techniques for U-series measurements. We then apply these techniques to better understand U-series environmental transport and develop/apply U-series chronometers in support of basic geoscience research for energy and waste concerns.

For U-series measurements using LA-MC-ICPMS, a crucial issue is having matrix-matched reference materials to correct for elemental fractionation during LA. We have completed high-precision U-Th disequilibrium measurements in a suite of Chinese Geological Standard Glasses with a range of composition including basalt, syenite, andesite, and soil (Denton et al., 2013a). The large disequilibria observed for some of the glasses (up to several %) along with the range in Th/U ratios should provide useful reference points for the U-series analytical community.

Studies of U-series disequilibria near uranium deposits can provide valuable information on the timing of actinide mobility over a range of spatial and temporal scales. In our most recent work (Denton et al., 2013b), we characterized the geochemical evolution of the Nopal I uranium ore deposit (Sierra Peña Blanca, Chihuahua, Mexico) in terms of mineral-fluid interactions as well as the role that vertical fractures play in U transport and retention. The Nopal I deposit is a possible analog for actinide transport from a nuclear waste repository in fractured, unsaturated tuff and an arid climate. Samples were obtained from a vertical drill core (PB-1b) that extends to ~250 m depth below the surface. Three samples were selected for study from the drill core at depths of 8.5 m, 67 m and 191 m. Since these are fine-grained materials, different whole-rock subsamples were selected based on differences in color. From these fractions we can evaluate U-Th model ages and whole rock isochrons for dating past actinide transport.

Drill core samples were dissolved and spiked with ^{229}Th and ^{233}U tracers. U and Th were separated from the rock matrix by ion exchange chromatography, and high-precision U-Th concentration and isotopic ratios were measured by MC-TIMS and MC-ICPMS. Our data show that uranium concentrations range from ~0.1- 0.8 wt. % and U/Th weight ratios range from ~50-700. The ore deposit contains ~0.57 wt. % U, therefore our results suggest that U has been mobile up to 200 m depth in the past. ^{234}U/^{238}U activity ratios in the drill core samples range from 0.66 to 2.44 and illustrate a complex evolution consistent with interaction between groundwater enriched in ^{234}U and a tuff matrix that is depleted in ^{234}U due to recoil-related leaching. Closed-system U-Th model ages are generally >200 ka, and U-Th whole rock isochrons yield ages >200 ka with one exception (Figure 1). Although mineral-fluid interaction is ongoing and more complex open system models are possible, the most consistent interpretation of these data is that the drill core samples have generally remained closed with respect to U and Th mobility for >200 ka. These results confirm our prior U-series chronology studies of horizontal-trending fractures at this site and also provide a baseline for more detailed mineral work on actinide mobility and retention using LA-MC-ICPMS.

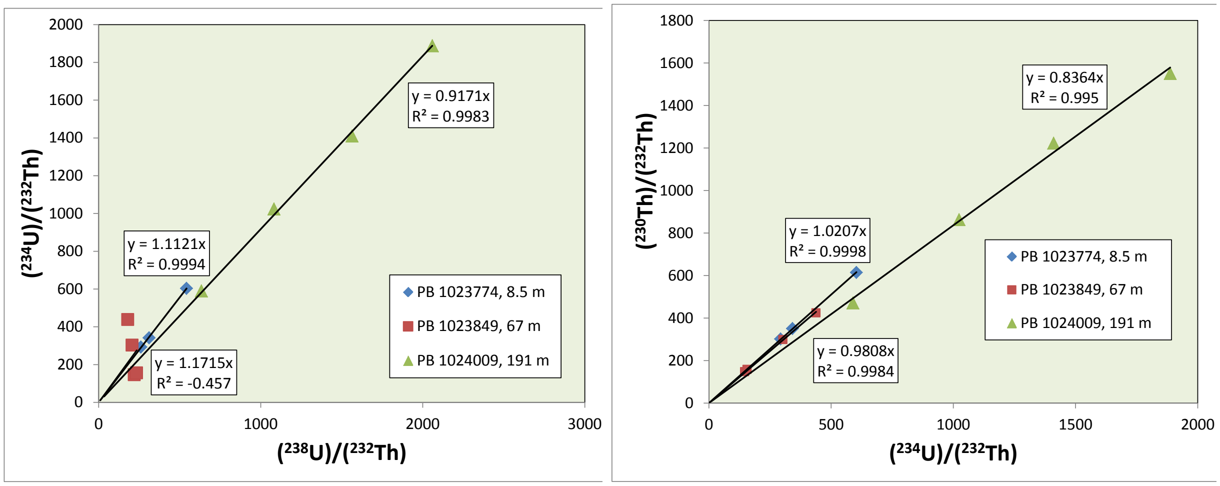

Figure 1. Isochron results for the whole-rock subsamples. Well defined U-Th isochrons are obtained for two of the samples, with ages of ~ 440 +/- 30 ka for the near surface sample and 211 +/- 3 ka for the deepest sample. The intermediate depth sample at 67 m does not lie on an isochron suggesting open system behavior for U.

2013 Publications:

Denton, J.S., Murrell, M.T., Goldstein, S.J., Nunn, A.J., Amato, R.S., Hinrichs, K.A., 2013a. Evaluation of new geological reference materials for uranium-series measurements: CGSG glasses and macusanite obsidian. *Anal. Chem*. **85**, 9975-9981.

Denton, J.S., Goldstein, S.J., Murrell, M.T., Nunn, A.J., Hinrichs, K.A., Amato, R.S., 2013b. A record of uranium-series transport in fractured, unsaturated tuff at Nopal I, Sierra Peña Blanca, Mexico. *Geological Society of America Abstracts with Programs*. **45**, 7.

Kinetic Isotope Fractionation in Laboratory and Natural Samples

Frank Richter
Department of the Geophysical Sciences, The University of Chicago

For the past ten years we have been demonstrating and quantifying large kinetic isotope fractionations by diffusion in systems ranging from water, silicate melts and minerals, and metal alloys. Our most recent work puts special emphasis on comparing what we find in laboratory experiments and in natural settings. We are also focusing increasingly on kinetic isotope fractionation by diffusion in minerals because in natural settings it is often the minerals that retain a record of the history of transport and thermal evolution even in cases where the large-scale transport was by fluid infiltration or by grain boundary diffusion. Because diffusion in minerals is slow, the experiments involving diffusion in minerals have to be run at relatively high temperature (~1000˚C), but the results should be applicable to much lower temperature situations if given a longer time than one can devote to a laboratory experiment.

I propose to focus on two particular aspects of our recent work kinetic isotope fractionation in geological materials.

1. I will present a number of experimental results where the isotopic measurements give unique insight into diffusive processes that are not at all apparent when one only considers concentration gradients. I will show results where step-like concentration profiles would not suggest that diffusion was the responsible process, but the isotopic fractionation give clear evidence that diffusion was indeed involved.
2. I will also show a number of case studies where we have found quantitative agreement between the kinetic isotope fractionation in our laboratory experiments and in natural geological settings. The laboratory and natural examples include both molten systems (i.e., diffusion boundaries between molten rhyolite and basalt) and minerals (pyroxenes and olivines from a lava lake, a lava flow, and from mantle xenoliths).

Time permitting I will also address some of the experimental and theoretical challenges that we are now faced with given our recent results.

Geologic Complexity in Surface Complexation Models

Dimitri A. Sverjensky
the Johns Hopkins University

Reactions between mineral surfaces and water proceeding via surface complexation reactions play an important role in the equilibria and kinetics of processes controlling the compositions of soilwaters and groundwaters, the fate of contaminants, and the subsurface storage of CO_2 and nuclear waste. However, no currently-available model of surface complexation can be used to analyze these processes by predicting surface protonation and adsorption of metallic cations, anions and organic species for the wide range of fluid compositions, minerals, and temperatures and pressures that exist in nature.

The geologic complexity affecting the chemistry of mineral-water interactions in shallow subsurface conditions involves a wide variety of variables. These include a wide variety of minerals, and poorly crystalline precursors to minerals, and a very wide range of aqueous species. My previous studies have shown that surface complexation can be applied in a predictive mode for many of the different types of minerals and mineral precursors. Using the extended triple-layer model (ETLM), the application of Born solvation theory enables prediction of adsorption onto many types of solids. However, the wide range of aqueous species is still a challenge. Despite this, the geologic reality is that most near-surface and shallow subsurface waters on the continents are predominantly Ca-bicarbonate-silica waters. Consequently, it is essential to be able to model the chemistry of the mineral-water interface in such waters. Remarkably, there is not much experimental information about how such waters behave at the surfaces of minerals. Recent efforts in the present project have been oriented towards developing predictive surface complexation models to address this issue. Progressively, my studies have been carried out on separate characterizations of the adsorption of Ca (and other divalent cations), bicarbonate adsorption, and silica adsorption, both with and without aqueous organic species present. It is now possible to carry out predictive calculations simulating the beginnings of this geologic complexity. One example that will be shown is the surprising effect of an organic acid anion (glutamate) on Ca adsorption on rutile. The surface charge on the rutile is completely reversed at pH values of about 7 to 9 by the adsorption of Ca. Under these circumstances, an organic anion can adsorb strongly when it would normally not adsorb. Experimental results are consistent with this behavior. This type of cooperative effect illustrates the need to account for the chemical and geologic complexity of the mineral-water interface in natural systems.

*Effect of Ca on the adsorption of an organic acid anion (glutamate) on rutile:

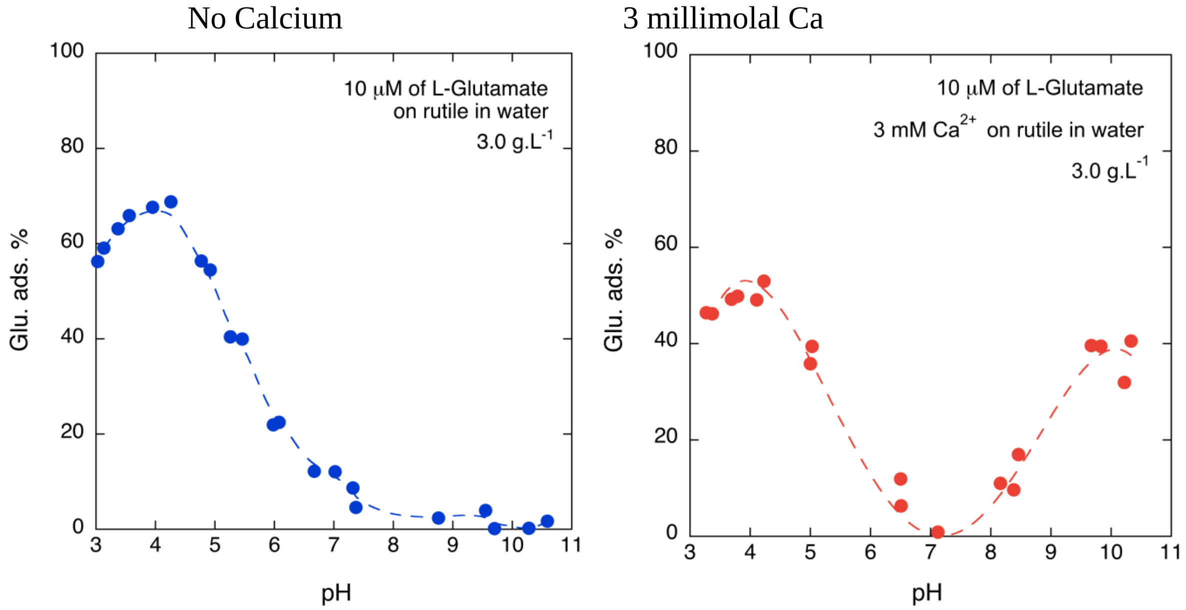

Recent Publications:

Lee, N., Hummer, D. R., Sverjensky, D. A., Rajh, T., Hazen, R. M., Steele, A., and Cody, G. D., 2012. Speciation of l-DOPA on Nanorutile as a Function of pH and Surface Coverage Using Surface-Enhanced Raman Spectroscopy (SERS). *Langmuir* **28**, 17322–17330.

Livi, K. J. T., Schaffer, B., Azzolini, D., Seabourne, C. R., Hardcastle, T. P., Scott, A. J., Hazen, R. M., Erlebacher, J. D., Brydson, R., and Sverjensky, D. A., 2013. Atomic-Scale Surface Roughness of Rutile and Implications for Organic Molecule Adsorption. *Langmuir* **29**, 6876-6883.

Geochemistry of Interfaces: From Surfaces to Interlayers to Clusters

Jeffery A. Greathouse[1], Louise J. Criscenti[1], Kevin Leung[2], Anastasia G. Ilgen[1], Lynn E. Katz[3], Heather C. Allen[4], and Randall T. Cygan[1]

[1]Geochemistry Department, Sandia National Laboratories, Albuquerque, New Mexico, 87185; [2]Surfaces and Interface Sciences Department, Sandia National Laboratories, New Mexico, 87185; [3]Department of Civil, Architectural and Environmental Engineering, University of Texas, Austin, Texas, 78712; [4]Chemistry Department, Ohio State University, Columbus, Ohio, 43210

This comprehensive project seeks to identify and evaluate the critical molecular phenomena at clay mineral and metal-oxide interfaces that control many geochemical and environmental processes. We combine advanced experimental and analytical methods with state-of-the-art molecular simulation to improve our understanding of the mineral-water interface and to develop a predictive capability for evaluating geochemical processes that are critical to water quality and treatment, fate and transport of contaminants, underground storage, resource extraction, materials stability and corrosion, and other related technologies. Specific tasks include the analysis of surface speciation, adsorption phenomena, surface complexation modeling, ion pairing, interlayer structures, structure and reactivity of the edge surfaces of clay minerals, and redox processes at clay mineral-water interfaces. Related subtasks incorporate nuclear magnetic resonance, X-ray absorption, second harmonic generation, sum frequency generation, infrared and Raman vibrational, and inelastic neutron scattering spectroscopies as well as more conventional characterization methods to understand the key molecular processes and help validate the modeling studies.

Our molecular simulation efforts employ both classical and quantum techniques to address structure, thermodynamics, kinetics, and physical properties of mineral-water systems. The development of improved edge-site models within our classical force field approach (Clayff) greatly expands the possible applications from basal surfaces to reactive edges. We have also performed potential of mean force simulations to calculate free energy profiles of ion pairs in solution and adsorbed on mineral surfaces. A variety of experimental and spectroscopic work complements the theoretical effort.

More recently, we have examined the reactivity of the clay structural Fe(II)/Fe(III) couple. We perform laboratory experiments in order to understand the exact mechanism by which structural Fe in phyllosilicates participates in redox reactions, the controls over capacity, pathways, kinetics and direction of electron transfer, and the effective redox potential of the clay structural Fe(II)/Fe(III) couple.

Sandia National Laboratories is a multi-program laboratory operated by Sandia Corporation, a wholly owned subsidiary of Lockheed Martin Corporation, for the United States Department of Energy's National Nuclear Security Administration under contract DE-AC04-94AL85000.

Atomic- to Pore-Scale Probes and Predictions of Mineral Reactivity

A.G. Stack, J.R.D. Godinho, L.M. Anovitz, G. Rother, A.A. Chialvo, D. J. Wesolowski, E. Mamontov, J.C. Borreguero, P.R.C. Kent, K. C. Littrell (ORNL), J.N. Bracco, S.R. Higgins (WSU), J.E. Stubbs, P.J. Eng, M. Rivers (U. Chicago), P. Fenter, S.S. Lee (ANL)

The overarching goal of the ORNL Geosciences program is to attain a fundamental, quantitative, and ultimately predictive understanding of geofluid speciation, mineral-fluid interfacial equilibria and dynamics, mineral reactivity, and the effect of these properties on the evolution of porous geologic media over wide ranges of temperature, pressure, composition and spatio-temporal scales. This goal is addressed by closely coupling key experimental, characterization and modeling efforts, including: 1) building validated and chemically-realistic atomic-molecular scale descriptions of structures, speciation and equilibria in geofluids and at fluid-mineral interfaces; 2) using new and quantitative dynamic and kinetic models of the processes controlling mineral growth and dissolution; and, 3) developing quantitative descriptions of natural and synthetic porous geologic media that reveal how geochemical equilibria and kinetic processes control their evolution.

In this talk, I will highlight some of our progress towards those goals. Initially I will discuss the criteria one might use to validate an atomistic computational model used to predict mineral surface reactions quantitatively. Such criteria include traditional parameters such as the dissolution free energy (lattice enthalpy), ion hydration energies, and bulk mineral structure, but also new data such as the interfacial structure measured by X-ray Reflectivity, the interfacial dynamics measured by Quasi-Elastic Neutron Scattering, and aqueous ion hydration structure from X-ray/neutron diffraction. A properly calibrated and validated model will reproduce the data from these, but improved functional forms of models are necessary, especially classical molecular dynamics force fields. Once models are calibrated/validated, rare event theories can allow an unprecedented ability to discover reaction mechanisms, and determine rates, equilibrium constants and activation energies for atomic-scale mineral growth and dissolution reactions. An understanding of these mechanisms tightly coupled to experimental measurements will help us to derive models of growth and dissolution that more faithfully portray the processes that actually occur on mineral surfaces. This in turn may lead to enhanced accuracy and improved predictive capacity.

In addition to the above, I will discuss mineral growth and dissolution in porous media, both model compounds and specific rock samples. While this work is in progress, we are using X-ray microtomography and small/ultra small angle neutron scattering coupled to analytical techniques to observe directly changes in pore structure resulting from reaction with aqueous solutions. A combination of methods allows us to measure changes in pore structure over approximately seven orders of magnitude in pore sizes.

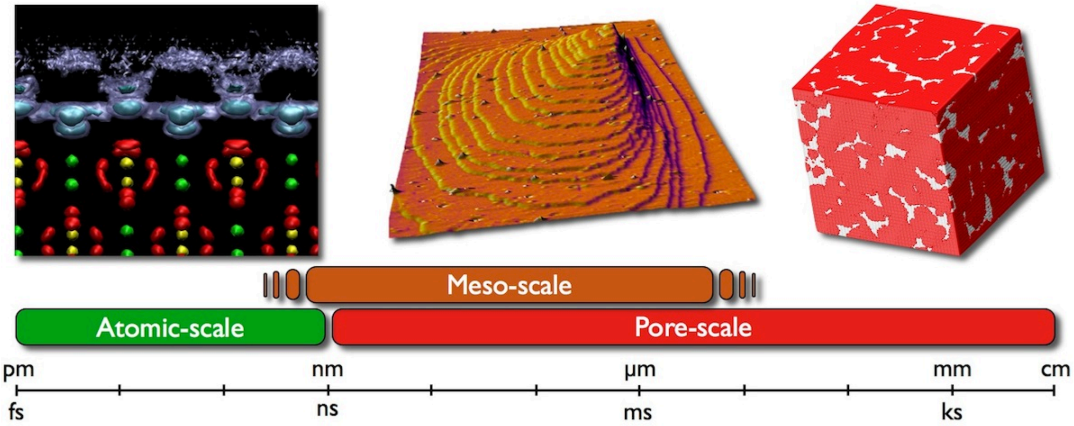

Figure 1: Atomic- to pore-scales of mineral surface structure and reaction.

Recent Publications

1. Anovitz, L. M.; Cole, D. R.; Rother, G.; Allard, L. F.; Jackson, A. J.; Littrell, K. C. Digenetic Changes in Macro- to Nano-Scale Porosity in the St. Peter Sandstone: An (Ultra) Small Angle Neutron Scattering and Backscattered Electron Imagining Analysis. *Geochim. Cosmochim. Acta* **2013**, *102,* 280-305.
2. Bracco, J. N.; Stack, A. G.; Steefel, C. I. Upscaling Calcite Growth Rates from the Mesoscale to the Macroscale. *Environ. Sci. Technol.* **2013**, *47,* 7555-7562.
3. Bracco, J. N.; Grantham, M.; Stack, A. G. Calcite Growth Rates as a Function of Aqueous Calcium-to-Carbonate Ratio, Saturation Index and Strontium Concentration: Insight into the Mechanism of Reaction and Poisoning by Strontium. *Cryst. Growth Des.* **2012** *12,* 3540-3548.
4. Raju, M.; Van Duin, A. C. T.; Fichthorn, K. A. Mechanisms of Oriented Attachment of TiO_2 Nanocrystals in Vacuum and Humid Environments: Reactive Molecular Dynamics. *Nano Lett.* **2014**, Accepted.
5. Parez, S.; Predota, M.; Machesky, M. The Dielectric Properties of Water at Rutile and Graphite Surfaces: Effect of Molecular Structure. *J. Phys. Chem. C* **2014**, Accepted.
6. Stack, A. G.; Gale, J. D.; Raiteri, P. Virtual Probes of Mineral-Water Interfaces: The More Flops, the Better! *Elements* **2013**, *9,* 211-216.
7. Stack, A.G.; Raiteri, P.; Gale, J.D. Accurate Rates of the Complex Mechanisms for Growth and Dissolution of Minerals Using a Combination of Rare Event Theories. *J. Am. Chem. Soc.* **2012**, *134,* 11-14.
8. Wang, H-W.; Anovitz, L. M.; Burg, A.; Cole, D. R.; Allard, L. F.; Jackson, A. J.; Stack, A. G.; Rother, G. Multi-scale Characterization of Pore Evolution in a Combustion Metamorphic Complex, Hatrurim Basin, Israel: Combining (Ultra) Small-Angle Neutron Scattering and Image Analysis. *Geochim. Cosmochim. Acta* **2013**, *121,* 339-362.

Measurements and Conceptual Models of the Reactivity of the World's Smallest Rocks: Bacteriogenic and Abiogenic Nanomineral Aggregates

M.F. Hochella, Jr.[1], J. Xu[1], M. Murayama[1], C. Roco[1], G. Singh[1], N. Qafoku[2]
[1]Department of Geosciences and ICTAS, Virginia Tech; [2]Pacific Northwest National Laboratory

The recognition that nanominerals and amorphous nanoparticles are common and widely distributed in the environment has greatly enhanced our understanding of many physical, chemical, and biological processes on Earth. Among the diverse factors that may affect the inventory of nanoparticles in nature, microorganisms, although being a vital group of contributors, have not been fully appreciated for their role in producing, transforming, and transporting nanoparticles. Nevertheless, the biogeochemical community has learned that bacteria can actively form nanominerals (down to a few nm in size) to enhance cell survival (e.g., magnetotactic bacteria) or passively as a result of cellular metabolism (e.g., sulfate-reducing bacteria). In either scenario, the nanomineral's reactivity *in situ* ultimately determines this material's fate in the environment, which in turn, helps regulate geochemical cycles.

The fundamental-level goal of our project is to study the particle size, crystal structure, surface reactivity, and in-situ structural transformation of bacteriogenic vs. abiogenic nanominerals of metal monosulfides. We also aim to search for potential biosignatures manifested in the physical and reactive characteristics of the bacteriogenic nanominerals through this comparative study. The bacteriogenic nanominerals used in this study are produced by a dissimilatory sulfate-reducing bacterium (dSRB), *Desulfovibrio desulfuricans*, in Zn-amended media. The abiogenic nanominerals are synthesized using a surfactant-based method. Metal monosulfide minerals and dSRB were chosen mainly because of their prevalence in low-temperature geochemical settings and relevance for contaminant geochemistry and environmental toxicology.

Our work is composed of several projects aligned to acheive our primary goal, including: (1) synthesis and characterization of abiogenic ZnS nanoparticles; (2) determination of optimal conditions for bacterial production of ZnS nanoparticles and characterization of the bacteriogenic nanoparticles; (3) investigation of oxidative dissolution mechanisms for both bacteriogenic and abiogenic ZnS nanoparticles; and (4) study of the roles and interplay of sulfate-reducing bacteria and redox-active metal sulfides in uranium sequestration in natural sediments.

Both bacteriogenic and abiogenic ZnS in our experiments are identified as sphalerite nanocrystals based on XRD powder patterns, HR-TEM images, and SAED analyses. The abiogenic nanoparticles (Fig. 1) have a uniform equidimensional shape and size (~5 nm), and in comparison, the bacteriogenic nanoparticles (Fig. 2) display more variation in both shape and size (in a range of 2-8 nm) as well as noticeable structural defects like stacking faults and twinning (Fig. 3a,b). The maximum tolerance of *D. desulfuricans* to Zn^{2+} was determined to be ~40 ppm by evaluating the cell viability using CTC staining coupled with epifluorescence microscopy and flow cytometry. To evaluate the direct role of bacterial cells in nano-ZnS formation, we also synthesized ZnS precipitates using the cell-free metabolite-containing medium. TEM micrographs (Fig. 4) show that these ZnS nanoprecipitates formed aggregates of up to ~50 nm in the absence of bacteria.

Oxidative dissolution experiments of bacteriogenic and abiogenic nano-sphalerite were carried out by submerging the TEM grids with freshly deposited ZnS nanoparticles into aqueous solutions over a range of pH's in stirred beakers open to the air. By observing the average size and shape changes of individual particles as well as electron diffraction using TEM, we were able to estimate the dissolution kinetics and identify secondary products of the oxidation process. Preliminary results show that the dissolution rate was much higher at lower pH and reached a minimum at pH 7 for the abiogenic ZnS. Elemental sulfur was also detected in the proximity of shrinking sphalerite nanoparticles at both pH 3 and 9. The dissolution experiments for bacteriogenic ZnS nanoparticles are being conducted. Besides the oxidation/dissolution mechanisms for each system, we will focus on evaluating the potential differences between the two.

To investigate the roles of sulfate-reducing bacteria and bacteriogenic metal sulfides (i.e., Fe,Cu-sulfide) in uranium sequestration in natural sediments, we conducted flow-through column studies to evaluate the uranium uptake by four different types of bioreduced sediments at the Rifle Site. Based on q-PCR analyses and mineralogical characterization (i.e., XRD and SEM-EDX), we found that LQ 107 and CD sediments were relatively more oxidized and contained significant amounts of Fe-(oxyhydr)oxides, whereas D08 was relatively more reduced and contained abundant SRB as well as biogenic framboidal pyrite. Interestingly, the aqueous chemistry data showed that most U was taken up by the D08 column, and thus, pointed to a positive correlation between U sequestration and the presence of SRB and/or biogenic Fe-sulfide.

Publications:

Veeramani H, Scheinost A, Monsegue N, Qafoku N, Kukkadapu R, Newville M, Lanzirotti A, Pruden A, Murayama M, Hochella MF Jr (2013). Abiotic reductive immobilization of U(VI) by biogenic mackinawite. Environmental Science & Technology, 47 (5), 2361-2369.

Veeramani H, Aruguete D, Monsegue N, Murayama M, Dippon U, Kappler A, Hochella MF Jr (2013). Low-temperature green synthesis of multivalent manganese oxide nanowires. ACS Sustainable Chemistry and Engineering, 1 (9), 1070-1074.

Veeramani H, Xu J, Qafoku N, Singh G, Pruden A, Hochella MF Jr (in submission). The roles and interplay of sulfate-reducing bacteria and redox-active metals sulfides in uranium sequestration in natural sediments. In preparation for submission to Geochimica et Cosmochimica Acta.

Supporting Figures

1&2: Transmission electron micrographs and electron diffraction patterns of abiogenic (1) and bacteriogenic (2) ZnS nanoparticles; 3: Observed structural defects in bacteriogenic ZnS nanoparticles; and 4: transmission electron micrographs for ZnS precipitates in cell-free metabolite-containing media.

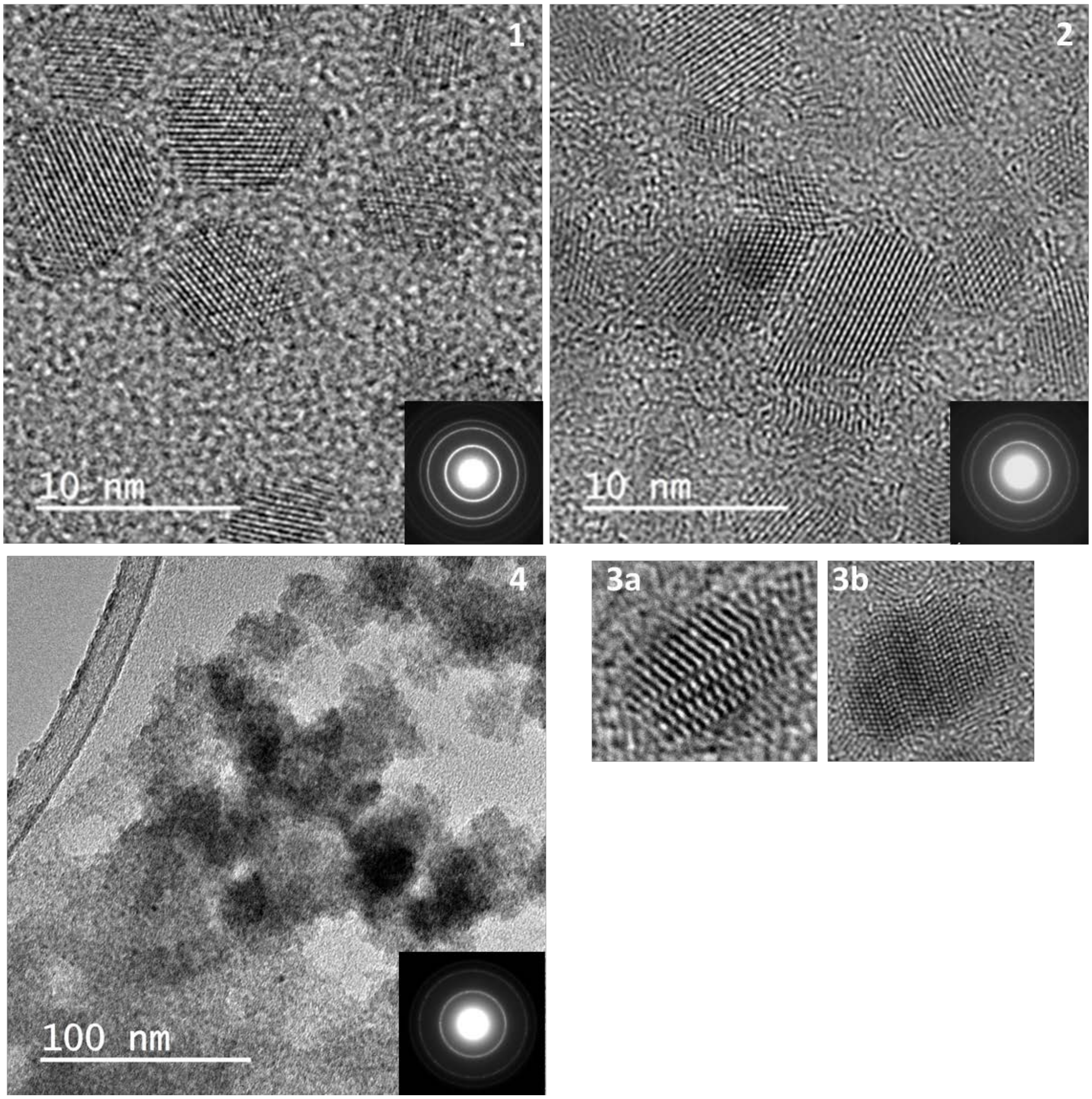

Molecular Mechanisms of Interfacial Reactivity in Near Surface and Extreme Geochemical Environments

A.R. Felmy, J.M. Zachara, A.M. Chaka, J. Loring, and S. Kerisit
Pacific Northwest National Laboratory, Richland, WA

The research program being conducted by scientists at the Pacific Northwest National Laboratory and associated Universities emphasizes the role of electron conduction on mineral transformations, the impact of mineral/water film nucleation and growth on geochemical processes, and the development and application of novel theoretical approaches. Examples of recent advances in these scientific areas will be given that will include: AFM and TEM studies of growth of otavite on surfaces of calcite, the development of *ab inito* thermodynamic models for magnesium carbonate phases, and the role of interfacial processes on mineral transformation in wet supercritical CO_2.

Specific studies designed to unravel the formation of a difficult to form magnesium carbonate phase, magnesite, will also discussed. These studies include long term equilibration studies at high partial pressures of carbon dioxide and the impact of providing seed crystals to enhance nucleation and growth. Research on mineral nucleation and growth will also be described which is driven by differences between surface and bulk temperature, as well as attempts to constrain systems to prevent water from entering the first solvation shell of the reacting cation. The overall presentation will emphasize research results made possible by the use of *In situ* methods that are especially important in unraveling mineral reactivity when the observed ex situ reactivity can change greatly during sample degassing or other changes in conditions. Finally, the use of atom probe tomography (APT) to characterize both the composition and reactivity of mineral phases will be described. The use of APT allows an atom by atom characterization of complex mineral phases in which not only the locations of minor components can be determined but also the presence of hydrated layers within the mineral phase which may represent area of enhanced reactivity relative to the overall bulk material (see Figure 1). This detailed characterization can allow researcher to distinguish differences in reactivity among apparently uniform mineral phases.

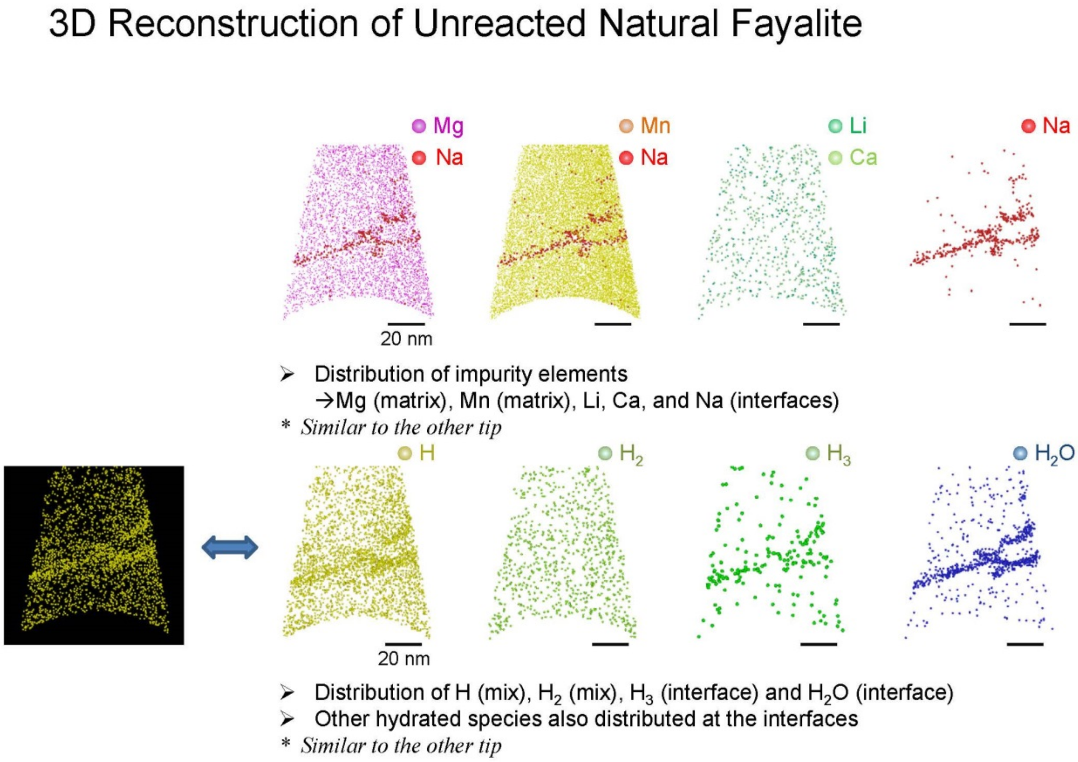
3D Reconstruction of Unreacted Natural Fayalite

- Distribution of impurity elements
  →Mg (matrix), Mn (matrix), Li, Ca, and Na (interfaces)

* *Similar to the other tip*

- Distribution of H (mix), H_2 (mix), H_3 (interface) and H_2O (interface)
- Other hydrated species also distributed at the interfaces

* *Similar to the other tip*

Figure 1. APT analysis of a fayalite sample showing the distribution of trace components, including Na and H_2O, in an apparently pure mineral sample. Reactivity is believed to be enhanced at locations where the water and/or sodium is concentrated.

Stable-isotope probe of nano-scale mineral-fluid redox interactions

Abby Kavner
Department of Earth, Planetary and Space Sciences, University of California Los Angeles

Objectives The goal of this research program is to understand the kinetic isotope effects associated with electrochemistry reactions. The project aims to 1) determine the chemical mechanism(s) responsible for isotope separation during electron transfer (redox reactions) 2) develop a framework to predict the kinetic isotope fractionation arising from simple electrochemical reactions; and 3) perform experimental tests of hypothesized isotope fractionations as a function of temperature and rate in a variety of electrochemical reactions involving Zn, Fe, and Li.

Results Measurements in a wide variety of metal electrochemical deposition systems including Fe, Zn, Li, Mo, and Cu have led to observations of isotope signatures of the electroplated metal compared with the electroplating solution. In all cases, light isotopes are preferentially electroplated, with the extent of fractionation dependent on rate and temperature. We have successfully interpreted our observations in terms of a competition between mass-transport-limited supply of ions to the electrode (which limits the extent of isotope separation) and the chemical kinetics of the deposition reaction (which creates the large electrochemical kinetic isotope effect) [Kavner and Black, 2014]. To help design future experiments, we have revisited our previous derivation of an electrochemical isotope effect based on Marcus theory [Kavner et al., 2005, 2008], which was based on behavior far from equilibrium, and did not deal explicitly with the pre-exponential reaction frequency factor. Our new derivation makes predictions of the expected kinetic isotope effect for single electron transfer reactions as a function of reaction rate and temperature.

J. R. Black, S. G. John, A. Kavner, (2014), Coupled effects of temperature and mass transport on the isotope fractionation of zinc during electroplating, *Geochim. Cosmochim. Acta*, 124, pp. 272-282.

A. Kavner, S. G. John, S. Sass, and E. A. Boyle, (2008), Redox-driven stable isotope fractionation in transition metals: Application to Zn electroplating. *Geochim. Cosmochim. Acta*, 72, pp. 1731-1741.

A. Kavner, A. Shahar, F. Bonet, J. Simon and E. Young, (2005), The isotopic effects of electron transfer: an explanation for Fe isotope fractionation in nature, *Geochim. Cosmochim. Acta,* 69, pp. 2971-2979.

Non-Gassmann Pore-fill Substitution in Heterogeneous Rocks

Gary Mavko, Nishank Saxena, Jack Dvorkin, Amos Nur
Stanford University

Gassmann's equations, introduced more than 60 years ago, continues to provide the foundation for modeling the seismic signatures of fluids in rocks. Aside from a few well-established limitations (e.g., well-connected pore space, low frequency, and low fluid viscosity), Gassmann's predictions depend only on constituent moduli, volume fractions, and the first moment of drained pore space compressibility; i.e., pore space heterogeneity does not enter into Gassmann's equations.

There are many elastic substitution problems that cannot be handled by Gassmann's theory. These include fluid substitution at high frequencies, substitution of solid or highly viscous materials (magma, heavy oil, creeping phases) in the pore space, substitution of one mineral phase for another (replacing feldspar with alteration products, replacement of calcite with dolomite, replacement of clay with kerogen), and chemical changes to the rock frame that accompany a change in pore fluid.

We have found a strategy to estimate the changes in rock elastic moduli when solids (or highly viscous fluids) are added to or removed from the pore space. The method is based on recursive use of the Hashin-Shtrikman bounds. We find that non-Gassmann substitution is inherently non-unique in the usual geophysical context – i.e. starting with initial values of effective elastic moduli, porosity, and composition. The reason is that non-Gassmann substitution depends on details of pore microgeometry that are generally not available. More specifically, solid substitution depends on the spatial variance of the pore space compressibility, in addition to the mean compressibility required by Gassmann.

The new substitution algorithms yields upper and lower bounds on the change in effective bulk and shear moduli upon solid or fluid substitution. The smallest possible change is usually larger than that predicted by Gassmann.

The non-uniqueness can be improved, but not eliminated when both initial bulk and shear moduli are known. We can bound the changes in effective elastic moduli upon substitution, with the lower bound always predicting non-Gassmann substitution better than existing methods.

Rock deformation at submicron scale

Ronaldo I. Borja, Martin Tjioe and Kane C. Bennett
Department of Civil and Environmental Engineering, Stanford University, Stanford, CA 94305

Deformation mechanisms at the grain scale are responsible for producing macroscopic deformations in porous rocks. They include cataclastic flow, dislocation creep, dynamic recrystallization, diffusive mass transfer, and grain boundary sliding, among others. Processes such as carbon sequestration, geothermal energy generation, hydrocarbon extraction, hydraulic fracturing, and mining rely on a solid understanding of these grain-scale mechanisms to better understand the emergent complex behavior. To address the theme of the workshop “Where are the rocks?” we investigate rock deformation at the submicron scale through state-of-the-art imaging and computational modeling. We focus on three dominant grain-scale mechanisms resulting from purely mechanical, isothermal loading: crystal plasticity, micro-fracturing, and creep. Crystal plasticity is assumed to occur as dislocations along the many crystallographic slip planes, whereas micro-fracturing entails slip and frictional sliding on micro-cracks. Creep is a time-dependent process independent of pore pressure transients, and is captured in the mechanistic model by viscoplasticity at the grain scale. To motivate the computational model, we conduct nano-resolution imaging through focused ion beam-scanning electron microscopy (FIB-SEM) and construct a volume representation of rock at submicron scale. We then use nonlinear finite element modeling to: (a) obtain a homogenization and develop the associated bifurcation condition for the grain-scale processes at the next higher scale (mesoscale), and (b) analyze and validate the results of nano-indentation tests on Woodford shale as a boundary-value problem. The oral presentation will cover both the mechanistic model development and submicron scale imaging conducted by our research team.

Rates of Fracture Array Growth and Sealing from a Model for Quartz Cementation and Implications for Fracture Size Scaling

S. E. Laubach,[1] R. H. Lander,[2] J. E. Olson,[3] and P. Eichhubl[1]

[1] Bureau of Economic Geology, The University of Texas at Austin, 10100 Burnet Road, Bldg. 130, Austin, TX 78758 USA, [2] Geocosm and BEG; [3] Department of Petroleum & Geosystems Engineering, The University of Texas at Austin

A new model accounts for crystal growth patterns and internal textures in quartz cement in sandstone fractures, including *massive sealing* deposits, *thin rinds* (or veneers) on open fracture surfaces and *bridge* structures that span otherwise open fractures. High-resolution cathodoluminescence imaging of bridge structures and massive sealing deposits indicates that they form in association with repeated micron-scale fracturing whereas thin rinds do not. Model results indicate that the three morphology types develop in response to (1) the ratio of the rates of quartz growth to fracture opening and (2) the substantially faster growth rate that occurs on non-euhedral surfaces in certain crystallographic orientations. Rind morphologies develop when the fracture opening rate exceeds two times the fastest rate of quartz growth (along the c-axis on non-euhedral surfaces) because growing crystals develop slow-growing euhedral faces. Massive sealing, on the other hand, develops where the net rate of fracture opening is less than half the rate of quartz growth on euhedral faces because all quartz nucleation surfaces along the fracture wall seal the fracture between fracturing events. Bridge structures form at fracture opening rates that are intermediate between the massive sealing and rind cases and are associated with crystallographic orientations that permit growth to span the fracture between fracturing events. Subsequent fractures break the spanned crystal, introducing new, fast-growing non-euhedral nucleation surfaces that grow more rapidly than the euhedral faces of non-spanning crystals. As the ratio of fracture opening to quartz growth rate increases, the proportion of overgrowths that span the fracture decreases and the c-axis orientations for these crystals becomes progressively closer to perpendicular to the fracture wall until the maximum spanning limit is reached. The model also reproduces “stretched crystal”, “radiator structure”, and “elongate blocky” textures in metamorphic quartz veins.

The model replicates a well-characterized quartz bridge from the Cretaceous Travis Peak Formation and reproduces quartz cement abundances, internal textures, and morphologies in the sandstone host rock and fracture zone using the same kinetic parameters while honoring fluid-inclusion and thermal-history constraints. The same fundamental driving forces, in both in the host rock and fracture system, are responsible for quartz cementation with the only significant difference being the creation of new fracture surfaces (non-euhedral surface area) for cases where overgrowths span fractures between fracturing events. Rates of fracture growth and sealing may be inferred from fracture cement textures using model results.

The presentation will describe tests of the model in replicating cement distributions in a wide range of other structural settings. We will also show how cement predictions are being incorporated into geomechanical models and show how modeled feedback between cement precipitation and fracture growth compares to fracture array histories reconstructed using fluid-inclusion assemblages. An interesting result is that the combined structural diagenetic model correctly predicts patterns of fracture size scaling, including the occurrence of both power-law and characteristic aperture size distributions.

Structural Heterogeneities and Paleo Fluid Flow in an Analogue Sandstone Reservoir

Atilla Aydin and David D. Pollard
Stanford University

The overarching goal of this project is to understand the tectonic circumstances and physical processes by which a complex suite of brittle structures can evolve in a sandstone reservoir/aquifer over a long geological time span, and how the resulting fabric of structural heterogeneities can affect fluid flow. The geological field work focuses on the Aztec Sandstone at the Valley of Fire State Park, Nevada. As we enter the final year of this project, we summarize the breadth of the acquired knowledge, the scope of the publications, and the number of graduate students and postdocs trained.

During the last three years, we focused on the distribution and orientation of compaction bands and joints in the Aztec and Navajo sandstones. The field data suggested a strong correlation between the occurrence and orientation of these structures and the orientation and nature of the cross beds in these aeolian sandstones. As part of an effort to understand this correlation, we studied the cross-bed induced strength anisotropy using a mechanical model (Tsai and Wu, 1971) based on a general strength criterion for anisotropic materials. We collected samples of the Aztec Sandstone and determined their stiffness anisotropy in the lab. It turns out the aeolian sandstones are strongly anisotropic as anticipated. However, this anisotropy is variable as a function of other types of heterogeneities in the sandstones. To facilitate fluid flow modeling in dunes with distributed compaction bands in various orientations, we determined porosity and permeability of compaction bands using image- and direct laboratory-based methods and compare and contrast the results from both approaches. This line of research includes actual flow modeling using both the distribution of compaction bands and joints, and their impact on up-scaled permeability.

We utilized the solution of Eshelby for the ellipsoidal inhomogeneous inclusion to study the mechanical behavior of compaction bands and shear-enhanced compaction bands in the Aztec sandstone. Attributes of this solution include: 3D ellipsoidal geometry; appropriate stiffness contrast between band and sandstone based on rock mechanics data; a prescribed remote triaxial stress state based on the tectonic history; a realistic compaction strain within the band based on measured porosity loss, and non-singular stress states along the band tipline. A new propagation criterion is proposed that is consistent with in-plane propagation, but leaves unresolved the micro-mechanical mechanism(s) that operate along the tipline. At the band tip the stress state is triaxial, suggesting that the eigenstrain within the band may not be purely uniaxial, as has been assumed. The result found here is consistent with a shear stress to compressive stress ratio of 1.3, under which shear-enhanced compaction bands are favored. We are developing a 3D discrete element method (DEM) computer code to characterize compaction strain within the band. The new code is able to create models that have similar elastic properties and failure behaviors to those recorded by rock mechanics laboratory testing. We are using the geometric characteristics of ‘wiggly’ compaction bands to constrain the propagation criterion for bands. Our goal is to develop a new capability through improved numerical models to forecast the presence and characteristics of these structural heterogeneities in sandstone reservoirs/aquifers.

Fractures in Rock: Swarms, Scaling & Intersections

Laura J. Pyrak-Nolte,[1,2,3] Eric Boomsma[1], Siyi Shao[1] and Brad Abell[1]

[1]*Department of Physics, Purdue University, West Lafayette, Indiana*
[2]*Department of Earth and Atmospheric Science, Purdue University, West Lafayette, Indiana*
[3]*School of Civil Engineering, Purdue University, West Lafayette, Indiana*

Within the last decade, researchers have worked to deploy nano- and micro-sensors into the subsurface to probe rock formations and the fluids they contain. Sensor mobility is a major challenge for any innovation that relies on the directed transport of nano- or micro- particles into the subsurface. Sensor mobility depends critically on the complexity of the flow paths in the rock, and on the size, shape and functionality of the sensors. A potential method for sensor deployment is the use of sensor swarms, i.e. groups of nano- or micro- sensors that are maintained as a coherent group to enable targeted emplacement into fractures. To control deployment of sensor swarms, a fundamental understanding is required of the physical processes that affect swarm transport.

This presentation covers three areas of research that relate to transport in fractured rock: (1) a scaling relationship between fluid flow and fracture specific stiffness that enables remote identification of the dominant flow paths in fractured rock; (2) global effects on the local behavior of swarms in fractures and (3) the ability to characterize fracture intersections for transport in fracture networks.

Scaling: Fractures with weakly correlated random aperture distributions were used to explore a fundamental scaling relationship between fracture stiffness and fluid flow in a fracture. Three computational methods were used (1) a stratified percolation approach to generate pore-scale fracture void geometry for fractures, (2) a combined conjugate-gradient method and fast-multipole method for determining fracture deformation, and (3) a flow network model for simulating fluid flow, fluid velocity and fluid pressures within a fracture. From this numerical study, fracture specific stiffness was determined to be a surrogate for fracture void area. Fracture specific stiffness captures the deformation of the fracture void geometry that includes both changes in contact area and aperture. The numerical flow-stiffness data, simulated at multiple length scales, was collapsed to a single scaling function that displays two exponential regions above and below the transition into the critical regime. The transition point is governed by the multi-fractal spectrum of stress dependent flow paths. This spectrum reveals that the flow path geometry deforms from a sheet-like topology to a string-like topology. The resulting hydromechanical scaling function provides a link between fluid flow and the seismic response of a fracture, because fracture specific stiffness affects seismic wave attenuation and velocity, which are routinely measured in the field. This relationship provides the first stepping stone for determining the dominant flow path through fractured rock for directing swarms.

Global versus Local Behavior of Swarms: In contrast to emulsions or dispersions, particle swarms are highly localized assemblages containing thousands to millions of particles. As a result of the hydrodynamic interactions among particles, a swarm travels 10x-1000x faster than an individual particle and it exhibits complex behavior. Swarms consisted of soda-lime glass beads (~8μm diameter) mixed in a 2% concentration by mass with the bulk fluid. The distance between the two walls was varied to determine the effect of fracture aperture on swarm behavior. Swarms were observed to travel farther and faster prior to break-up in an optimal aperture range, contrary to traditional Stokelet theoretical methods that predict a monotonic asymptotic increase in velocity with increasing aperture. Experiments that controlled global boundary conditions, along with computational studies with COMSOL, demonstrated that swarms induce global advection currents at finite Reynolds number and in finite geometries. Coupling of the swarms to the global advection currents is affected by fracture aperture and the degree of confinement.

Intersections: The ability to link fracture specific stiffness to fluid flow provides a method for delineating potential pathways for swarm release and control. Although fracture intersections often provide connectivity among fractures and fracture sets, few studies have focused on methods to characterize intersections and the response of intersections to changes in stress. An experimental investigation was performed to determine if distinct elastic-wave modes exist that propagate along fracture intersections. Ultrasonic waves propagated along the intersection between two orthogonal, synthetic fractures in aluminum were compared with waves that were propagated through the bulk and along single fractures as a function of stress. Intersections give rise to several elastic-wave modes not observed for a single fracture. Intersection waves have the potential to provide a new method to monitor fracture intersections and their contribution to transport in rocks.

Geophysical Monitoring of Fluid Invasion

Steve Pride, Greg Newman, Michael Commer, Don Vasco, Seiji Nakagawa, Stephen Breen and Jim Berryman

Lawrence Berkeley National Laboratory

The goal over the next three years (2014 – 2016) for the BES-funded Geophysics Cluster at Lawrence Berkeley National Laboratory (nine scientists in all) is to develop procedures that allow time-lapse geophysical data acquired while fluids are being injected into the Earth to be inverted in order to quantify where the injected fluids go and what they do vis-a-vis fracturing or other alterations to the state of the subsurface. Specific applications are to geothermal systems and CO_2 sequestration among others.

In this presentation, several of our avenues of research are spelled out and initial results acquired over the last six months presented. The overall flow diagram of the inversion scheme is to first model how geophysical properties (specifically, electrical conductivity and seismic properties) are changing due both to fluid substitution effects (e.g., warm and saline brine being replaced by relatively cool and fresh water) and to fluid-pressure-induced deformation and damage. Such altered geophysical properties allow geophysical synthetic data sets to be determined and compared to time-lapse geophysical data. The goal of the inversion is to obtain the initial values of the permeability and porosity that were present prior to fluid injection (i.e., the changes in permeability and porosity through time are being modeled from these initial values) as well as a handful of parameters at each voxel that control how the electrical conductivity and seismic properties change with the hydrogeological or damage fields. As part of this endeavor, we are also performing research into the forward model for how injected fluids move through the subsurface which is non-trival when there are any of 1) saline plumes, 2) immiscible fluids and 3) fluid-induced damage. This project thus requires us to develop: (1) novel forward (hydrogeological) models of the invasion process; (2) models for how changing fluids, changing fluid pressures and changing fracturation alter the geophysical properties; and (3) novel methods for addressing the inverse problem.

The types of invasion problems we aim to model are extensive (immiscible invasion, invasion of fluids with contrasting salinity and temperatures compared to the host rocks, invasion that causes measurable elastic rock deformation and invasion that causes fracture damage). In the presentation, focus is limited to the first fields we have allowed for; namely, the dispersive development of a saline plume caused by injecting a fluid of contrasting salt concentration compared to the native brines along with the associated fluid-induced changes in deformation. Movies of how the geophysical properties are changing will be presented. Our approach to obtaining the Frechet derivatives for the least-squares inverse problem will also be shared. The type of laboratory data we are collecting to constrain our procedures will be presented as well. In future years, the methods being developed will be applied to data collected from actual field sites.

New Measurements of Elasticity in Earth Materials Guiding a New Theoretical Approach

Paul Johnson
Los Alamos National Laboratory

In the last 10 years, application of elastic nonlinear behavior has expanded markedly to imaging in the earth, to medicine and to nondestructive evaluation of materials. Many of these areas rely on the fact that elastic nonlinearity is extremely sensitive to damage—dislocations, cracks, macrocracks—at many scales. We are developing new, sensitive measures of elastic nonlinear behavior and a new theoretical approach in order to ultimately extract the average dimension of the features responsible for bulk nonlinearity, as well as ultimately attempting to quantify damage or crack density from such measures. Such a development would be a significant breakthrough for numerous applications. The new, highly sensitive measurement methods are based on 'Dynamic Acousto Elasticity', where the material is perturbed by a low frequency disturbance and probed with a high frequency, repeating pulse. The theoretical approach under development is an extension of the Arrhenius model.

Publications/Patents

15 Patents in progress or granted in the last 6 years.

Book

Nonlinear Mesoscopic Elasticity: The Complex Behaviour of Rocks and Soil, R. A. Guyer and P.A. Johnson, Wiley-VCH Verlag GmbH Berlin, 410 p. August 2009.

Recent Publications

Haupert, S., J. Rivière, B.E. Anderson, Y. Ohara, T.J. Ulrich, P.A. Johnson, Optimized dynamic acousto-elasticity applied to fatigue damage and stress corrosion cracking. *J. NonDestruct. Eval.*, DOI 10.1007/s10921-014-0231-2 (2014).

Riviere, J., G. Renard, R. Guyer and P. Johnson, Pump and probe waves in dynamic acousto-elasticity: comprehensive description and comparison with nonlinear elastic theories, Journal of Applied Physics 114 (2013) DOI: 10.1063/1.4816395

Renaud, G., J. Riviere, P.Y. Le Bas and P. Johnson, Hysteretic nonlinear elasticity of Berea sandstone at low vibrational strain revealed by dynamic acousto-elastic testing, Geophyscial Research Letters 40, 715-719, doi:10.1002/grl.50150 (2013).

Riviere et al.., Nonlinear ultrasound: potential of the cross-correlation method for osseointegration monitoring, J. Acoust. Soc. Am., 132 EL202-EL207 (2012).

Renaud G., P-Y. Le Bas, and P. Johnson, Dynamic Measures of Elastic Nonlinear (Anelastic) Behavior: Dynamic Acousto-Elasticity Testing (DAET), J. Geophys. Res., B06202, 17 PP. doi:10.1029/2011JB009127 (2012).

Riviere, J., Ulrich, T.J. Haupert, S., Laugier, P. and Johnson, P., Time Reversal Nonlinear Elastic Wave Spectroscopy applied to osseointegration monitoring through two mock models, J. Acoust. Soc. Am., **131** 1922-1927 DOI: 10.1121/1.3683251 (2012).

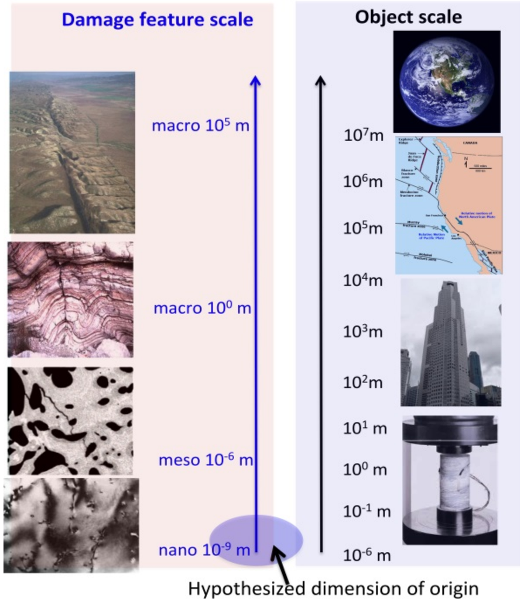

Two scale-lines are shown—(a) the damage feature scale (left) that is responsible for the nonlinear signatures. The feature may be nano-damage at the dimension of dislocation, meso-damage in the form of cracks, macro-damage in the form of large fractures, and mega-damage at the tectonic scale—faults zones. (b) The object scale of the material that hosts the damage—lab samples, buildings, tectonic plates and potentially, the whole earth.

Modeling shale anisotropy based on microstructure, fabric, pore and grain geometry - comparison of simulations with experiments

Hans-Rudolf Wenk, Roman Vasin, and Waruntorn Kanitpanyacharoen
Department of Earth and Planetary Science, University of California, Berkeley

The significance of shales as unconventional hydrocarbon reservoirs, nuclear waste repositories, and geological carbon storage has opened new research frontiers in geophysics. Among many of its unique physical properties, elastic anisotropy has long been investigated by both experimental and computational approaches. Here we present results for two classical examples where elastic properties have been determined experimentally, Kimmeridge shale from the North Sea and Cretaceous Muderong Shale from Australia. We compare experimental data with modeling results based on self-consistent averaging using microstructural information. The microstructure is quantified with TEM, SEM, X-ray microtomography. Of particular importance is crystallographic preferred orientation distributions of phyllosilicate minerals that are based on synchrotron X-ray diffraction experiments and the volume fraction and shape of pores. Preferred orientation is very strong, with alignment of up to 6 multiples of a random distribution and this is the main contribution to seismic anisotropy. Model results compare satisfactorily with values derived from ultrasonic velocity measurements, confirming the validity and reliability of our approximations and averaging approach. Major uncertainties on the modeling side are single crystal elastic properties as well as quantitative assessments of pore distributions. On the experimental side multiple path methods may better constrain elastic properties and we are preparing for a similar study on a shale sample where acoustic velocities are measured on spheres.

Rheological description of mantle rocks: Comprehensive in situ analysis of mantle minerals deforming at high pressure

N. A. Dixon[1], W. B. Durham[1], D. L. Kohlstedt[2], S. Mei[2], J. Homburg[2]
[1]*Massachusetts Institute of Technology, Cambridge, MA 02139*
[2]*University of Minnesota, Minneapolis, MN 55455*

Unresolved issues in geodynamics demand a better understanding of the bulk mechanical properties of mantle minerals, as well as careful analysis of the complex lattice-scale physics behind these properties. The continuing improvement of synchrotron x-ray diffraction techniques used in conjunction with the D-DIA apparatus now offers unprecedented richness of data for each experiment and allows a new approach to rheological experiments. Instead of probing the mechanical properties of a material by testing the relationship between “bulk” stress and strain rate in a sample at a variety of conditions (varying P, T, water content, and other environmental variables), synchrotron x-ray diffraction now allows us to observe, in situ, the active deformation physics in much greater detail. This approach includes in-situ monitoring of plastic anisotropy and local stress heterogeneity, grain size, the development of lattice-preferred orientation (LPO), and even the partitioning of stress between multiple phases in the same polycrystalline sample. Here, we present results obtained with the use of the *MTEX* toolbox for Matlab and energy-dispersive x-ray diffraction, showing the in-situ development of LPO in deforming dry San Carlos olivine samples, at pressures from 2 to 7 GPa. These measurements hint at the active dislocation mechanisms for these conditions. The ability generate a broad range of mantle conditions in the D-DIA, while precisely measuring the structure and conditions within our sample at the grain and lattice scale, demonstrates the promising future of deformation experiments as a means to understanding the evolution of the deep Earth.

In search of processes driving clumped-isotope (dis)equilibrium in geoscience systems: New insights from data and theory

Aradhna Tripati
University of California, Los Angeles

Over the last decade, the clumped isotope thermometer has emerged as a tool used throughout the geosciences to study the temperature history of surface and subsurface environments. It is based on measurements of the proportion of ^{13}C and ^{18}O isotopes bound to each other within carbonate minerals in $^{13}C^{18}O^{16}O_2$ groups (heavy isotope "clumps"). However, although most geothermometry implicitly presumes carbonate crystals have attained lattice equilibrium (i.e., independent of solution chemistry), several non-temperature factors may influence mineral isotopic signatures. Therefore it is important to develop a realistic assessment of the uncertainties associated with the application of this temperature proxy and to understand the potential influence of other variables such as pH and growth rate. Therefore we are using a combination of experimental and theoretical approaches to study the processes controlling clumped isotope signatures in minerals. Specifically, we are using precipitation experiments to determine ^{13}C-^{18}O bond abundances of CO_3^{2-} and HCO_3^- molecules at a nominal temperature-dependent equilibrium. We are using *ab initio* cluster models based on density functional theory to predict equilibrium as a function of temperature in ^{13}C-^{18}O bond abundances of different DIC species and carbonate minerals. Additionally, we are exploring the effects of pH, salinity, precipitation rate, and enzymatic activity on clumped isotope signatures in minerals. We are determining acid digestion fractionation factors for different carbonates, including witherite, calcite, dolomite, and siderite. Finally, we are comparing results from experiments and theory to geological samples. For example, we have measured samples that may have attained lattice equilibrium from the slow-growing Devils Hole vein calcite in Nevada, as well as deep-sea corals of differing mineralogy. These geological materials are carbonates with some of the slowest growth rates that have been documented. Data for these and other geological samples allow us to test the conceptual framework that is emerging for interpreting clumped isotope data in geological systems based on theory and experiments, and identify specific processes that need to be explored further.

Quartz Cements and Basin Evolution: Illinois Basin and Wisconsin Arch

John W Valley, Anthony D Pollington, Ayumi Hyodo, Reinhard Kozdon

Department of Geoscience, University of Wisconsin, Madison, WI 53706

The thermal, mechanical, and chemical evolution of a sedimentary basin exerts important controls on porosity and permeability of reservoir rocks. Oxygen isotope ratios of individual diagenetic cements record evidence of this history, but cannot be accurately analyzed by conventional techniques. Recent improvements for in situ analysis by ion microprobe provide high precision and accuracy at 3–10 µm-scale. In combination with cathodoluminescence imaging, in situ analysis of δ^{18}O(quartz) from the Cambrian Mt. Simon Sandstone and overlying Eau Claire Shale in the Illinois Basin reveals gradients *within* single overgrowths of as much as 7.7‰/50 µm (1). While the inner portions of overgrowths remain approximately constant in δ^{18}O across the basin, the δ^{18}O of the rim becomes lower with depth. These data suggest that overgrowths formed during burial and heating, possibly with minimal changes in δ^{18}O of pore fluids. A majority of analyzed healed microfractures cutting detrital grains have low δ^{18}O and formed in the pre-sedimentary parent rocks. Thus the percentage of these fractures does not provide an estimate of burial depth. In contrast to the Illinois Basin, samples of sandstone and shale from the Wisconsin Arch have not been buried deeply (< 1 km), overgrowths are not zoned in δ^{18}O, and quartz cementation was at low T (< 40°C). In the Illinois Basin, both δ^{18}O and δ^{30}Si of quartz are consistent with local derivation of silica, largely from pressure solution of originally igneous detrital quartz. If δ^{18}O (H_2O) = -3‰, the highest temperature calculated for the rim of an overgrowth is 107ºC at a paleo-depth of 3.5 km. The variability both in average δ^{18}O of overgrowths and zoning patterns from individual overgrowths correspond with a geotherm of 30ºC/km. Thus there is no evidence of quartz precipitation from higher temperature hydrothermal fluid events, and quartz overgrowths likely formed over a period of 100-200 million years synchronous with deposition in the basin.

(1) Anthony D. Pollington, Reinhard Kozdon, and John W. Valley (2011) Evolution of quartz cementation during burial of the Cambrian Mt. Simon Sandstone, Illinois Basin: In situ microanalysis of δ^{18}O. Geology accepted.

Kinetic isotope fractionation during mineral growth and fluid phase transport

D. J. DePaolo, J. N. Christensen, B.M. Kennedy, M.E. Conrad, Ian Bourg

Lawrence Berkeley National Laboratory, Berkeley, CA 94720

Differences in mass between isotopic molecular and atomic species lead to differences in isotopic composition due to both equilibrium partitioning and non-equilibrium chemical processes. These isotopic differences, as well as variations in trace element concentrations, are used extensively to infer conditions of formation of natural minerals. Because non-equilibrium effects are poorly described by existing theories, equilibrium is generally assumed for data interpretation even though it is unlikely to apply. We are focused on developing the theory and the necessary experimental validation to produce better models for isotopic and trace element fractionation produced by combined equilibrium and kinetic effects during mineral growth and chemical transport. Kinetic isotope effects also function as a unique probe of microscopic mineral surface processes and fluid phase reactions. The focus on kinetic fractionation is stimulated by the growing body of data on isotopic fractionation of metals such as Li, Mg, Si, K, Ca, Mo, Fe, Sr, and U. The link between isotopes and trace impurity constituents is useful because the latter can typically be measured with higher spatial resolution.

Our theoretical work on isotopic and trace element fractionation during mineral precipitation was initially based on Ca isotopes in calcite (DePaolo, *GCA*, 2011; Nielsen et al., *GCA*, 2012, 2013). Fractionation due to ion desolvation was also investigated using MD simulations (Hofmann et al., *PNAS*, 2012). This work is now being extended with new calcite precipitation experiments (Watkins et al., 2013; 2014 in review), which are allowing us to assess the effects of ionic strength, and extend the treatment to O isotopes, and eventually also C isotopes and clumped isotopes. We have demonstrated that O isotope ratios of calcite precipitated at 5-25°C at near-neutral pH are subject to kinetic fractionation effects of 1-2 per mil, corresponding to 4-8°C differences in inferred temperature. Larger kinetic fractionation effects are predicted at high pH. Establishing equilibrium isotopic fractionation factors is a challenge for all elements; and appears to require study of natural systems where mineral growth rates are extremely slow.

Measurements of natural systems are important not only because they access a much greater range of time and length scales, but because they usually provide evidence of other controls on fractionation. To interrogate other sources of kinetic fractionation we have made measurements of Ca and K isotopes in vascular plants, Ca in an alkaline lake, hydrothermal calcite, and most recently serpentinized peridotite and associated alkaline springs and travertine. The alkaline lake results partially confirm that Ca isotope fractionation is affected by the $Ca^{2+}:CO_3^{2-}$ ratio of water. Hydrothermal calcites and epidote appear to have kinetic Ca isotope effects, but somewhat smaller than low-temperature calcite.

[*] The title of the project is “Integrated isotopic studies of geochemical processes.” The grant supports radiogenic, stable, and noble gas isotopic studies. BES provides core support for labs involving 2 TIMS, 2 Noble gas and 2 stable isotope mass spectrometers, and an MC-ICPMS.

NMR Spectroscopy of Aqueous Solutions to 2.0 GPa

W. H. Casey[1,2], Brent Pautler[1], Chris Colla[2], Rene Johnson[1], Steve Harley[3] and Peter Klavins[4]

[1]Dept. of Chemistry, University of California, Davis. CA, 95616 , [2]Department of Earth and Planetary Sciences, University of California, Davis, One Shields Ave, Davis California 95616
[3]Lawrence Livermore National Laboratory, 7000 East Avenue, Livermore, California 94550
[4]Dept. of Physics, University of California. Davis. CA, 95616

Understanding the chemistry of high-pressure aqueous solutions, and making useful predictions, is essential to geochemist, and we have compiled data and built models for predicting solution chemistry to 5 kbars and several hundreds of degrees Celsius. These extrapolations have been limited by measurements of the dielectric constant of water, which was recently extended to 60 kbars via molecular-dynamic simulations [1, 2]. What the models cannot do is identify new species or estimate reaction kinetics at extreme conditions. For this reason we have designed a simple NMR probe that can be used at crustal pressures.

The probe design is based upon a microcoil [Fig. 1] that contains a sealed PEEK tube containing 20-40 μl of solution and is calibrated to work up to 20 kbars of pressure. The entire apparatus costs only about $20,000 and can be used by any geochemist in a standard wide-bore NMR magnet. The design allows for single- or two-nuclei NMR spectroscopy and temperature is controlled via a circulating fluid. The coil passes through tungsten-carbide and berylco cylinders to a standard radio-frequency circuit that is designed for the specific nucleus. Pressure is measured by the fluorescence of a ruby chip glued to an *in situ* fiberoptic cable and is highly reproducible. With this design one can measure equilibrium constants, rates of reactions, diffusion coefficients and identify new aqueous complexes from the NMR resonances [Fig. 2] at pressures to 20 kbars.

References Cited

1. Sverjensky, D.A., B. Harrison, and D. Azzolini, *Water in the deep Earth: The dielectric constant and the solubilities of quartz and corundum to 60 kbars and 1200°C.* Geochimica et Cosmochimica Acta, 2014. **129**(0): p. 125-145.
2. Pan, D., et al., *Dielectric properties of water under extreme conditions and transport of carbonates in the deep Earth.* Proceedings of the National Academy of Sciences, 2013. **110**(17): p. 6646-6650.

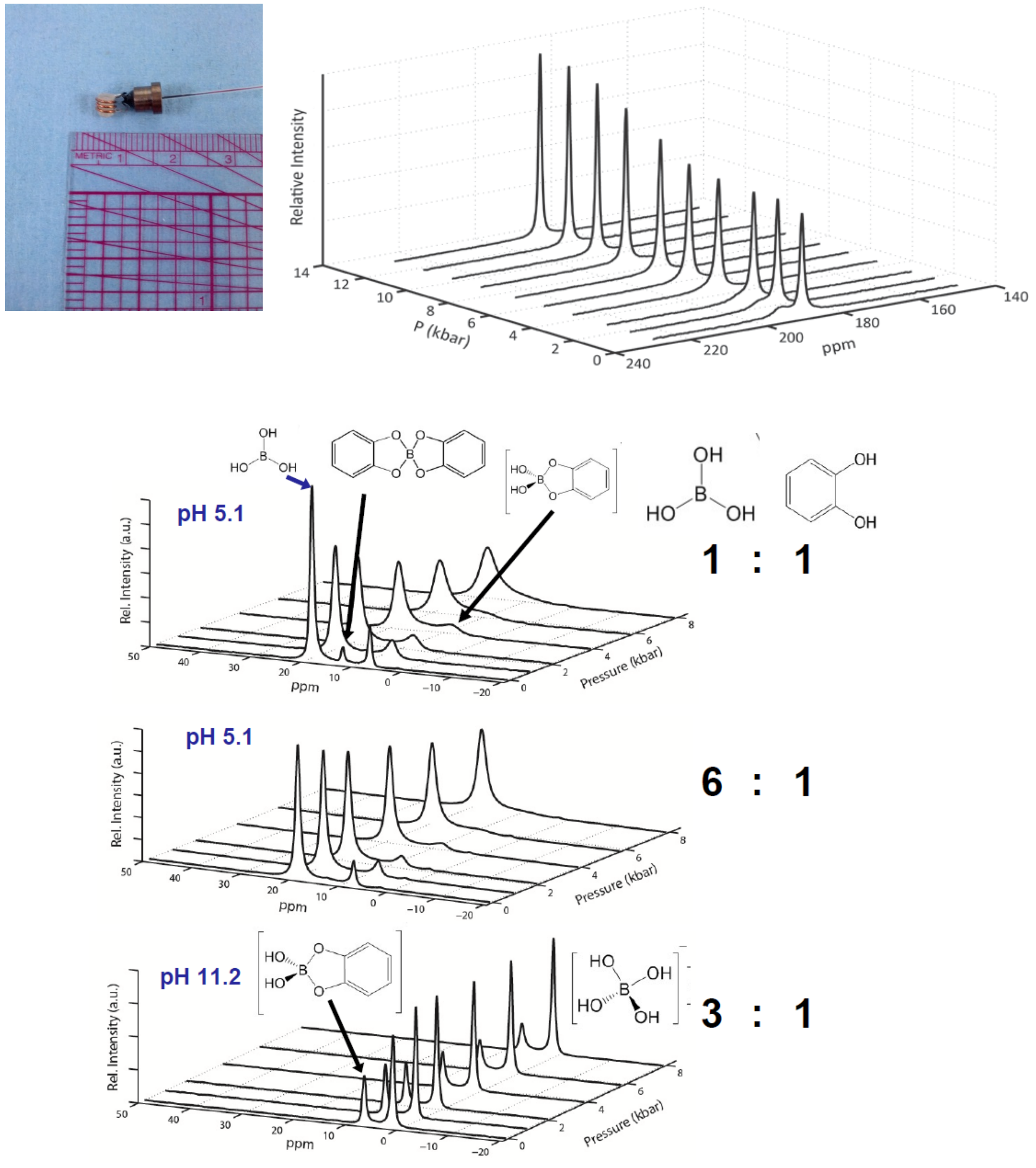

Figure:(**top left**) A 20-40 microliter sample and microcoil is all that is needed to collect NMR spectra to 20 kbars at temperatures to 100°C (**top right**) ^{11}B-NMR spectra for a 0.1 M sodium borate solution to 12 kbars. The narrowing and growth of the central peak corresponds to oligomers dissociating as pressure increases to 12 kbars. (**bottom three figures**) Boron changes coordination from three- to four-coordination to oxygens as pressure increases and boron-diol species form. At pH=5.1, the ^{11}B sites reach rapid-exchange equilibrium as pressure is increased to 8 kbars at 40°C. At pH=11, rates of site exchange remain slow with pressure and the peaks remain distinct.

In situ transformation of amorphous calcium carbonate (ACC): Structural and compositional changes

Richard J. Reeder and Brian L. Phillips
Stony Brook University

Overall goals of our research program include development of structure-stability relationships for different types of amorphous calcium carbonate (ACC) and identification of structural changes associated with transformation to crystalline calcium carbonate. Our focus has been on model systems that have application to initial stages of calcium carbonate precipitation in terrestrial and marine systems, both inorganic and biogenic. These studies are intended to provide a structural basis for understanding and predicting reactivity of ACC in different environments and in applications related to CO_2 sequestration. We have also studied natural ACC for comparison with model systems. Our experimental approach has utilized synchrotron-based X-ray total scattering and X-ray absorption spectroscopy in combination with ^1H and ^{13}C NMR spectroscopic methods to assess short- and medium-range structure in ACC. These methods have allowed characterization of structural changes resulting from dehydration and transformation of ACC to crystalline phases.

Our most recent work has been focused in two closely related areas: (1) structural consequences of dehydration of ACC and its relation to crystallization, and (2) *in situ* studies of ACC crystallization, assessing both kinetics and the influence of environmental factors. The most useful approach was found to combine *in situ* and *ex situ* experiments using total X-ray scattering and NMR techniques to examine rates and pathways for crystallization of ACC synthesized by three different methods. The samples studied differ mainly in their hydrous components, and ^1H NMR was found to be valuable in distinguishing hydrous components. Thermal treatment was used to control hydration state

Hydrous components, including structural H_2O and in some instances OH^-, are present in biogenic and synthetic amorphous calcium carbonate (ACC) in variable amounts depending on the conditions of formation. These hydrous components can be differentiated on the basis of NMR data, and are found to include translationally rigid structural H_2O, restrictedly mobile H_2O, fluid-like H_2O, and OH^-. ACC samples that differ in their hydrous components also exhibit differences in stability and transformation behavior, as well as differences in crystallization temperature with heating.

Thermal treatment was used to create ACC samples over a range of hydration states, quantified using TGA-DSC. Only subtle changes were observed in total X-ray scattering and pair distribution function (PDF) analysis over a wide range of hydration states. NMR results show that different populations of hydrous components are lost as a result of thermal treatment of fresh ACC. Samples exhibit different transformation behaviors with heating depending on hydration state, as well as synthesis method. In view of the minimal differences observed in PDFs, the structural roles of different types of hydrous components appear to be the main factors that control transformation behavior of ACC.

In situ transformation studies were conducted using synchrotron X-ray total scattering. Crystallization kinetics and pathways were found to vary according to synthesis method, corresponding to different populations of hydrous components as determined by NMR. Depending on synthesis method, initial crystalline product was either calcite or a coeval mixture of calcite and vaterite. Transformation kinetics were also found to differ with solution composition. Crystallization rates were lower in calcite-saturated solution compared to deionized water, as would be expected.

The results demonstrate that variations in the amount and types of hydrous component of ACC influence the stability and transformation behavior of amorphous calcium carbonate. Furthermore, the detailed insight to these structural aspects contributes to the basis for modifying ACC to control its behavior in environmental and engineered environments.

NMR and Computational Modeling of Clay-Organic Composites with H_2O and CO_2 Fluids

R. James Kirkpatrick,[1] Geoffrey M. Bowers,[2] A. Ozgur Yazaydin,[3] Marimuthu Krishnan,[3] Moumita Saharay,[3] Brennan O. Ferguson,[2] David W. Hoyt,[4] Sarah D. Burton,[4] Tamas Varga.[4]

[1]College of Natural Science, Michigan State University, East Lansing, MI 48824, [2]Division of Chemistry, Alfred University, 1 Saxon Drive, Alfred, New York 14802, [3]Department of Chemistry, Michigan State University, East Lansing, MI 48824, [4]William R. Wiley Environmental Molecular Sciences Laboratory, Pacific Northwest National Laboratory, Richland, WA 99305

The interaction of organic matter (OM) with mineral surfaces plays an important role in controlling the binding and transport of naturally occurring and anthropogenic organic and inorganic species in the earth's near-surface environment and may also play a similar role in deeper geological conditions related to sequestration of CO_2. We present here the results of experimental NMR and computational molecular dynamics (MD) studies of OM-clay (hectorite) composites that provide significant new molecular scale insight into how OM interacts with mineral surfaces and how this interaction affects the behavior of cations, H_2O, and CO_2 near the interface. Variable temperature ^{23}Na and ^{43}Ca NMR data for hectorite-NOM composites synthesized using Suwannee River natural organic matter (NOM) and its humic acid (HA) and fulvic acid (FA) fractions obtained at atmospheric pressure show that the two cations behave quite differently. For samples equilibrated at 43% R.H. and as pastes, ^{43}Ca yields only one resolvable resonance for proximity restricted Ca^{2+} that becomes progressively more shielded (more negative chemical shift) and loses intensity with increasing temperature. The loss of signal intensity is due to dynamical processes in the 10 - 100 kHz range. The paste sample also shows dynamical line narrowing with increasing temperature. The ^{23}Na spectra at 43% R.H. show one resonance for proximity restricted Na^+ that loses intensity with increasing temperature due to dynamical processes. In contrast, there are two resonances for the paste samples. One is similar that of the 43% R.H. sample and represents proximity restricted Na^+. The other has very narrow peaks due to solution-like mobility near room temperature but broadens continuously with decreasing temperature. This resonance is similar to that for the clay without OM and less tightly bound Na^+. MD simulations of hydrated Na-hectorite-OM composites modeled at near-neutral pHs (only carboxylic groups deprotonated) show that hydrated Na^+ bridges the OM molecules and the clay surface through the carboxylic groups and that the Na^+ is mobile, as for the clay without OM. ^{13}C and ^{23}Na NMR spectra for 43% R.H. Na-hectorite and a Na-hectorite-humic acid composite obtained at 90 bars CO_2 pressure and 50^oC show that supercritical CO_2 interacts more strongly with the composite than with the base clay and that it enters the interlayer galleries of both samples. ^{13}C NMR shows that the CO_2 does not react to form carbonate species. The CO_2 causes increased ^{23}Na signal intensity, reduced peak widths, more rapid T_1 relaxation rates, and more positive chemical shifts. The effects are greater for the composite than the base clay. We interpret these changes to be due to supercritical CO_2 increasing the rate of Na^+ site hopping, as also shown in MD simulations for hectorite-polymer (PEG) composites containing CO_2 under supercritical conditions. The MD simulations provide a detailed picture of the effects of nano-confinement on polymer structure and show that the local (nearest molecular neighbor) structure of CO_2 in clay-organic systems is similar to that of crystalline CO_2 and thus that the dry ice structure is a useful reference structure the way water ice is for H_2O.

Investigating the Physical Basis of Biomineralization

Patricia M. Dove[1], James J. De Yoreo[2] and Anthony .J. Giuffre[1]

[1]Department of Geosciences, Virginia Tech, [2]Physical Sciences Division, Pacific Northwest National Laboratory

During the process of biomineralization, living organisms use macromolecules to direct the nucleation and growth of organic-mineral composite materials. Over geologic time, biologically-directed mineral formation has facilitated carbon sequestration in the form of carbonate sediments. The products of biomineralization are preserved in the rock record and chronicle the interplay of biota and environment. Attempts to use the fossil record as an indicator of paleoenvironments require a fundamental understanding of the physical and chemical controls on biomineral formation. In addition, this understanding will allow us to harness the ability of organisms to form structures with complex topologies, hierarchical design, and unique materials properties. Moreover, this knowledge is critical to the goal of artificially sequestering carbon as well as developing new strategies towards synthesis of novel materials for applications to diverse technologies.

This project uses quantitative molecular-scale techniques to explore calcium carbonate mineralization. In particular, we are investigating how biomolecular interactions alter calcite nucleation barriers, kinetics, polymorph selection (Wang et al., 2012), and impurity and isotope incorporation (Han et al., 2013; Blue et al., in review; Giuffre et al., in prep B). Our studies are revealing the importance of cooperative restructuring of both the organic and mineralizing constituents during template-driven nucleation, and we are further developing in situ TEM methods that we pioneered through support from this project to understand particle mediated growth processes in both calcium carbonate and iron oxide systems. Our objective is to develop a comprehensive picture of the physics and chemistry underlying the controls exerted through the interconnected matrix-mineral-solvent interactions over calcium carbonate, silica and iron oxide nucleation.

During this project period, we are pursuing four questions: (1) biomolecular controls on heterogeneous and cooperative nucleation (Giuffre et al., 2013, *PNAS;* Giuffre et al., in prep A); (2) matrix-controlled patterning at substrates (Hamm et al., 2014, *PNAS*), (3) the interplay of substrates and simple model tissues during nucleation (in progress) and (4) the mechanisms and controls on particle mediated crystallization (Hu et al., 2012; De Yoreo, 2013; more in progress). These studies are using in situ AFM and optical measurements of nucleation rates in confinement and on model organic matrices, dynamic force spectroscopy measurements of crystal-crystal and crystal-substrate binding free energies, in situ transmission electron microscopy investigations of nucleation, nanoparticle aggregation and fusion during oriented nanoparticle attachment. In new work, we are also testing the theories that describe the role of confinement — a common feature in mineralizing environments — over the barriers to nucleation. We are also working toward a quantitative description of particle mediated mineral growth based on in situ molecular scale observations.

Selected Publications from this Project

Blue, C., and P.M. Dove (in review) Chemical controls on the magnesium content of amorphous calcium carbonate. *Geochimica et Cosmochimica Acta*.

De Yoreo JJ. 2013. Nucleation: More than one pathway. *Nature Materials* 12:284.

Giuffre, A.J., L.M. Hamm, J.J. De Yoreo, P.M. Dove (2013) Polysaccharide chemistry regulates kinetics of calcite nucleation through competition of interfacial forces. *Proceedings of the National Academy of Sciences*.

Giuffre, A.J., A. Gagnon, J.J. De Yoreo, P.M. Dove (in prep.) Deciphering the pathway to crystallization of amorphous calcium carbonate using isotope tracers. *Geochimica Cosmochimica Acta*.

Hamm, L.M., Giuffre, A.J., Han, N., J.J. De Yoreo, P.M. Dove (2014) Reconciling disparate views of template-directed nucleation through measurement of calcite nucleation kinetics and binding energies. *Proceedings of the National Academy of Sciences*. 111:1304-1309.

Han, N., C.R. Blue, J.J. De Yoreo, P.M. Dove (2013) The effect of carboxylates on the Mg content of calcites that transform from ACC. *Water-Rock International.*

Hu, Q., Nielsen, M.H., Freeman, C.L., Hamm, L.M., Tao, J., Lee, J.R.I, Han, T.Y.J., Becker, U., Harding, J.H., Dove, P.M., De Yoreo, J.J. (2012) The thermodynamics of calcite nucleation at organic interfaces: Classical vs. non-classical pathways. *Faraday Discussion: Biological Crystallization*, 159, 509-523.

Wang, D., T. Echigo, A.J. Giuffre, L.M. Hamm, J.D. Rimstidt, J.J. De Yoreo, J. Grotzinger, P.M. Dove (2012) Revisiting geochemical controls on patterns of carbonate deposition through the lens of multiple pathways to mineralization. *Faraday Discussion: Biological Crystallization*, **159**, 371-386.

Unexpected crystal structures in biominerals

Ross T. DeVol[1], Claire B. Salling[1], Adam Z. Blonsky[1], Christopher E. Killian[1], Lee Kabalah-Amitai[2], Boaz Pokroy[2], Assaf Gal[3], Steve Weiner[3], Lia Addadi[3], Pupa U. P. A. Gilbert[1]

[1]University of Wisconsin - Madison, USA; [2]Technion-Israel Institute of Technology, Haifa, Israel; [3]Weizmann Institute of Science, Rehovot, Israel

In this talk we will show compelling evidence for unexpected $CaCO_3$ structures formed by living organisms, including double-crystalline structures, crystal lattice tilting, and particle-mediated crystal formation, which is not alternative but occurs in combination with classical ion-by-ion growth from solution. The double-structure of vaterite could only be revealed because the tunicate *Herdmania momus* makes the largest and most perfect crystals of vaterite ever observed (1). In mollusk shells we observed tilting of the crystal lattice. In a geologic crystal tilting of the crystal lattice would produce a curved crystal habit, but in columnar nacre the morphology of the aragonite tablets does not change, it is only the crystal lattice that tilts (2), as revealed by Polarization-dependent Imaging Contrast (PIC) mapping (3) at the mesoscale (10nm-10µm). In the prismatic outer layer of mollusk shells, calcite crystal lattice tilts over a larger scale, on the order of 100µm, hence it needed a micro-diffraction experiment to be revealed (4). Finally, diverse fresh, forming biominerals such as sea urchin spicules (5), mollusk shell calcite prisms, and aragonite nacre tablets all reveal morphology and composition patterns that are only consistent with concomitant particle-mediated and ion-by-ion crystal formation mechanisms, occurring nearly simultaneously (6).

PUBLICATIONS

1. L Kabalah-Amitai, B Mayzel, Y Kauffmann, AN Fitch, L Bloch, PUPA Gilbert, B Pokroy. *Vaterite crystals contain two interspersed crystal sructures*. Science **340**, 454, **2013**.
2. IC Olson, AZ Blonsky, N Tamura, M Kunz, PUPA Gilbert. *Crystal nucleation and near-epitaxial growth in nacre*. J Struct Biol **184**, 454, **2013. JOURNAL COVER**.
3. PUPA Gilbert. *Polarization-dependent Imaging Contrast (PIC) mapping reveals nanocrystal orientation patterns in carbonate biominerals*. J Electr Spectrosc Rel Phenom, special issue on Photoelectron microscopy, Time-resolved pump-probe PES **185**, 395, **2012**.
4. IC Olson, RA Metzler, N Tamura, M Kunz, CE Killian, PUPA Gilbert. *Crystal lattice tilting in prismatic calcite*. J Struct Biol **183**, 180, **2013**.
5. YUT Gong, CE Killian, IC Olson, NP Appathurai, AL Amasino, MC Martin, LJ Holt, FH Wilt, PUPA Gilbert. *Phase transitions in biogenic amorphous calcium carbonate*. Proc Natl Acad Sci USA **109**, 6088, **2012**.
6. A Gal, K Kahil, N Vidavsky, RT DeVol, PUPA Gilbert, P Fratzl, S Weiner, L Addadi. *Particle accretion mechanism underlies biological crystal growth from an amorphous precursor phase*. submitted, **2014**.

How should we interpret the carbon isotope composition of terrestrial rocks? Insight from controlled plant-growth experiments

A. Hope Jahren[1] and Brian A. Schubert[2]

[1]*University of Hawaii, SOEST, Honolulu, HI 96822, USA*
[2]*University of Louisiana at Lafayette, School of Geosciences, Lafayette, LA 70504, USA*

Changes in the carbon isotope composition ($\delta^{13}C$) of terrestrial substrates have been widely observed throughout the geologic record and often coincide with critical transitions such as the Permian-Triassic, the Cretaceous-Tertiary and the Paleocene-Eocene, to name a few. Upon quantification, such changes have been variously interpreted, usually invoking any one of the myriad ways in which the environment exerts control over plant biology. Many environmental parameters have been demonstrated to influence the $\delta^{13}C$ value of plant tissue, using both empirical fieldwork and controlled laboratory experiments. Changes in soil moisture availability and associated water-use efficiency give rise to per-mil scale changes in carbon isotope composition of leaves. Species-to-species variability in $\delta^{13}C$ value is often cited, as differing proportions of plant lipids (especially) may lead to per-mil scale differences between major groups (e.g., angiosperms vs. gymnosperms). This has led several researchers to suggest that perturbations in the carbon isotope record within terrestrial sediments may be interpreted as a change in environmental water availability, or a change in biome distributions, respectively. Atmospheric carbon dioxide is the primary carbon source for photosynthesis and pCO_2 level has been shown to influence multiple aspects of plant functioning, leading workers to hypothesize as early as 1960 that there could be a direct influence of pCO_2 upon the net carbon isotope fractionation between plants and the atmosphere ($\Delta\delta^{13}C$). However, prior to our controlled growth experiments, the magnitude of this response was uncertain. We report here upon multiple growth experiments involving both C_3 and C_4 plants that have quantified the relationship between pCO_2 and $\Delta\delta^{13}C$ across the levels of atmospheric pCO_2 hypothesized for the entire Phanerozoic using previous proxies. Our work has revealed an increase in $\Delta\delta^{13}C$ value within increasing pCO_2 (see Figure), which is quite different for C_3 and C_4 plants reflecting the different role of respiration between the two photosynthetic types. Upon the strength of these relationships, we suggest that changes in the $\delta^{13}C$ of terrestrial organic matter during periods of known carbon cycle disruption are best interpreted as resulting from changes in atmospheric pCO_2. We discuss our ongoing work to further quantify this relationship and describe its mechanism, such that it may be useful as a new terrestrial proxy for ancient pCO_2 levels.

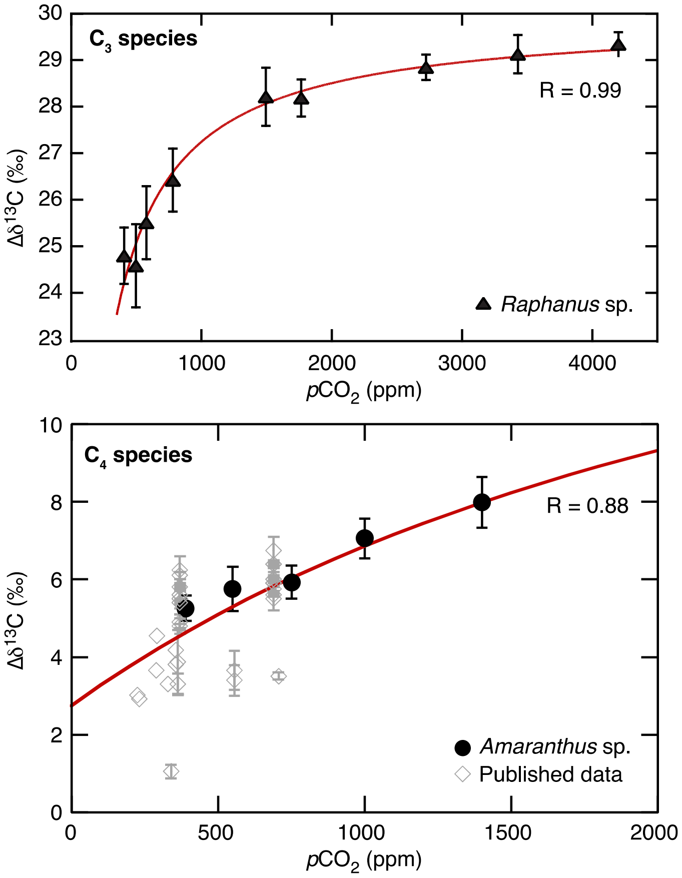

The effect of pCO$_2$ level on carbon isotope fractionation ($\Delta\delta^{13}C$) in C$_3$ (top) and C$_4$ (bottom) land plants. Both plant types show an increase in $\Delta\delta^{13}C$ with increasing pCO$_2$, but the shape of the relationship differs. Solid symbols indicate our data.

High Resolution X-ray CMT imaging of Supercritical CO_2 in Porous Media: Pore-scale Results in Support of Larger-Scale Implementation of CO_2 Storage

A.L. Herring, L. Andersson, and D. Wildenschild
School of Chemical, Biological and Environmental Engineering, Oregon State University, Corvallis, OR, USA

Geologic CO_2 sequestration has been proposed as a climate change mitigation strategy to limit emissions of CO_2 to the atmosphere from large fossil-fuel burning CO_2 point sources; however, there are concerns associated with the long-term stability of a mobile subsurface CO_2 plume. Capillary trapping of supercritical CO_2 ($scCO_2$), wherein the CO_2 is held in place by capillary forces, is a more secure form of subsurface storage than structural trapping, which relies on an impermeable caprock to contain the buoyant CO_2 plume.

To understand the multiphase physics of CO_2 transport, and to subsequently produce quantitative estimates of potential CO_2 capillary trapping, it is necessary to study field, core, and pore-scale processes. X-ray computed microtomography (microCT) allows for three-dimensional (3D) in-situ visualization and quantification of the porous medium, as well as the fluid phases within the pore structure, at the pore-scale. Initial work using this methodology has focused on proxy fluid-based systems and experiments carried out at ambient conditions. As the interfacial tension, viscosity, and carbon dioxide injection (as well as subsequent brine flood injection) rates are varied, trends have been observed with the type of porous medium (unconsolidated vs. consolidated), varying wetting and nonwetting phase viscosity, and flow rates. The injection scenario has been studied for its effect on topology and connectivity of the trapped nonwetting phase (i.e., the supercritical carbon dioxide), and initial results suggest that trapping is optimized as nonwetting phase connectivity after injection is minimized.

To study these processes under in-situ conditions, we have designed and built a mobile experimental set-up capable of running at pressures up to 2000 PSI and temperatures up to 50^oC. Our experimental procedure includes pressurizing, mixing, and separating fluids; and subsequently running immiscible drainage and imbibition flow experiments with brine and supercritical CO_2. These complete scCO2 injection and trapping experiments are then conducted at the Advanced Photon Source, and x-ray microCT data is used to quantify the resulting trapping efficiency.

Results so far indicate that carbon dioxide injection can be manipulated to facilitate optimal trapping of residual carbon dioxide, both in terms of amount and with respect to size/ connectivity characteristics that may favorably support subsequent trapping reactions (e.g., dissolution and mineral formation). Future work should include test on larger samples and involve numerical modeling to substantiate the trends found at the pore-scale.

Thermodynamically Consistent Multiscale Models of Transport Phenomena in Porous Medium Systems

Cass T. Miller and William G. Gray
University of North Carolina

Natural porous medium systems span a wide range of length scales from the molecular scale to the kilometer scale where critical problems related to energy are of importance to society. It is generally understood that models are essential and at the field scale these models must be based upon an overlapping continuum representation where quantities are represented in an averaged sense at what is termed the macroscale. Typically, macroscale models are posed directly at the scale of interest and closure relations, often based upon experimental observations, are posited to produce a solvable system. This traditional approach is deficient in multiple respects: (1) the macroscale models are posed in terms of variables that are not precisely defined; (2) an explicit connection between quantities at the scale of interest and smaller scales does not exist; (3) underlying physics known to be important from a microscale perspective are not explicitly represented in macroscale models; and (4) thermodynamic constraints on the allowable form of posited closure relations are not known or enforced. These common limitations make it impossible to demonstrate the consistency of a macroscale model with a well-understood microscale model, where the phase distributions are fully resolved with time.

The thermodynamically constrained averaging theory (TCAT) has been developed as a means to overcome these limitations associated with conventional modeling approaches. We demonstrate the elements of TCAT including microscale conservation and balance equations, thermodynamics, multiscale averaging theorems, macroscale conservation and balance equations, evolution equations, upscaled thermodynamic theory, and entropy inequality expressions. A framework is presented to show the role that these components play in TCAT model development. These components are used to generate models for example systems that have a desirable set of characteristics, which overcome the limitations noted above. A range of systems are considered, including single and two-fluid-phase porous medium systems. Example results are analyzed and the extensibility of the formulation is discussed. Approaches to model the needed closure relations are considered using both experimental and microscale modeling and analysis methods.

Recent Project Publications

1. Gray, W.G., and C.T. Miller (2014) Introduction to the Thermodynamically Constrained Averaging Theory for Porous Medium Systems, Series Title: Advances in Geophysical and Environmental Mechanics and Mathematics, Series Editor: K. Hutter, Springer, Heidelberg, Germany, 582 pp, ISBN 978-3-319-04010-3.
2. Gray, W.G., C.T. Miller, and B.A. Schrefler (2013) Averaging Theory for Description of Environmental Problems: What Have We Learned, Advances in Water Resources, Vol. 51, pp. 123--158. doi:10.1016/j.advwatres.2011.12.005.
3. Miller, C.T., C.N. Dawson, M.W. Farthing, T.Y. Hou, J. Huang, C.E. Kees, C.T. Kelley, and H.P. Langtangen (2013) Numerical Simulation of Water Resources Problems: Models, Methods, and Trends, Advances in Water Resources, Vol. 51, pp. 405--437. doi:10.1016/ j.advwatres.2012.05.008.
4. Sciume, G., S.E. Shelton, W.G. Gray, C.T. Miller, F. Hussain, M. Ferrari, P. Decuzzi, and B.A. Schrefler (2013) A Multiphase Model for Three-Dimensional Tumor Growth, New Journal of Physics, Vol. 15, No. 015005, 35 pp, doi:10.1088/1367-2630/15/1/015005.
5. Dye, A.L., W.G. Gray, C.T. Miller, and J.E. McClure (2013) Description of Non-Darcy Flows in Porous Medium Systems, Physical Review E, 033012, pp. 1--14, doi:10.1103/PhysRevE.87.033012.
6. Gray, W.G., and C.T. Miller (2013) A Generalization of Averaging Theorems for Porous Medium Analysis, Advances in Water Resources, Vol. 62, pp. 227--237, doi:10.1016/j.advwatres.2013.06.006.
7. McClure, J.E., J.F. Prins, and C.T. Miller (2014) A Novel Heterogeneous Algorithm to Simulate Multiphase Flow in Porous Media on Multicore CPU-GPU Systems, In press: Computer Physics Communications.

Nanopore Confinement of C-H-O Mixed-Volatile Fluids Relevant to Subsurface Energy Systems

David R. Cole[1], Alberto Striolo[2], David Tomasko[1], Siddharth Gautam[1], Salim Ok[1], Tingting Liu[1]
[1] The Ohio State University, [2] University College London

Collaborators: K. Mueller, David Hoyt, Nancy Washton, Amity Andersen, PNNL/EMSL
G. Rother, M. Gruszkiewicz, E. Mamontov, A. Kolesnokov, ORNL
A. Asthagiri, Philip Grandinetti, The Ohio State University
Steve Greenbaum, Hunter College

The overarching objective of this effort is to obtain a fundamental atomic- to macro-scale understanding of the sorptivity, structure and dynamics of simple and complex C-H-O fluids at mineral surfaces or within nanoporous matrices over temperatures, pressures and compositions encountered in near-surface and shallow crustal environments. To achieve this goal we (a) assess the adsorption-desorption behavior of methane, related hydrocarbons and CO_2 on a variety of mineral substrates and in nanoporous matrices, (b) characterize the microstructure and dynamical behavior of methane and related HC volatiles at mineral surfaces and within nanopores with and without H_2O present at relevant P-T-x subsurface conditions, and (c) utilize molecular-level modeling to provide critically important insights into the interfacial properties of these mineral-volatile systems, assist in the interpretation of experimental data and predict fluid behavior beyond the limits of current experimental capability. A scientifically diverse, multi-institutional team (Ohio State University, University College London, Oak Ridge National Lab, Pacific Northwest National Lab, Hunter College) are utilizing novel experimental and analytical techniques in concert with state-of-the-art theory, modeling and simulation approaches to address these issues. There is a special emphasis on building synergistic links between results obtained from various neutron scattering and NMR studies which are integrated into our research portfolio with molecular dynamics modeling, to provide new phenomenological insights.

Thus far, we have conducted a number of different kinds of experiments focusing on the behavior of propane, ethane, methane, carbon dioxide or their mixtures with or without water present interacting with different types of mesoporous matrices (e.g., SiO_2, Al_2O_3, TiO_2, ZrO_2). High temperature-high pressure gravimetric measurements on these fluids have revealed profound fluid densification in nanopores as the density (pressure) approaches that of the bulk critical density followed by a dramatic density decrease (fluid depletion). Densification of propane in model silica pores has been observed in MD simulations, in qualitative agreement with experiments. The CO_2 adsorption on TiO_2 has been modeled with density functional theory (DFT) that employs a new version of the dispersion correction. Quasielastic neutron scattering (QENS) experiments have been conducted at Oak Ridge National Laboratory on the system propane-mesoporous silica with or without CO_2 present. Results from these experiments are interpreted in terms of translational "diffusive" motion of propane, residence times between diffusion jumps and the jump distances. Interestingly, the presence of CO_2 seems to enhance the mobility of propane in the mesopores. Mixed water-methane and water-ethanol systems have also been investigated using MD simulations, suggesting that preferential adsorption might be responsible for the results observed experimentally in mixed systems. We used a recently developed high-pressure Magic Angle Spinning (MAS) NMR system (EMSL) to investigate methane interacting with mesoporous silica having 200 nm particle size and 4 nm pores, a high surface area non-porous silica and montmorillonite. The proton decoupled ^{13}C NMR spectra were acquired with high-pressure MAS probe at 30, 60 and 120 bars. At each pressure, the temperature was varied from 34 ^oC to 73 ^oC. The experiments revealed that pressure induces shifts in the methane peak position: ~0.25 ppm going from 30 to 60b, and ~0.50 ppm shift going from 30 to 120b. The magnitudes of these spectral chemical shifts have been emulated by Amity Andersen at EMSL using DFT. The simulations indicate that the chemical shifts reflect the effects of "molecular crowding" and adsorption on magnetic shielding.

Genesis, Storage, Producibility, and Natural Leakage of Shale Gas

Arndt Schimmelmann and Maria Mastalerz
Indiana University, Bloomington, Indiana

Shales are important source and reservoir rocks for hydrocarbons (shale gas, oil). The three research goals of this project encompass: (1) Quantification of the character and development of porosity in organic-rich rocks as a function of organic matter content, type of organic matter, thermal maturity, and the degree of compaction; (2) evaluation of the natural outgassing of methane from shales into the atmosphere and its potential contribution to global warming by delivering potent methane greenhouse gas; and (3) testing of shales' ability to generate thermogenic gas (or natural gas via catalysis) at relatively low temperatures (60, 100 and 200 °C) and different pressures (ambient, 100 MPa, 300 MPa) over months to years.

A variety of porosimetric methods was used to assess macro- meso- and microporosity in shales (e.g., Mastalerz et al., 2012). Porosity strongly depends on the presence of organic matter and its thermal maturity. Porosity in shales at low maturity initially diminishes due to ongoing compaction, but incipient thermal cracking at the beginning of the oil window generates new porosity. Further into the oil window, the generation of additional liquid hydrocarbons fills pores and reduces the open pore space available for gas storage. At even higher maturity, secondary cracking and gas generation expels some liquid hydrocarbons from pores and opens new pore spaces for gases Mastalerz et al., 2013). Traditional low-pressure gas adsorption isotherms for porosimetry of shales do not take into account the solubility of gases in liquid hydrocarbon phases. Our PhD students are currently re-evaluating gas adsorption porosimetry of shales across the oil window. High-resolution chemical mapping of organic matter in macerals and pore fillings (as well as of inorganic components) in shales by novel micro-FTIR techniques proved to be a valuable tool for assessing shales' microstructure (methodology developed and applied by our PhD student Yanyan Chen; Chen et al., 2013, 2014).

Natural outgassing of shale gas into the atmosphere in the absence of drilling and fracking was evaluated during field work in several states. A naturally occurring spectacular "eternal flame" and associated non-burning shale gas seeps in western New York State mark a gas macroseepage system of dominantly thermogenic origin emanating directly from deep shale source rocks (Etiope et al., 2013). The chemical and isotopic compositions of the gas could be traced to deep Upper Devonian shales. This seep gas holds the current world record with regard to the highest ethane and propane concentration ever reported for a natural gas seep ([ethane + propane] ≈ 35 vol. %). Microseepages along geologic fault lines are abundant. The occurrence of gas seepages fed by deeper shales through tectonically-induced conduits proves that strong fluxes and point sources of shale gas can indeed contribute to atmospheric greenhouse gas loading, although much ascending methane seems to be microbially oxidized to carbon dioxide by methanotrophs before it reaches the atmosphere. This is well demonstrated in limestone caves in Kentucky and Indiana that overlie deeper shales and often receive gas seepages. Our results show that the semi-stagnant air in caves typically contains less methane and more carbon dioxide than in the atmosphere, presumably because methanotrophic microbes are lining the walls of underground gas passageways and intercept hydrocarbons (research project of our PhD student Kevin Webster).

The hypothesis of catalytic gas generation from shales at low temperatures in the absence of methanogenic microbes is being tested by sterile incubation of shales in the presence of deuterium-enriched waters under different temperatures and pressures. Experiments by our PhD student Lin Wei last from 6 months to two years due to slow kinetics. Low-temperature methanogenesis is indeed observed from some shales and decreases with increasing hydrostatic pressure. Hydrogen stable isotope ratios of methane indicate that hydrogen from water does not enter newly generated methane at a significant level, which means that methanogenesis likely occurs at catalytic centers within hydrophobic organic domains.

PUBLICATIONS

Mastalerz, M., L. He, Y.B. Melnichenko, and J.A. Rupp (2012) Porosity of coal and shale: Insights from gas adsorption and SANS/USANS techniques. *Energy & Fuels* **26**, 5109−5120. http://dx.doi.org/10.1021/ef300735t

Mastalerz, M., A. Schimmelmann, A. Drobniak, Y. Chen (2013) Porosity of Devonian and Mississippian New Albany Shale across a maturation gradient: Insights from organic petrology, gas adsorption, and mercury intrusion. *AAAP Bulletin* **97** (10), 1621–1643. http://dx.doi.org/10.1306/04011312194

Chen, Y., L. Dethere Caro, M. Mastalerz, A. Schimmelmann, A. Blandón (2013) Mapping the chemistry of resinite, funginite and associated vitrinite in coal with micro-FTIR. *Journal of Microscopy* **249** (1), 69-81. http://dx.doi.org/10.1111/j.1365-2818.2012.03685.x

Etiope, G., A. Drobniak, A. Schimmelmann (2013) Natural seepage of shale gas and the origin of “eternal flames” in the Northern Appalachian Basin, USA. *Marine and Petroleum Geology* **43**, 178-186. http://dx.doi.org/10.1016/j.marpetgeo.2013.02.009

Chen, Y., A. Furmann, M. Mastalerz, A. Schimmelmann (2014) Quantitative analysis of shales by KBr-FTIR and micro-FTIR. *Fuel* **116**, 538–549. http://dx.doi.org/10.1016/j.fuel.2013.08.052

Subsurface Flow and Transport Tomography Using Streamlines

Akhil Datta-Gupta,
Texas A&M University

The goal of this project is to examine the viability of time-lapse seismic monitoring using an integrated modeling of fluid flow, including chemical reactions, geomechanical effects and seismic response. A critical aspect here is computational efficiency so that the approach can be suitable for large-scale field applications using high resolution geologic and seismic models. Our work focuses on fully integrating fluid flow and seismic data for monitoring injected CO_2 fronts by developing robust methods for reservoir characterization via coupled seismic and fluid flow modeling and joint inversion of seismic and fluid flow data. For computational efficiency and suitability for large-scale field applications, we are developing streamline-based compositional modeling of CO_2 sequestration including compressibility, stress-sensitivity, compositional and geochemical effects. For data integration and uncertainty assessment, we adopt an efficient Bayesian framework using multistage Markov Chain Monte Carlo (MCMC) methods.

We developed a novel approach to incorporate gravity and capillary effects into compositional streamline simulation of CO_2 injection without adversely impacting its computational efficiency (Tanaka et al., 2014). We use an orthogonal projection method to reformulate the streamline transport equations so that the fluxes of capillary and gravity are separated into components parallel and orthogonal to the total velocity defining the streamline trajectories. Fluxes parallel to total velocity are included within the solution of the convective flow equations on streamlines. The remaining terms are calculated on the underlying three dimensional grid. Our proposed formulation still uses an operator splitting approach, but the size of the remaining transverse flux correction terms is significantly reduced, allowing for large time steps. We have also introduced a novel parameterization approach to mitigate the challenges associated with field-scale calibration of geologic models to time-lapse seismic data. The reservoir property field is mapped to and updated in a low-dimensional transform domain using a linear transformation basis. The transformation basis vectors are the eigenvectors of a Laplacian matrix that is constructed using grid connectivity information and the main features in a given prior model. Finally, we use multi-objective optimization to simultaneously integrate 4-D repeat seismic surveys with multiphase flow and transport data using streamlines. The joint inversion is performed using streamline-based sensitivities that are derived analytically without additional flow simulations. Our previous approach to seismic data integration have mostly incorporated saturation effects but the pressure effects have not been accounted for (Rey et al., 2012). We propose, for the first time, streamline-based analytic approaches to compute parameter sensitivities that relate the seismic data to reservoir properties while accounting for both pressure and saturation effects via appropriate rock physics models. The efficacy of our approach is demonstrated with both synthetic and field applications.

PUBLICATIONS

Rey, A., Bhark, E., Gao, K., Datta-Gupta, A. and Gibson, R., Streamline-based integration of time-lapse seismic and production data into petroleum reservoir models," *Geophysics*, 77 (6), (2012).

Tanaka, S., Datta-Gupta, A. and King, M. J., Compositional Streamline Simulation of CO_2 Injection Accounting for Gravity and Capillary Effects Using Orthogonal Projection, SPE 169066, presented at the SPE Improved Oil Recovery Symposium held in Tulsa, Oklahoma, USA, 12–16 April 2014. (Submitted to *SPE Journal*).

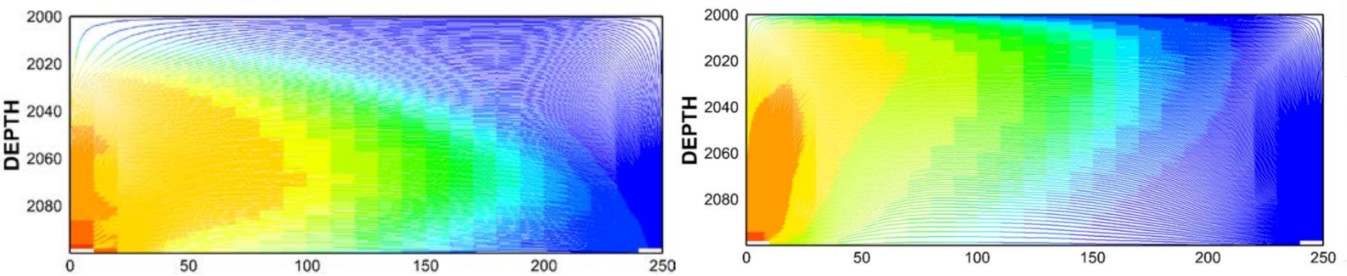
(a) Convection only

(b) With Gravity and Capillarity

Figure: An Illustration of incorporating Gravity and Capillarity in Streamline-based Transport of CO_2 Using Orthogonal Projection

Low temperature H_2 production in serpentine aquifers

Templeton, A.S., Miller, H.M., and Mayhew, L.E.
Department of Geological Sciences University of Colorado, Boulder, CO 80309-0399.

Collaborators: Mark Conrad, LBNL, Peter Kelemen, Columbia University, and Tori Hoehler, NASA AMES Research Center.

The low temperature water-rock reaction pathways that occur during the anoxic alteration of ultramafic rocks are not currently well constrained, particularly at shallow subsurface temperatures from 25-100°C. There are wide discrepancies in the predicted amount of H_2 and/or energy that will be generated through the oxidation of Fe during olivine and pyroxene hydration and carbonation, and ongoing debate about the possible pathways of associated CO_2 consumption and potential mineral carbonation.

We are examining the connections among the geochemical behavior of iron, and the extent of hydrogen, methane or carbonate mineral formation, during the aqueous alteration of olivine and pyroxene bearing rocks at near surface temperatures and pressures. Geologically-produced H_2 gas is of interest because H_2 can drive the biological and/or abiotic synthesis of methane and low molecular weight organics, and the concomitant utilization of CO_2, depending upon the geochemical conditions. Alternatively, dissolved CO_2 may be significantly consumed in mineral carbonation reactions that not only suppress H_2 generation, but result in the formation of stable Ca, Mg and Fe carbonates.

In our most recent work, we have determined that dunites and harzburgites from the Oman ophiolite can generate extensive quantities of H_2 at 100°C, greater than any other single mineral or peridotite experimentally serpentinized to date at these temperatures. The rates of H_2 generation, and the δD of the H_2, is highly sensitive to the aqueous geochemistry. In addition, prolonged periods of H_2 generation are then followed by persistent declines in pH_2 with increasing reaction time. We are now trying to determine the pathways of H_2 consumption under abiotic conditions, when we transition to a state where the rate of H_2 production is less than the rate of H_2 consumption. Possible H_2-sinks include surface-catalyzed reduction of volatile species, such as CO_2.

To explore the feasibility of this hypothesis, we have measured the total organic acids present in Oman peridotite hydration experiments vs. controls after 1 year of water/rock reaction, and can reproducible generate 100-250 micromolar concentrations of total C1-C5 organic acids at pH 9, where formate is the dominant organic acid produced. Therefore, these acids may be quantitative sinks for CO_2 in our experiments, and we are now working to measure the partitioning of ^{13}C between aqueous forms of CO_2, mineral forms of CO_2 and organic compounds during progressive water/rock interaction.

We will also discuss pathways of Fe-oxidation coupled to H_2 generation during the continued alteration of partially-serpentinized rocks, and the of δD H_2 produced experimentally vs. measured under *in-situ* conditions, in order to provide mechanistic insights into the extent of modern H_2 generation and consumption that may be occurring in shallow peridotite aquifers.

Role of iron chemistry in oxyhydroxide nucleation and olivine carbonation

B. Gilbert, B. Legg, M. Zhu, H. Zhang, G. D. Saldi, D. Duval, K. G. Knauss, G. A. Waychunas, J. F. Banfield

Lawrence Berkeley National Laboratory

Several research groups within the Berkeley Geochemistry Project are studying different aspects of the geochemistry of iron. We will summarize results from two recent studies that highlight how the high affinity of iron(III) for oxyanions leads to strong effects on the rates of important mineral formation and mineral dissolution processes.

First, we studied the initial stages of the precipitation of iron oxyhydroxide minerals during the neutralization of acidic solutions. This mineral formation pathway occurs during the neutralization of acid mine drainage, typically in the presence of high concentrations of nitrate or sulfate. We applied stopped-flow methods for fast optical and X-ray observations of the formation of molecular clusters and mineral nuclei. In this system, the early stages of precipitation depend markedly on the dynamics of iron hydrolysis and the extent of sulfate binding. Slow hydrolysis produces molecular clusters, while faster hydrolysis produces ferrihydrite and schwertmannite. Sulfate binding appears to control the pathway for mineral transformations. At low pH sulfate binds more strongly, stabilizing molecular clusters, but as hydrolysis proceeds increasing pH leads to cluster destabilization and ferrihydrite formation. At high sulfate compositions schwertmannite forms at the expense of ferrihydrite indicating it is the stable phase.

Second, we studied the effects of iron, and iron redox state, on carbonation reactions of olivine for carbon dioxide (CO_2) sequestration. Olivine, $(Mg,Fe)_2SiO$, is an abundant mineral in basalts and ultramafic rocks and its conversion to Mg-carbonates is expected to trap most of the CO_2 introduced within these systems. The experimental results of a series of batch and flow-through reactor experiments, conducted at 150 °C in a CO_2 saturated fluid, provide clear evidence of formation of Fe–Si-rich interfacial layers that slow olivine dissolution. The passivating effect of these layers is a function of the aqueous fluid composition and is related to the permanence of oxidizing conditions in the system. The consumption of $O_2(aq)$ during the course of the reaction and the consequent establishment of anoxic conditions lead to the breakdown of the pre-formed Fe-Si layers.

Note: Prof. Evans was unable to attend the meeting.

Designing seals: Integration of field observations, experimental analysis, and numerical modeling to constrain the long-term effectiveness of engineered storage systems

Elizabeth Petrie[1], Steven Bauer[2], Santiago Flores[1,4], Stephen Radua[3], Peter Mozley[3],
James P. Evans[1]

[1]Dept. of Geology, Utah State University, Logan, UT 84322-4505; [2]Sandia National Laboratories, Geomechanics Research Department 6914 Albuquerque, NM 87185; [3]Department of Earth and Environmental Science, New Mexico Tech, Socorro, New Mexico 87801; [4]Chesapeake Energy, Oklahoma City, OK

We characterize the nature of mineralized and barren fractures and small faults that transect interfaces between reservoir-seal systems in Paleozoic and Mesozoic rock exposed in central and southeastern Utah. We use these analogs to constrain the mechanical rock properties, determine the mechanisms of possible seal failure, and predict their behavior in forward models of pressurized reservoirs. Outcrop evaluation of the microscale to mesoscale (mm- to m-scale) variability in fracture density and morphology is combined with variability in elastic moduli derived from geophysical wireline logs and rock strength measurements to characterize the rock. An integrated approach of field, borehole geophysical, burial and stress history modeling, rock strength testing, and numerical modeling are used to understand the effects changing material properties, rock strength, and stress history have on sealing capacity.

Permeability for units of interest was determined using field mini-permeameter and laboratory measurements. Field measurements were obtained using a TinyPerm II field mini-permeameter, capable of measuring permeabilities between 10 and 10,000 mD. All seal rocks evaluated in this study are heterolithic, and low permeability (0.001 to 0.12 D), often below the detection limits of the mini-permeameter. Reservoir permeabilities are much higher and range from 5 – 20 D. Laboratory derived permeability measurements were done via mercury injection capillary pressure measurements (MICP) and show that deformation bands within the reservoirs range from 0.416 to 16.10 mD, much lower than the reservoir host rock and are expected to act as barriers to fluid flow and compartmentalize the reservoir. MICP results also show that the zones of deformation bands are capable of trapping a 3-m column of fluid. MICP of the overlying seal shows a range in permeability that varies with rock type, carbonate permeability was 4 nD-0.454 µD and siliciclastic shale and siltstone have permeability values that range between 0.149 to 1.16-µD. The presence or creation of fractures or faults within the overlying caprock creates preferential permeability pathways adversely affecting the subsurface carbon sequestration system.

We create geomechanical models for finite element analysis and modified Mohr-Griffith-Coulomb failure analysis by combine outcrop observations with the unique loading history and resultant uniaxial strain model at each locality to understand the changes in stress magnitude through time, timing of fracture initiation and paleo-tectonic stress orientation if it differs from the current dominant crustal stress orientation. The stress magnitudes for each scenario and elastic moduli derived from geophysical wireline log data are used in 3D FEA to understand the effects changes in material properties and depositional stacking has on strain distribution and fracture occurrence.

Structure summary

Outcrop-based analyses of the Jurassic Navajo Sandstone and Carmel Formation reservoir-seal pairs document a range of behaviors, including slip on faults in permeable reservoir sandstone that change updip to fracture networks in the low permeability siliciclastic Carmel, with joints, opening-mode+shear faults, and opening-mode veins. The fractures in the caprock show evidence of seal failure that include multiple mineralization events and host-rock bleaching, likely from transport of reducing fluids within the fractures. Seal failure is most likely where fracture density is highest, and fracture density is highest in three settings: fracture clusters, where fold curvature is highest, and near faults.

Small displacement, reservoir-scale faults in the Cedar Mesa Sandstone transition to bleached and mineralized fracture swarms and shear fractures within the overlying seal of the Organ Rock Formation. Bleached zones crosscut the entire vertical thickness of the Organ Rock Formation (120 m /394 ft) and can be observed in air photo images extending for several km.

Microscale observations of mineralized faults and fractures in all seal lithologies indicate that subsurface flow of reducing fluids, responsible for the bleaching, and alteration of the caprocks, occurred repeatedly at depth. Migration of fluids into the adjacent rocks occurred as diffuse flow away from subvertical fractures, and along bedding planes. Multiple fluid flow events are also supported by observations from the underlying reservoirs, where UV illumination of uranium-rich calcite mineralization within deformation band faults documents reactivation of the faults by open-mode fractures. Cross-cutting relationships and varied vein mineralogy are also observed within the reservoir fracture sets suggesting multiple fluid chemistries and fluid flow events.

Material properties

Material properties of the rocks are determined from inversion of wireline log sonic data, correlated with gamma ray logs to define caprock lithological-sonic log response populations, which are used to derived dynamic values for Young’s moduli and Poisson’s ratio. We observe meter scale variability in unconfined compressive strength obtained in outcrop and fracture densities, analysis of wireline logs also show similar scale of variability in dynamic elastic moduli. Using material properties derived from wireline logs and tying them to outcrop observations of deformation features allows us to test subsurface finite element models and obtain vertical strain distributions. These data are used to understand the effects changes in rock properties have on strain distribution expanding the scale of investigation from outcrop analog to that of subsurface storage systems.

Results from laboratory tests including unconfined compression tests (UCS), Brazil tensile strength tests, and triaxial compression tests are used to constrain the mechanical properties in the modified Griffith – Mohr-Coulomb fields. Tensile rock strength, derived from indirect tensile strength tests range from 2.3 MPa in siltstone to 11.5 MPa in calcareous shale, and are lithology dependent. The shapes of the predicted failure envelopes in the tensile fields vary, indicating that the pore-fluid pressures necessary for mechanical failure vary between rock types and this variation may induce pure tensile failure, mixed mode shear and opening mode faults, or sheared faults, depending on the rock properties/type. Fracture mode will have an effect on permeability and fluid flow in the subsurface and the presence of pre-existing fractures will alter the rock strength.

Modeling summary

Characterization of fracture patterns, rock strength variability and the modeled changes in subsurface strain distribution evaluates the response of low-permeability rocks to changing stress in the subsurface, and is applicable to multiple geo-engineering scenarios such as exploitation of natural resources, waste disposal, and management of fluids in the subsurface. The meso-scale (cm to m) variability in fracture distributions and morphology and heterolithic nature of the caprock seals evaluated here highlights the strong link between variations in material properties affecting rock strength and response to changing stress conditions. The variable connectivity of fractures and the changes in fracture density at the meso-scale plays a critical role in subsurface fluid flow.

Meso-scale changes in rock strength are expected to affect the distributions of localized stress and thereby influence fracture propagation and fluid flow behavior within the seal. Burial history models evaluated in this study suggest that most formations reach a maximum burial depth > 1.6 km and experience an overburden stress of up to 50 MPa. As lithostatic load increases with burial depth the potential for initiation of natural hydrofractures increases because the excess pressure above the hydrostatic gradient required for failure decreases. Once zones of weakness have been established within the caprock they exist as loci for future deformation and fluid flow.

Results of 3D geomechanical finite-element modeling reveals that mismatches in elastic moduli results in gradients in local strain magnitudes at locked mechanical interfaces, suggesting that mechanical mismatches between layers will create differential strain distribution in the subsurface. This variability in strain distribution can be used to predict the rock response manifested as more fractures in high-strain regions and few fractures in low-strain regions. These data can also be used to predict where future fracture formation is more likely; and when combined with knowledge of rock properties can be used in the prediction of fracture mode.

Note: Prof. Navrotsky was unable to attend the meeting.

Thermodynamics of Minerals Stable Near the Earth's Surface

Alexandra Navrotsky,
University of California, Davis

PROGRAM SCOPE

The project "Thermodynamics of Minerals Stable Near the Earth's Surface" uses specialized calorimetric techniques in the Peter A. Rock Thermochemistry Laboratory at UC Davis to obtain new thermochemical data for materials, often of nanoscale dimensions, encountered in the Earth's "critical zone," the near surface region of the planet most directly affecting and affected by human activity. This project focuses on the transformations from ions in solution to clusters, to nanoparticles, to precipitates and finally to well crystallized minerals (and the reverse transformations during weathering and dissolution) representing a continuous spectrum of events. This project expands on our previous studies of the energetic driving forces for such transformations these, with a strong emphasis on transition metals and redox reactions, especially involving iron and manganese oxides.

We continue exploring the gradual transformation from nanoclusters in solution to nanoparticles to crystalline minerals, with an emphasis on transition metal oxides of variable valence, especially iron and manganese. A new area is the large effect of particle size on the thermodynamics of redox reactions. To succeed in calorimetry on the above problem, we must fine tune calorimetric, analytical, and structural techniques to control and delineate oxidation states, water contents, and structural features of materials containing one or more transition elements of variable valence and structural and adsorbed H_2O. In particular, we are confident now that we can do reliable oxide melt solution calorimetry on phases which simultaneously contain ferrous and ferric iron and water, as well as materials containing several transition metals. This capability opens the door to detailed studies of minerals containing these combinations of elements, for which enthalpies of formation are still surprisingly poorly known. These include spinels containing Cr, Mn, Fe, Co, Ni, and Cu, as well as complex sulfides, silicates, and borates containing transition metals.

FY 2013 HIGHLIGHTS

We have documented rapidly reversible size- and water- induced redox reactions in manganese oxides. Chemisorption of water onto anhydrous nanophase manganese oxide surfaces promotes rapidly reversible redox phase changes as confirmed by calorimetry, X-ray diffraction, and titration for manganese average oxidation state. Surface reduction of bixbyite (Mn_2O_3) to hausmannite (Mn_3O_4) occurs in nanoparticles under conditions where no such reactions are seen or expected on grounds of bulk thermodynamics in coarse-grained materials. Additionally, transformation does not occur on nanosurfaces passivated by at least two percent coverage of what is likely an amorphous manganese oxide layer. The transformation is due to thermodynamic control arising from differences in surface energies

Aluminum hydroxide ions in the ε-Keggin structure provide geochemical models for how structure affects reactivity, and consequently, how aqueous ions evolve to bulk precipitates. Here we report a systematic comparison of heterometal substitution into the MAl_{12} ε -Keggin structure, where M = GaIII, AlIII, or GeIV. We use direct calorimetric techniques to compare the energetics of these substituted structures and complement these measurements with density functional theory, DFT, to further examine this structure as a host to alternative heterometals. The measured enthalpy of solutions, ΔHsoln, at 28 °C in 5 N HCl for the selenate salts of $GaAl_{12}^{7+}$ and $AlAl_{12}^{7+}$, was measured as -869.71 ± 5.18 and -958.04 ± 2.79 $kJ \cdot mol^{-1}$, respectively. The enthalpies of formation from the elements, ΔH°f,el, for the selenate salts of $GaAl_{12}^{7+}$ and $AlAl_{12}^{7+}$, are -23334.18 ± 60.38 and -23075.02 ± 61.68 $kJ \cdot mol^{-1}$, respectively, supplanting previous values. We compare structural relationships to both experimental and calculated energies to identify the driving forces that control these substitutions and stability, and establish that tetrahedral M-O bond lengths are closely related to the strain and stability of the structure. We show that substitution depends on the size and valence of the heterometal through energetics, and we extend our thermodynamic and structural relationships to other not yet synthesized MAl_{12} clusters (M= SiIV, FeIII, BeII, MgII, or ZnII).

"Rapidly Reversible Redox Transformation in Nanophase Manganese Oxides at Room Temperature Triggered by Changes in Hydration" N. Birkner and A. Navrotsky, *Proc. Natl. Acad. Sci.*, Submitted (2013).

"Energetics of Heterometal Substitution in ε-Keggin $[MO_4Al_{12}(OH)_{24}(OH_2)_{12}]^{6/7/8+}$ Ions" D. Reusser, W. H. Casey, and A. Navrotsky, *Amer. Miner.*, Under Revision (2014).

ABSTRACTS

POSTER PRESENTATIONS

Poster 1

Constitutive Modeling Approaches for High Porosity Sandstone

Kathleen A. Issen[1] and Mathew D. Ingraham[2]
[1]*Mechanical and Aeronautical Engineering, Clarkson University, Potsdam, NY 13676*
[2]*Geomechanics Department, Sandia National Laboratories, Albuquerque, NM 87185*

High porosity sandstone exhibits a range of deformational responses: at low mean stress, dilatant shear bands form; at intermediate mean stress, compactant shear bands and/or compaction localization occurs; while at high mean stress, non-localized cataclastic compaction occurs. Predicting and modeling these deformation responses requires development of mathematical constitutive frameworks that represent fundamental mechanical behaviors, determined from experimental characterization. This work examines three aspects of this process: 1) constitutive response and failure observations from true triaxial testing, 2) evaluation of strain localization predictions, and 3) development of improved constitutive frameworks.

In prior work, a suite of true triaxial tests were conducted on Castlegate sandstone, covering a wide range of mean stresses (brittle to ductile response) and a full range of deviatoric stress states (axisymmetric compression to axisymmetric extension, with three stress states in between). The onset of localization and the band angle were determined using located acoustic emissions (AE). In the present work, we determine predicted band angles (angle between band normal and direction of maximum compression) using the Rudnicki and Rice (1975) localization framework. At low mean stresses, predicted band angles are typically within a few degrees of observed band angles. As expected, both observed and predicted band angles decrease with mean stress. At intermediate mean stresses, compaction localization manifests as low angle zones of localized AE (approximately 20 mm thick), in contrast with the relatively thin shear bands at low mean stress. The relatively diffuse compaction localization in Castlegate does not fit the traditional definition of a deformation band. Additionally, predicted band angles are notably higher than observations, suggesting that use of localization theory may not be applicable for this deformation mode.

Evaluation of localization predictions requires partitioning strain to separate the inelastic strain required to determine localization parameters. For Castlegate, the elastic moduli evolve with both stress and plastic strain. For simplicity, we assume the bulk modulus depends on mean stress and plastic volume strain, and the shear modulus depends on shear stress and plastic shear strain. These expressions for the strain separation were employed to determine predicted band angles. Through this process, we observed the well-known experimental result, that the plastic strain increment is not normal to the yield surface, necessitating the use of non-associated plasticity. However, there are known problems with use of non-associated plasticity, for example, the possibility of negative work. Thus, the third thrust of the present work is development of alternate constitutive frameworks, derived using thermomechanics principles, which capture the observed constitutive response (stress and plastic strain dependence of moduli, apparent non-normality). Key requirements and associated difficulties are examined in the context of available mechanical data.

Poster 2

Bulk and Interfacial Cation Behavior in OM-H_2O and Clay-OM-H_2O Composites: Molecular Scale Insights

Geoffrey M. Bowers,[1] Brennan O. Ferguson,[1] Venkateswara Reddy,[2] A. Ozgur Yazaydin,[2] R. James Kirkpatrick[3]

[1]Division of Chemistry, Alfred University, Alfred, New York 14802; [2]Department of Chemistry, Michigan State University, East Lansing, MI 48824; [3]College of Natural Science, Michigan State University, East Lansing, MI 48824

One thrust of our ongoing DOE-BES funded work is to explore ion and fluid (H_2O, CO_2) dynamics at smectite-fluid interfaces in the presence of natural organic polymers (e.g. natural organic matter, humic acid, fulvic acid [OM]). The interfacial behavior of these polyorgano-mineral composite materials has yet to be explored in detail on the molecular-scale, leaving a sizable gap in our understanding of physical and chemical behavior at authentic "dirty" mineral surfaces. Such behaviors have significant implications for soil biogeochemistry; plant nutrition and nutrient cycling; soil-microbe interactions; heterogeneous catalysis in natural systems; the global carbon balance; and a variety of fundamental chemical processes in the environment including weathering reactions and the transport/remediation of metal, radionuclide, pharmaceutical, and other organic contaminants. Here, we present new molecular-scale insights into cation binding and dynamics at mineral-OM-H_2O interfaces from studies of cation-OM aggregate and cation-smectite-OM composite systems. For Ca-fulvic acid equilibrated at 100% R.H., there is one ^{43}Ca resonance that becomes progressively broader with decreasing temperature, reflecting a decreasing rate of atomic motion in this OM fraction with a relatively large O-content (carboxylic and phenolic groups). For Ca-humic acid, the single relatively narrow resonance near room temperature broadens and resolves into two peaks at low temperature, reflecting a decreasing rate of atomic motion and the presence of two Ca^{2+} sites with larger mean Ca-O distances and mean coordination numbers than the Ca-fulvic acid aggregate. In contrast, for clay-OM composite samples equilibrated at 43% R.H. and as pastes with a 1.5:1 H_2O:solid ratio, ^{43}Ca yields only one resolvable resonance associated with proximity restricted Ca^{2+} that becomes progressively more shielded (more negative chemical shift) and loses intensity with increasing temperature. The loss of signal intensity and line narrowing are due to dynamical processes in the 10-100 kHz range. This is generally similar to what is observed for ^{43}Ca resonances in the base clay without OM, however, the presence of OM in the composite shifts the resonances at fixed H_2O activity to ~ 2 ppm lower resonance frequency at all temperatures, leads to broadening of the resonances at all temperatures, and yields evidence of a unique dynamic transition between 198 K and 173 K not observed in the OM-free system. These results suggest that direct Ca^{2+}-OM interactions are present for some fraction of the Ca^{2+} in the clay-OM composites. The ^{43}Ca is behavior is similar for composites made with all fractions of Suwannee River OM. Na^+ in hectorite-OM composites was present in two different proximity-restricted coordination/dynamic environments rather than the single Na^+ site observed in base Na-hectorite. One is associated with H_2O-accessible Na^+ and the other inaccessible Na^+ trapped in an environment like that of interlayer Na^+ in an anhydrous OM-free clay. However, the dynamics of Na^+ in these two sites differ significantly from the base clay. Supporting SEM/EDS, helium ion microscopy, and XRD data show that very thick organic coatings (> 3 microns thickness) form on our samples and the presence of diffraction peaks similar to those assigned to graphene-like stacking and aliphatic side-chain spacing in coals, which may indicate clay surface structural templating of the sorbed OM. The data also suggest that more OM enters the interlayers of the Na-hectorite composites than in the Ca-hectorite composites. MD simulations of hydrated Na-hectorite-OM composites modeled at near-neutral pHs (only carboxylic groups deprotonated) show that hydrated Na^+ bridges the OM and the clay surface by coordination to the carboxylic groups and that the Na^+ is mobile, as for the clay without OM. Together, these data suggest that the presence of organic matter in surface soils and clay-rich rocks such as shales can profoundly influence the transport and solubility of some surface-sorbed charged species in these environments, affecting many of the (bio)geochemical processes in these systems.

Poster 3:

Stress deformation of unconsolidated porous media and its impact on pore geometry and phase trapping

V. A. Torrealba[1], Z. T. Karpyn [2], H. Yoon[2], K. A. Klise[2], D. Crandall[2]

[1]Pennsylvania State University and [2]Sandia National Laboratory

Abstract: Understanding the coupled effect of rock compaction and changing stress conditions on multiphase flow in porous media is of fundamental importance for many subsurface activities including enhanced oil recovery, water drawdown from aquifers, and geologic carbon storage. Geomechanical properties of complex porous systems are dynamically linked to flow conditions, but their feedback relationship is often oversimplified due to the difficulty of representing pore-scale stress deformation and multiphase flow characteristics in high fidelity. In this work we performed pore-scale experiments of single- and multi-phase flow through bead packs at different confining pressure conditions to elucidate compaction-dependent characteristics of granular packs and their impact on fluid flow. A series of drainage and imbibition cycles was conducted on a water-wet soda-lime glass bead pack under varying confining stress conditions. Simultaneously, X-ray micro-CT was used to visualize and quantify the degree of compaction and fluid distribution corresponding with each stress condition and injection cycle. Micro-CT images were segmented using a gradient-based method to identify fluids (e.g. oil and water), and solid phase redistribution throughout the different experimental stages. Results demonstrate that the degree of compaction has a significant influence on phase trapping. It was found that an increase in confining pressure has a stabilizing effect on the displacing front during both drainage and imbibition. Alternatively, the compaction process was found to promote the disconnection of non-wetting blobs during imbibition, which in turn results into poor oil recovery by water flooding. In addition, the changes of both porosity, tortuosity, and specific surface area were dampened as the confining pressure was increased.

Poster 4

Comparison between modeled, measured, and predicted $\delta^{13}C$ and pCO_2 values from terrestrial sediments

Brian A. Schubert[1] and A. Hope Jahren[2]

[1]University of Louisiana at Lafayette, School of Geosciences, Lafayette, LA 70504, USA
[2]University of Hawaii, SOEST, Honolulu, HI 96822, USA

A multitude of proxies and models exist for reconstructing past levels of atmospheric carbon dioxide (pCO_2), yet each of these methods are limited by their temporal and/or spatial resolution. Here we present a new geochemical proxy for reconstructing paleo-pCO_2 based upon the $\delta^{13}C$ value of C_3 plant content within terrestrial organic matter. We have shown that this method accurately predicts pCO_2 level across a wide range of temporal resolutions and depositional environments *via* three independent tests. First, we tested the proxy's ability to reconstruct small (<100 ppm) changes in pCO_2 from $\delta^{13}C$ measurements made on fossil leaves, bulk organic matter, and *n*-alkanes across the Last Glacial Maximum through the Holocene (30,000 to 100 years BP). Comparison of our predicted pCO_2 levels to pCO_2 values measured from ice core records showed that all three terrestrial substrates accurately reconstruct the well-documented pCO_2 change, but greatest precision is provided by measurements made on fossil leaf material. Second, we tested the proxy's potential for improving models of atmospheric carbon release during carbon isotope excursions events by constraining estimates for the absolute minimum and maximum pCO_2 levels reached during these brief intervals of rapid pCO_2 rise and global warming. Third, we tested the potential for this proxy to reconstruct pCO_2 levels across large intervals of Geologic history with a preliminary reconstruction of pCO_2 across the entire Cenozoic Era (see Figure). Our reconstruction indicates the highest pCO_2 levels of the last 65 million years occurred during the early Paleogene, followed by a significant drop in pCO_2 levels to the relatively low pCO_2 levels experienced throughout much of the Neogene and Quaternary, as is consistent with models of long-term carbon cycling and previous proxy estimates. Each of these three examples suggests a wholly new way of interpreting changes in the $\delta^{13}C$ value of terrestrial substrates, and demonstrates the wide-ranging potential of using this proxy to reconstruct pCO_2 levels across the last 400+ million years of Earth history by exploiting the abundant terrestrial organic matter in the geologic rock record.

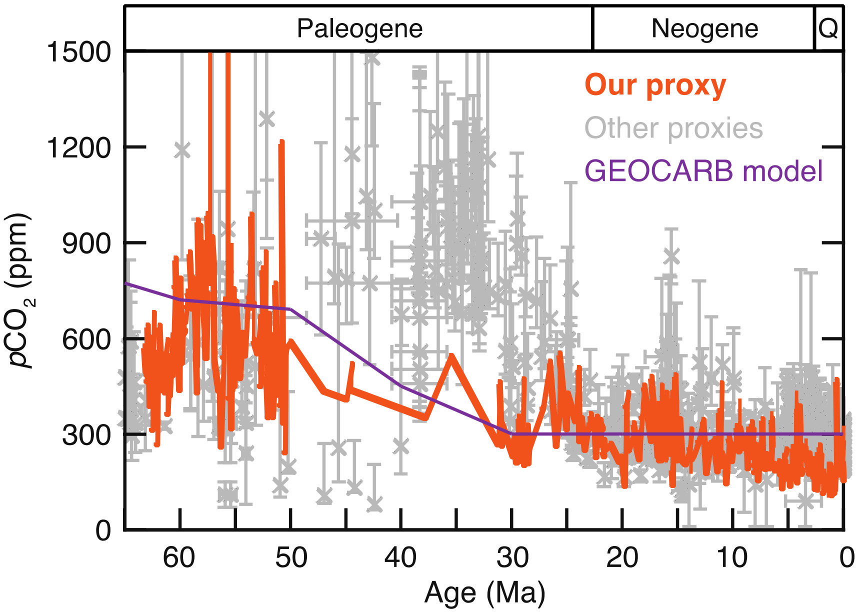

Reconstruction of pCO$_2$ across the Cenozoic Era (65-0 Ma). Our pCO$_2$ reconstruction using the δ^{13}C value of terrestrial organic matter (orange) follows similar trends observed in other published proxy values (gray) and a model of long-term carbon cycling (purple).

Poster 5

Internal Erosion, Particle Transport, and Channelization Drive by Fluid Flow

Arshad Kudrolli, Vikrant Yadav, and David Scheff
Clark University

The goal of the project is to investigate internal erosion and transport of particles leading to heterogeneity and channelization of a porous granular bed driven by fluid flow. Understanding this system is of fundamental importance to a number of geophysical processes and in the extraction of hydrocarbons in the subsurface. Focusing on the work performed over the last year, we will discuss a system where channels form in a bed composed of granular and clay particles confined under pressure. A continuum three phase model was developed recently which shows that channels can develop from small differences in packing in an otherwise homogeneous medium which leads to increased porosity and nonlinear feedback. To build on this model, an erodible porous medium composed of millimeter scale grains and Bentonite clay was prepared in a Hele-Shaw cell. Thus in addition to granular friction and confinement pressure, cohesive interactions exist between the granular medium which resist the action of the fluid. The cohesive strength between the grains can be varied since it is found to be directly proportional to the amount of clay binder. When water is pumped through this porous medium, we find three distinct regimes as heterogeneity develops in the system. First, a discontinuous spatially rough fluid front moves through the system which fully saturates the medium as it advances but which does not initially change the internal structure. Then, a deformation of the particulate medium into finger-like structures is observed akin to the development of a slow fracture network. We obtain the spatio-temporal development of heterogeneity of the medium including its deformation field to differentiate it from a Saffman-Taylor instability observed in viscous fluids. As fluid flow increases through these features, we find a third stage to the development of the heterogeneity as the binder dissolves and loose beads are sheared away. Here, viscous fluid stresses and lift forces are important to the local rate of erosion. We discuss the measured integrated rates of erosion as well as the statistical development of heterogeneity and comparison with the three-phase model as a function of binding strength and consolidation of the medium. We then investigate the effect of the particle size on the onset of particle motion in channels within the bed. The Shields criteria given by the ratio of the viscous shear and normal stresses is used to understand the onset of motion at the boundaries. We find systematic variation with particle Reynolds Number at the interface. In particular we find that that Shields criteria gives different values depending on if the shear rate is changed or if the particle size is changed. We compare and contrast the values obtained assuming no-slip boundary conditions with those observed using florescent tracer particles to measure the fluid flow profile near the porous interface.

Image:

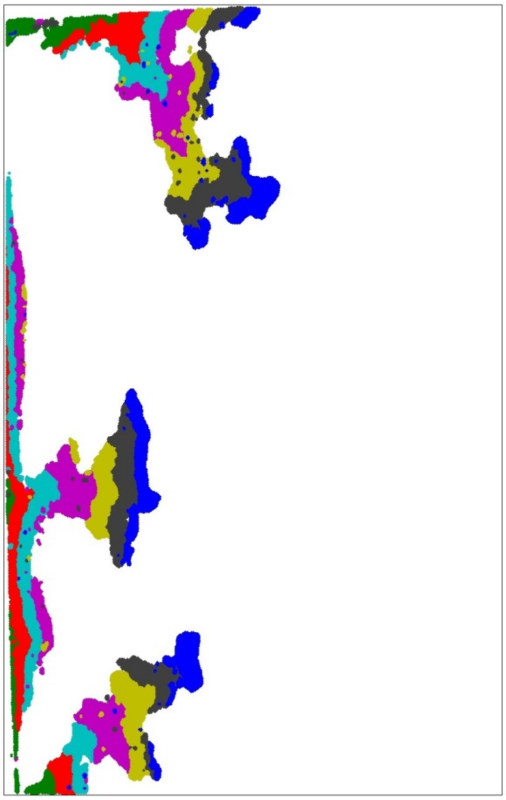

Development of heterogeneity and channel flow observed as fluid is injected uniformly from the left into a quasi-two dimensional system composed of granular matter and clay which serves as a binder. The various colors correspond to the advance of the channel features with time.

Poster 6

Porosity/Permeability Evolution and Pore-Confined Fluid Properties in Natural and Synthetic Geologic Media

Lawrence M. Anovitz, G. Rother, M.S. Gruszkiewicz, S.L. Brantley, D.R. Cole, P.T. Cummings, C. McCabe, S. Hlushak, L. Vlcek, E. Mamontov, A.K. Kolesnikov, N. Choudhury,
ORNL and Penn State University

The nano-structural features and evolution of pore space are critically important factors controlling fluid properties in geological formations, including the migration and retention of water and hydrocarbons, sequestration of wastes, the formation of ore deposits, and the evolution of geologic systems. The size, distribution and connectivity of these confined geometries dictate how fluids migrate into and through these environments, wet and react with the solid surfaces over length scales ranging from the nano- to the macro-scale and, at the smaller scales, the properties of the fluids themselves. The goal of this project is to understand and ultimately predict how geochemical and geological processes control the evolution of porous fluid-rock systems and the properties of geofluids.

We investigate the multiscale pore structure of rock materials representative of important geologic processes using a combination of small and ultra-small angle neutron scattering and image processing. Results show significant differences in the overall pore structures of varying rock types and stages of reaction. Multi-scale pore structure found in rocks can often be precisely characterized using a combination of fractal concepts and standard petrography. Carbonates and shales show combined mass plus surface fractal behavior that transitions to a surface fractal dominated structure. Sandstones, by comparison, show no evidence of mass fractal behavior. While apparent surface fractal behavior is common, this can often be decomposed into assemblages of pores at different scales, often with no evident surface fractal behavior. These patterns are, however, modified by geological processes. For instance, our analysis suggests that overgrowth formation in sandstones tends to fill larger pores first, while reactive crystallization may primarily fill smaller pores. Work is ongoing to further elucidate how the pore structure, and thus the pathways for reactive transport, is modified by such processes.

The physical properties of fluids in the nanopore systems play important roles in the formation of subsurface geofluid reservoir formation and geofluid extraction. Using a combination of experimental and computer modeling tools, we investigate the structure and dynamics of pure and mixed fluids in synthetic and natural porous rocks. Experimental studies rely on excess sorption, vibrating tube, and neutron scattering techniques. Combined analysis of excess sorption and small-angle neutron scattering data yields the volume and mean density of the sorption phase for different conditions of pressure, temperature, composition and pore structure/surface chemistry. The dynamic properties of pore fluids are measured as a function of pore loading with inelastic, quasielastic, and coherent spin-echo neutron scattering methods. Computer modeling using Density Functional Theory, Monte Carlo techniques, and Molecular Dynamics simulation is extensively utilized to gain atomistic level insight into the structural and dynamic behavior of pore and interfacial fluids and enhance interpretation of experimental data in both the nanometer (confinement) and sub-nanometer (ultra-confinement) regimes. In the latter, minerals with channel structures (e.g. beryl) that can be obtained in large single crystals are used to quantify directional variations, perpendicular and parallel to the channel directions, in the dynamics of the confined fluid. In beryl these are significantly anisotropic and, somewhat counter-intuitively, show that vibrations parallel to the c-axis channels are significantly more hindered than those perpendicular to the channels, suggesting quantum tunneling between symmetrically- identical orientations of the ultra-confined water molecules.

Recent Publications

1. Anovitz, LM. Mamontov, E., Ishai, PB, and Kolesnikov, AI (2013) Anisotropic dynamics of water ultra-confined in macroscopically oriented channels of single-crystal beryl: A multi-frequency analysis. *Physical Review E*, 88(5) 052306.
2. Anovitz, LM, Cole, DR, Rother, G, Allard, LF JR., Jackson, A, and Littrell, KC (2013) Diagenetic changes in macro-to nano-scale porosity in the St. Peter Sandstone: an (Ultra) small angle neutron scattering and backscattered electron imaging analysis. G*eochimica et Cosmochimica Acta*, 102, 280-305.
3. Bazilevskaya, E., Lebedeva, M., Pavich, M., Rother, G., Parkinson, D. Y., Cole, D. R., Brantley, S. L. (2012) Where fast weathering creates thin regolith and slow weathering creates thick regolith, *Earth Surface Processes and Landforms*, DOI: 10.1002/esp.3369
4. Buss, H. L., Brantley, S. L., Scatena, F. N., Bazilevskaya, E., Blum, A., Schulz, M., Jimenez, R., White, A. F. (2013) Probing the deep critical zone beneath the Luquillo Experimental Forest, Puerto Rico, *Earth Surface Processes and Landforms*, DOI: 10.1002/esp.3409.
5. Jin, L., Mathur, R., Rother, G., Cole, D. R., Bazilevskaya, E., Williams, J., Carone, A., Brantley, S. L. (2013) Evolution of porosity and geochemistry in Marcellus Formation black shale during weathering, *Chemical Geology*, 356, 50-63.
6. Navarre-Sitchler, A. K., Cole, D. R., Rother, G., Jin, L., Buss, H. L., and Brantley, S. L. (2013) Porosity and surface area evolution during weathering of two igneous rocks, *Geochimica et Cosmochimica Acta*, 109, 400-413.
7. Wang, H-W, Anovitz, LM., Burg, A, Cole, DJ, Allard, LF, Jackson, AJ, Stack, AG, and Rother, G (2013) Multi-scale characterization of pore evolution in a combustion metamorphic complex, Hatrurium basin, Israel: Combining (ultra) small-angle neutron scattering and image analysis. *Geochimica et Cosmochimica Acta*, 121, 339-362.

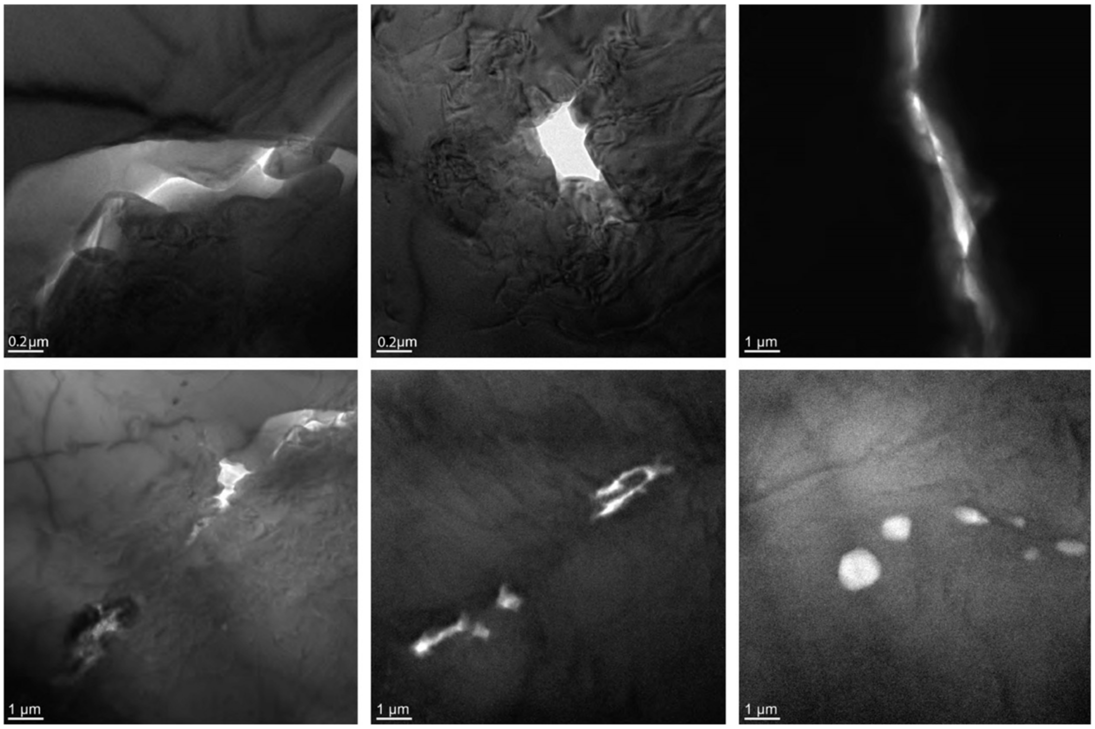

TEM images of micron to submicron porosity in the St. Peter Sandstone (Anovitz et al. 2013)

Poster 7

Permeability Evolution and the Mechanisms of Porosity Change

Wenlu Zhu[1] and Meg Tivey[2]

[1]*Department of Geology, University of Maryland*
[2]*Department of Marine Chemistry & Geochemistry, Woods Hole Oceanographic Institute*

Understanding subsurface fluid flow is of critical importance to such geological and engineering applications as faulting mechanics, hydrothermal venting and resource recovery. Mechanical, chemical and thermal loads can significantly alter microscopic pore geometry and thus affect macroscopic permeability. Recently, we measured the permeability and porosity of massive anhydrite deposits recovered from various seafloor hydrothermal vent fields. Together, these deposits comprise anhydrite samples that have undergone different stages of formation. For anhydrite samples with porosities greater than 5%, the dependence of permeability to porosity change is best characterized by a power--law relationship with an exponent n~9. At porosities less than 5%, a much gentler trend of n~1 is observed. These permeability—porosity relationships (PPRs) in anhydrite deposits are in stark contrast to those of Fontainebleau sandstone, a quartz arenite with various degrees of quartz cementation. Fontainebleau sandstone shows a power-law dependence of PPR with an exponent of n~3 for samples with porosities greater than 7%, and a much steeper trend of n~8 at low porosities[Bourbie and Zinszner,1985]. Microstructural analysis and numerical models suggest that the significant loss in pore connectivity below 7% is responsible for the steeper PPR trend in Fontainebleau sandstone [Zhu et al., 1995]. In anhydrite deposits, petrographic analyses show evidence for both dissolution and precipitation, consistent with the observed PPRs resulting from pore-size controlled solubility. Precipitation of anhydrite takes place preferentially in large pores within the anhydrite deposits, with precipitation limited in small pores, which is proposed to be due to the change in interfacial energy of the growing crystal (e.g., as described by Emmanuel and Ague[2009]). With abundant large voids in high porosity anhydrite samples, the growth of sulfates would result in a drastic loss of pore connectivity and permeability decrease (n~9). As precipitation continues, there would be an increase in population of small pores. Effective solubility generally increases with decreasing pore size, thus enhancing dissolution and likely keeping fluid paths open, thus explaining the observed more gradual permeability reduction (n~1). This observation of distinct PPRs at higher versus lower porosities, and the proposed mechanism, provide important constraints for modeling hydrothermal recharge zones. Reliable permeability models require integration of the mechanisms of porosity change to the upscaling methods.

Poster 8

Experimental and Computational Methods Used to Probe the Behavior of Fluids in Nanopores

S. Gautam[1], A. Striolo[2], A. Phan[2], S. Ok[1], K. Mueller[3], D. Hoyt[3], N. Washton[3] and D. Cole[1]
[1]The Ohio State University, [2]University College London, [3]PNNL/EMSL

Fluids are the main transport agents for the flow of energy and matter throughout the lithosphere and are often found confined in the pores or fractures of various complex materials like rocks and soil. For example, hydrocarbons trapped in shale formations have recently attracted great interest due to the industry exploration and exploitation of shale gas. An important aspect is the effect of confinement on the hydrocarbon properties. Under confinement, the properties of fluids in general are known to be affected profoundly by the confining media. Understanding the interplay of these factors is essential in order to extract and ultimately exploit hydrocarbons from their natural environments. We have made a synergistic use of experiments and computer simulations to study these effects. While computer simulations provide information not accessible to experiments and aid the interpretation of experimental results, experimental data is used to validate the reliability of computer simulations. Nuclear Magnetic Resonance (NMR) is an experimental technique well suited to study the molecular structure and dynamics at interfaces by following the chemical shift and the longitudinal and transverse relaxation rates for the molecular species of interest. We have probed methane interacting with mesoporous silica having 200 nm particle size and 4 nm pores and a high surface area non-porous silica using NMR [1]. The goal was to compare the impact of pore confinement versus surface-only effects on methane as a function of pressure and temperature. The interaction of methane and mesoporous silica yielded two signals, one likely due to a combination of pore-wall and reduced dimensionality effects in the 4 nm pores and the other exhibiting more bulk-like behavior as benchmarked by the control experiment of pure methane only. Whereas no shifts were observed in the baseline experiments on varying temperature, pressure was found to induce shifts in the methane peak position: ~0.25 ppm going from 30 to 60b, and ~0.50 ppm shift going from 30 to 120b. Another important tool in studying fluid behavior in confinement is neutron scattering. This is because the energy and wavelength of cold and thermal neutrons fall in the same range as that of the motions and spatial structure respectively of molecules confined in porous materials. In particular we have used quasielastic neutron scattering (QENS) to study the dynamical properties of propane under confinement in nanopores of silica aerogel [2]. The effects of pressure changes are found to dominate the effects of temperature variation on the dynamics of adsorbed propane. At lower loadings of propane, the QENS signal shows that most of the propane molecules are adsorbed on the silica aerogel surface, only a small fraction is free to move. As the propane loading is increased, more molecules become freely available to take part in the diffusional dynamics and thus enhance the diffusivity at higher pressures. A change in the mechanism of motion from low pressure to high pressure has also been observed. While at low pressure the propane molecules take part in a continuous diffusion, at higher pressures the diffusion occurs via the mechanism of jumps. The presence of CO_2 is seen to enhance the jump rate of propane molecules (by about an order of magnitude) thereby increasing the diffusion coefficient. The experimental efforts mentioned above have been supplemented with Computer Simulations. In particular, we focused on the behavior of hydrocarbons such as methane and propane under confinement in silica pores. In one recent study [3] we focused on the solubility of methane in water when water is confined in a 1 nm silica slit pore. We found two unexpected results: (1) methane solubility in confined water can be ~ 1 order of magnitude larger than that in bulk water at similar T (298K) and P (15-26 MPa) conditions; and (2) we found some evidence of hydrate cages, despite the pore was too narrow for the comfortable formation of hydrate cages, and despite the T and P conditions were not conducive to the formation of hydrates in bulk systems. In another computational study [4], we have found that in case of propane and CO_2 mixture in mesoporous SiO_2 the CO_2 – SiO_2 interaction plays a dominant role. CO_2 is thus seen to have a tendency to replace propane adsorbed on a SiO_2 surface corroborating our QENS results.

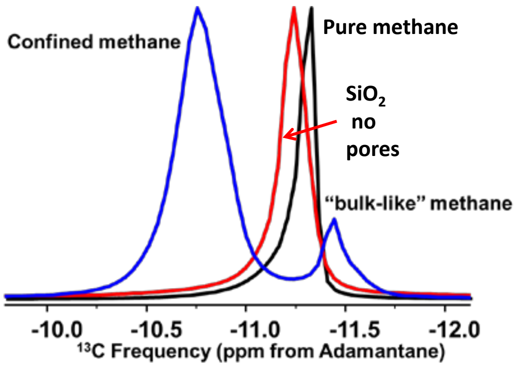

Fig. 1 Proton decoupled ^{13}C NMR spectra of pure CH_4, CH_4 interacting with mesoporous SiO_2 (blue) and SiO_2 powder (red) [1]

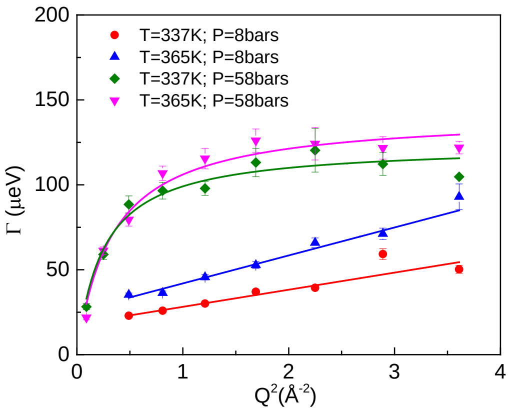

Fig. 2 Variation of quasielastic width of propane in silica aerogel. A change in the behavior is due to surface effects at low pressure that suppress the motion of propane molecules [2]

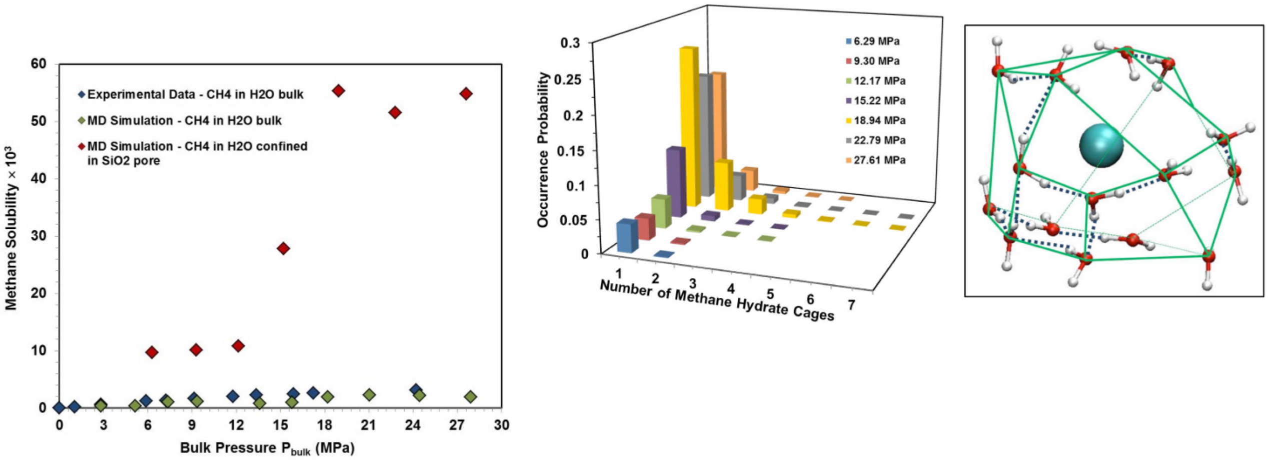

Fig. 3. (left) Methane solubility in liquid water as a function of bulk pressure. Simulation data for confined systems from this work are shown as red diamonds. Simulated bulk CH_4 solubility data in liquid water at 298K as reported by Sakamaki et al. (2011) [5] are shown as green diamonds. The corresponding experimental data for CH_4 in bulk water are shown as blue diamonds. (right) There is evidence for the formation of hydrate cages, although they are imperfect and short-lived [3].

References

[1] Salim Ok, Julie Sheets, Sue Welch, David Hoyt, Karl Mueller, Nancy Washton, Amity Andersen and David Cole, (under review)

[2] Siddharth Gautam, Tingting Liu, Gernot Rother, Niina Jalarvo, Eugene Mamontov, Susan Welch, Michael Droege, and David Cole, *J. Chem. Phys.* (2014) (under review)

[3] A. Phan, D.R. Cole, A. Striolo, *J. Phys. Chem. C* (2014) **118** 4860.

[4] T. Le, D.R. Cole, A. Striolo, *Chem. Eng. Sci.* (2014) submitted.

[5] R. Sakamaki, A. K. Sum, T. Narumi, R. Ohmura, and K. Yasuoka, *J. Chem. Phys.* 2011, 134

Poster 9

Geoscience Challenges for Extracting Energy Safely from the Earth: The Rocks Matter

Elizabeth A. Eide,
Board on Earth Sciences and Resources, National Research Council (NRC),
500 5th Street, NW, Washington, DC 20001

Geological resources (petroleum, natural gas, coal, uranium and thorium, and geothermal) supported nearly 90 percent of the energy produced in the United States in 2012.[1] The rocks from which these resources are extracted contain information needed for effective, safe, and reliable use of these forms of energy. As part of the work it undertakes for the Department of Energy to provide neutral, independent guidance to the nation on Earth resource issues, the Board on Earth Sciences and Resources has overseen projects that have examined development of conventional and unconventional hydrocarbon resources, geothermal energy, and carbon capture and sequestration (CCS) and the rocks that are fundamental to these systems. This contribution outlines some of the results of recent work (NRC, 2013) that has addressed understanding of induced seismicity related to fluid injection and withdrawal during development of these three energy technologies and to disposal of wastewater through underground injection. Although only a small fraction of injection and extraction activities in the United States has induced seismicity at levels felt by the public, understanding the potential for inducing felt seismic events and for managing the occurrence of felt seismicity is important to state and federal agencies, industry, and the public.

Several findings emerged from the NRC report: (1) Induced seismicity associated with fluid injection or withdrawal in energy projects seems to be caused in most cases by a change in pore pressure that contributes to change in stress in the subsurface in the presence of faults with specific properties and orientations and a critical state of stress. The factor with most bearing on inducing seismic events is the net fluid balance (total balance of fluid introduced into or removed from the subsurface). (2) Energy technology projects that maintain a balance between the amount of fluid being injected and withdrawn, such as most oil and gas and geothermal projects, appear to produce fewer seismic events than projects that do not maintain fluid balance. (3) The process of hydraulic fracturing as presently implemented for shale gas recovery does not pose a high risk for inducing felt seismic events. (4) Injection for disposal of wastewater derived from energy technologies does pose some risk for induced seismicity, but few events have been documented over the past several decades relative to the large number of disposal wells in operation. (5) CCS, due to the proposed large net volumes of injected fluids, may have potential for inducing larger seismic events.

Understanding and characterizing the rocks in the subsurface has bearing on technology development, environmental planning, hazard and risk assessment, regulation, development of best practices, and public perception. The NRC report determined crustal stress conditions; faults, fault properties, and fault locations; pore pressure; and rock permeability to be among the significant natural characteristics of rocks in the subsurface where more data, characterization, monitoring, and knowledge would help in understanding the potential to generate felt seismic events during fluid injection or withdrawal.

Reference

National Research Council, 2013. Induced seismicity potential in energy technologies. The National Academies Press, Washington, DC.

---

[1] Energy Information Administration, http://www.eia.gov/energyexplained/?page=us_energy_home

Poster 10

Iron Oxide Redox Transformation Pathways: The Bulk Electrical Conduction Mechanism

Michelle Scherer, *University of Iowa* and Kevin M. Rosso, *PNNL*

Despite decades of research on the reactivity and stable isotope properties of Fe oxides, the ability to describe their redox behavior in the environment is still quite limited. Here, we focus on understanding reductive transformation of phases such as hematite (α-Fe_2O_3) and goethite (α-FeOOH) in Fe(II) aqueous solution. These oxides serve as excellent model systems for studies of electron conduction processes in semiconducting minerals more generally, and provide valuable insights into the effect of nanoscale conduction on reactivity relevant to subsurface fate and transport of contaminants and geodisposal of radionuclides. Our goal is to provide insight into environmental redox reactions involving semiconducting minerals, focusing on the influence of bulk electrical conduction. The objective is to develop a detailed understanding of relationships between interfacial electron transfer processes, surface structure and potential, and mineral semiconducting properties so that we can predict the extent of involvement of the bulk conduction mechanism in semiconducting mineral redox behavior.

Using synthetic ^{56}Fe-dominant goethite and hematite crystallites tailored for specific particle sizes and morphologies, we have performed ^{57}Fe(II) isotope tracer studies in anoxic solution to investigate the redox recrystallization of goethite and hematite via time-dependent partitioning of the two Fe isotopes between solid and solution compartments. To evaluate whether the concentration of aqueous ^{57}Fe(II) influences the isotope mixing and extent of Fe atom exchange in goethite, we conducted experiments over a range of aqueous Fe(II) concentrations (**Figure 1**). We lowered the pH of these experiments to 6.8 (from 7.5 used in our previous work) to avoid precipitation of ferrous hydroxide at the higher Fe(II) concentrations. XRD of the goethite particles after experiments indicated no formation of additional phases. A plot of the change in ^{57}Fe(II) in the aqueous phase over time for the different initial Fe(II) concentrations shows that as the aqueous Fe(II) concentration decreases, faster decay of the ^{57}Fe(II) tracer from solution is observed and a larger fraction of the goethite atoms is thus exchanged. We also ran a series of experiments where we varied the loading of goethite and kept the aqueous Fe(II) concentration constant at about 1 mM Fe(II) (**Figure 1**). At lower goethite loadings we observed slower decay of the ^{57}Fe(II) tracer and a smaller extent of goethite atoms exchanging with the aqueous phase. The two kinds of experiments and associated results have the similarity that a lower amount of Fe(II) relative to Fe(III)-oxide yields larger amounts of exchange. This result is consistent with the expectation from equilibrium thermodynamics that with increasing $Fe(II)_{(aq)}$ the stability field of the Fe(III)-oxide widens, according to $FeOOH + 3H^+ + e^- \leftrightarrow Fe^{2+} + 2H_2O$, and likewise $Fe_2O_3 + 6H^+ + 2e^- \leftrightarrow 2Fe^{2+} + 3H_2O$. However, in contrast, examination of the pH dependence shows that for constant Fe(II) concentration and goethite loading, less isotopic exchange occurs as the pH is lowered. The lower pH of 6.8 resulted in significantly less exchange than we previously observed at pH 7.5 (about 94%). Data collected at pH 5.0 indicate even less exchange, on the order of 3 to 8%. We hypothesize that this effect results from lower Fe(II) sorption and hydrolysis that occurs with decreasing pH, effects that decrease the frequency of Fe(II)(aq)-Fe(III)oxide encounter complexes that underlie the interfacial electron transfer reaction, and that lower the driving force for the interfacial electron transfer reaction itself, respectively.

With respect to particle size effects, initial experiments with hematite indicate that the extent of atom exchange correlates with particle size; high surface area hematite nanoparticles (~10 nm) exhibit complete exchange of iron atoms with aqueous Fe(II) whereas larger particles (~40 nm) undergo partial but significant exchange (i.e., ~ 25%). Highly crystalline hematite platelets (~10 μm) exhibit no measureable exchange. Similar to goethite, we also observe less exchange at lower pH values (decreasing from 25% to 2% as pH is lowered from 7.5 to 3.0). Thus the key master variables in this system are phase stabilities, which increase with increasing Fe(II)(aq) relative to Fe(III)-oxide and with increasing particle size, and pH, which when lowered impedes the interfacial electron transfer step that forms the basis for the isotopic exchange and recrystallization process. Detailed molecular simulations focusing on key steps in the recrystallization process are currently underway, towards development of a comprehensive mechanistic multiscale model that encompass the experimental observations and comprise a basis for expansion into a broader range of semiconducting mineral transformations.

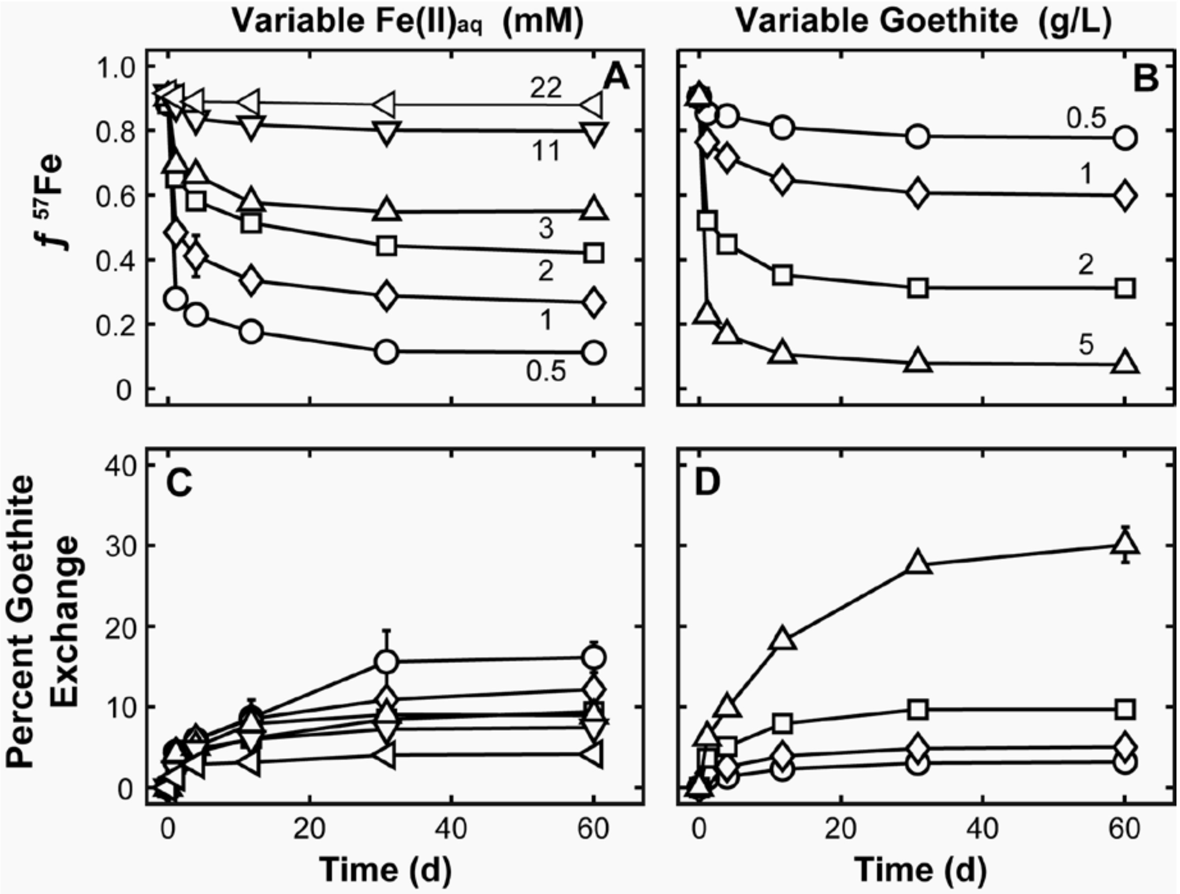

Figure 1. Temporal variation of the mole fraction of ^{57}Fe in $Fe(II)_{aq}$ with a range of **(A)** initial $Fe(II)_{aq}$ concentrations and a fixed goethite loading (i.e., 2 g L^{-1}) and **(B)** variable goethite concentrations with a constant initial $Fe(II)_{aq}$ concentration (i.e., 1 mM). Percent goethite exchange for variable **(C)** $Fe(II)_{aq}$ and **(D)** goethite concentration experiments. Percent goethite exchange (eq X) was calculated from ^{57}Fe variations in $Fe(II)_{aq}$. Reaction conditions: pH 6.8, 25 mM MOPS, and 25 mM KBr.

Recent Project Publications

Katz J.E., Zhang X., Attenkofer K., Chapman K.W., Frandsen C., Zarzycki P., Rosso K.M., Falcone R.W., Waychunas G.A., and Gilbert B. (2012) Electron small polarons and their mobility in iron (oxyhydr)oxide nanoparticles. *Science* 337, (6099) 1200-1203.

Chatman S.M.E., Zarzycki P., Preocanin T., and Rosso K.M. (2013) Effect of surface site interactions on potentiometric titration of hematite (α-Fe_2O_3) crystal faces. *Journal of Colloid and Interface Science*, **391**, 125-134.

Jordan D.S., Hull C.J., Troiano J.M., Riha S.C., Martinson B.F., Rosso K.M., and Geiger F.M. (2013) Second harmonic generation studies of Fe(II) interactions with hematite (α-Fe_2O_3). *Journal of Physical Chemistry C*, **117**, 4040-4047.

Chatman S.M.E., Zarzycki P., and Rosso K.M. (2013) Surface potentials of (001), (012), (113) hematite (α-Fe_2O_3) crystal faces in aqueous solution. *Physical Chemistry Chemical Physics*, 15, 13911-13921.

Handler R.M., Premartne, W.A.P Jeewantha, Frierdich, A.J., Beard B.L., Johnson C.M., Wang C., Rosso K.M., Latta, D.E., Neumann, A., Pasakarnis, T., and Scherer M.M. (2014) Fe(II)-catalyzed recrystallization of goethite revisited. *Environmental Science and Technology*, **Drafted**.

Zarzycki P. and Rosso K.M. (2014) Transient surface potential gradients as a driving force for the bulk conduction mechanism of iron oxide recrystallization. *Journal of Physical Chemistry*. **Drafted**.

Katz J.E., Zarzycki P., Zhang X., Attenkofer K., Chapman K.W., Rosso K.M., Falcone R.W., Waychunas G.A., and Gilbert B. (2013) Ferrous iron detachment is the rate-limiting step in the reductive dissolution of ferric iron oxide. *Environmental Science and Technology*, **Drafted.**

Frierdich, A.J., Helgeson, M., Liu, C., Rosso, K.M., Johnson, C.M., Beard, B.L., and Scherer, M.M. (2014). Fe(II)-catalyzed recrystallization of hematite. *Environmental Science and Technology*, **In Preparation**.

Zarzycki P. Frierdich, A.J., Scherer, M.M. Rosso K.M. (2014) Methods for quantifying heterogenous atom exchange. *Journal of Physical Chemistry*. **In Preparation**.

Poster 11

Pb and Cd Sorption to the Calcite-Water Interface: Structure and Process

Erika Callagon[1], Kathryn L. Nagy[1], Neil C. Sturchio[1]
Sang Soo Lee[2], Nouamane Laanait[2], Paul Fenter[2]

[1]*Department of Earth and Environmental Sciences, University of Illinois at Chicago*
[2]*Chemical Sciences and Engineering Division, Argonne National Laboratory*

Heavy metals, common environmental pollutants, are a threat to human health, and their transport in surface waters and groundwater is controlled in part by adsorption and precipitation reactions at mineral surfaces. The interaction of Pb and Cd with the calcite (104) surface was investigated through *in situ* observations of the surface in contact with metal-containing solutions, including high-resolution X-ray reflectivity (XR), resonant anomalous XR (RAXR), X-ray reflection interface microscopy (XRIM), and atomic force microscopy (AFM). Specular XR and RAXR reveal that Pb and Cd incorporate in several near-surface layers of calcite by substituting for Ca in the crystal. In the case of Pb, the different size of Pb vs. Ca induces strain that is manifested as vertical displacements of the incorporated Pb ion with respect to the Ca site. *In situ* AFM images obtained during reaction show that the Pb incorporation process occurs by a dissolution-regrowth mechanism, indicating that sequestration of Pb in calcite takes place through formation of an epitaxial but strained Pb-rich calcite solid solution at the interface. Similar results for Cd sorption show the formation of multiple Cd-rich layers at the calcite surface, i.e. a strained otavite-calcite solid solution. This type of solid solution may represent a widespread metastable host phase for Pb and Cd in groundwater aquifers and soil pore fluids.

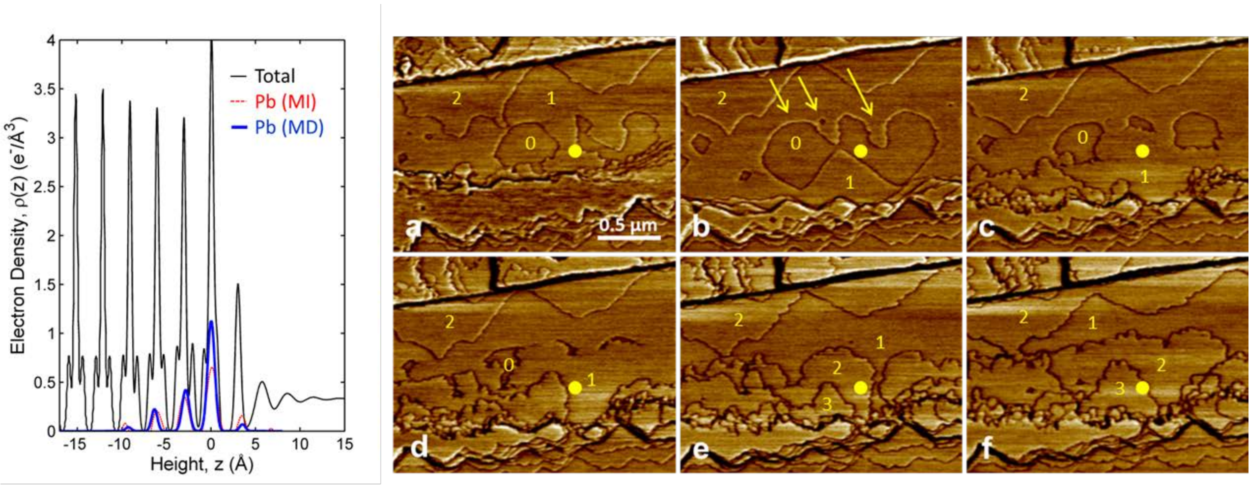

(Left) Laterally averaged total electron density profile (black line) and Pb-specific profiles (red and blue lines) after equilibration of calcite with an Pb-containing solution. (Right) AFM images of the changes in the calcite surface topography, including an initial transient dissolution and subsequent growth that explain the ability of Pb to incorporate below the calcite surface. (From Callagon et al., 2014)

Poster 12

Reactivity of structural iron in natural nontronite and synthetic Fe-phyllosilicate

Anastasia Ilgen and Jessica Kruichak
Sandia National Laboratories, Albuquerque, NM

Heterogeneous redox reactions on clay mineral surfaces affect the mobility of redox-sensitive contaminants and nutrients in soils. Clay minerals commonly have structural iron (Fe) due to substitution for aluminum (Al) in the octahedral sheet, and it can directly participate in electron transfer reactions. We investigated the redox properties of two substrates: nontronite clay NAu-1 (supplied by the Clay Repository of the Clay Minerals Society), and synthetic Fe-phyllosilicate, which we synthesized and characterized in our laboratory. The redox behavior of these two substrates was tested in batch experiments with redox active elements - arsenic (As), chromium (Cr), and selenium (Se). The aqueous speciation was analyzed using liquid chromatography coupled to an inductively coupled plasma mass spectrometer (LC-ICP-MS). Solid phase speciation of the trace metals was analysed using synchrotron-based X-ray Absorption Spectroscopy (XAS) techniques.

Our results indicate that structural Fe in both synthetic Fe-phyllosilicate and natural NAu-1 clay exhibit similar reactivity trend with respect to As(III) oxidation: some structural Fe(II) is necessary for the structural Fe(III) to oxidize As(III) to As(V). We also tested whether this mechanism is applicable to Se(IV) oxidation. We tracked changes in the speciation of selenium, initially added as Se(IV), in a fully oxidized and partially reduced NAu-1 (~20% of structural iron is Fe(II)) suspensions. The analysis of XAS data indicates that Se(IV) is not oxidized to Se(VI) over the 48 hour reaction time in the presence of either substrate. This difference in reactivity between As(III) and Se(IV) systems can be potentially attributed to the difference in the standard redox potentials of the homogeneous redox reactions, or to the differences in the sorption complex geometry – while arsenic forms inner-sphere bi-dentate complexes, selenium is predominantly adsorbed as an outer-sphere complex. Oxidation experiments with Cr(III) under oxic conditions indicate that all examined Fe-rich substrates enhance the rate of Cr(III) oxidation to Cr(VI) under oxic conditions over 24 hours, compared to the homogeneous control system with no clay substrates.

Sandia National Laboratories is a multi-program laboratory managed and operated by Sandia Corporation, a wholly owned subsidiary of Lockheed Martin Corporation, for the U.S. Department of Energy's National Nuclear Security Administration under contract DE-AC04-94AL85000.

Poster 13

Controlling and measuring water potentials and water film thicknesses on mineral surfaces

T.K. Tokunaga, Y. Kim, J. Wan, S. Wang, A. Lanzirotti, M. Newville, S. Sutton, W. Rao, and S. Wirrick
Lawrence Berkeley National Laboratory and University of Chicago

Water films influence and even control flow, reactions, and transport in unsaturated geologic environments including soils, the vadose zone, geothermal reservoirs, and oil/gas reservoirs. We are investigating how constraints imposed by physical scale (pore size), geochemical properties (mineral surface chemistry and aqueous geochemistry), and the potential energy status of water control its adsorption and capillary retention in geologic materials. Understanding water and gas (air) distribution at the pore scale is needed to improve the physicochemical basis for predicting macroscopic flow and transport properties. Goals of recent BES Geosciences research are to (1) develop conceptual models for constraining capillary influences on film thicknesses, (2) develop experimental approaches for testing surface capillary relations to surface roughness, and (3) develop a new method for controlling water activities in the environmentally important region very near 100% relative humidity.

We developed predictions for the matric (disjoining) potential dependent adsorbed water film thickness on different mineral surfaces, based on the Derjaguin-Landau-Verwey-Overbeek (DLVO) analysis of van der Waals and electrostatic interactions, including influences of solution chemistry and interfacial (mineral-water and gas-water) charge. These predictions are in good agreement with measurements that span more than 5 orders of magnitude in matric potential.

We developed a novel approach for equilibrating water films at very near-zero matric potentials (-10 kPa to -50 Pa), on surfaces with arbitrary roughness. X-ray microprobe based measurements of films on rough surfaces demonstrate the primary importance of surface capillarity at near-zero matric potentials.

For more negative potentials (-0.1 MPa to -10 MPa), we predicted that several previously untested saturated salt solutions could control relative humidities in the very high range of 0.999 to 0.90; conditions often occurring in the subsurface. These predictions were confirmed through water activity measurements, and used control very high humidities in water vapor adsorption isotherm experiments. New experiments on ion diffusion in adsorbed water films will utilize this method for regulating unsaturated systems at very high humidities, and contribute to efforts to understand salinity influences on ion diffusion to be conducted within the LBNL Geochemistry Project.

Poster 14

Optimizing capillary trapping for storage of CO_2: Lattice Boltzmann simulations of the Brine-CO_2 system for reservoir conditions

Marcel G. Schaap[1] and Dorthe Wildenschild[2]

[1]Department of Soil, Water and Environmental Science, College of Agriculture and Life Sciences, University of Arizona, Tucson, Arizona
[2]School of Chemical, Biological, and Environmental Engineering (CBEE) , Oregon State University, Corvallis Oregon

This project is a collaboration between Oregon State University (led by Dr. Dorthe Wildenschild) and the University of Arizona to investigate pore-scale aspects of capillary trapping to enhance the efficiency of geological CO_2 sequestration in deep saline aquifers where super-critical conditions prevail. Compared to most current reservoir-scale studies, our research takes several steps back in scale to observe and model trapping at the pore-scale using a combination of computed micro-tomography imaging (performed by OSU) and multi-phase/multi-component lattice Boltzmann (LB) simulations (carried out by UA). The main objective is to quantify how pore-scale mechanisms translate into continuum scale properties that can subsequently support improved modeling of sequestration at large spatio-temporal scales.

For the purposes of this project it is essential to correctly simulate the physical conditions under which super-critical CO_2 will be present after injection into the host rock. In practice this means that the LB model should be able to handle the pressures (*P*), densities (□), temperatures (*T*) that prevail in deep geological media. A logical way of dealing with is is to combine a single-component LB model with and Equation of State (EOS) that describes the physical interrelations among *P*, □and *T* (*Yuan and Scheafer*, 2006). Previously, we showed that the Peng-Robinson (PR) EOS provides an excellent fit to super-critical conditions for the pure CO_2 system (Figure 1). However, simulating pure-CO_2 systems is not sufficient as the super-critical CO_2 will co-exist (and interact) with brine present in the saline aquifers. In effect this means that we need to simulate multi-component systems: one phase being the super-critical CO_2, the other phase being a brine of varying salinity. A natural extension to the work under is to also treat the brine with an EOS. The brine will of be in a *sub-critical* state (the critical point of pure water is at 647 K and 22.064 MPa), thus it is important to find an EOS that can faithfully match the physical conditions of brine between temperatures of 300 and 400K and pressures between 7 and 30 MPa. Figure 2 shows a modified van-der Waals EOS equation that appears suitable for simulating brine under reservoir conditions.

This poster will present a number of EOS alternatives that attempt to correctly capture the density of the liquid branch of the water system for relevant temperatures and pressures and allow for a mismatch between modeled and experimental vapor densities. Comparison simulations with micro-tomography data recently obtained by the OSU group are still underway and the authors hope these numerically intensive simulations will be ready for presentation at the Geosciences meeting.

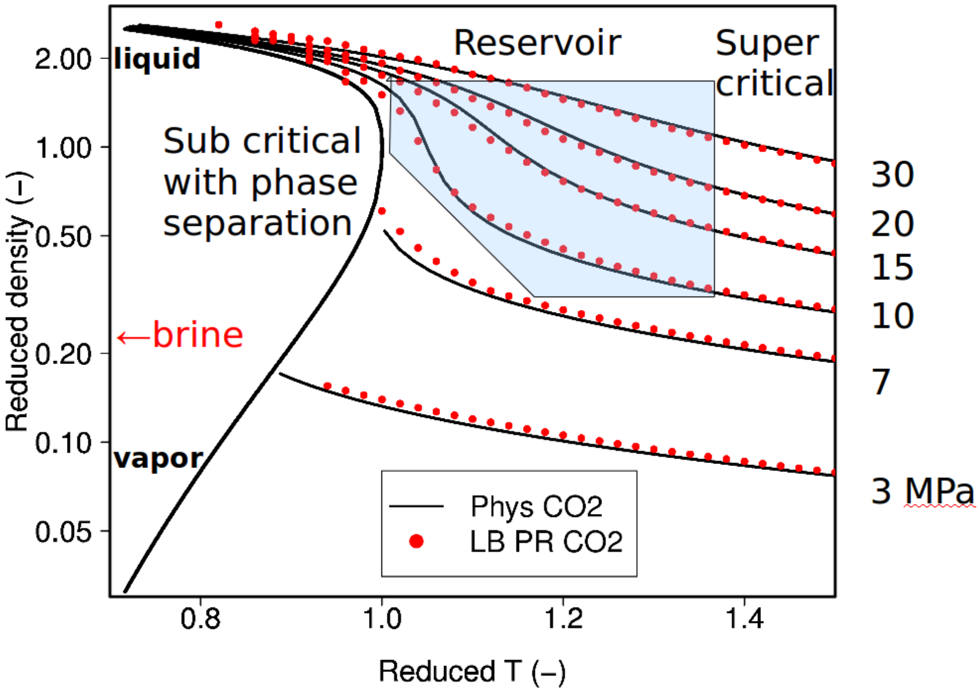

Figure 1. Peng-Robinson equation of state for the pure CO_2 system. Black lines are experimental data from the literature (NIST), red dots are LB simulated values based on the Peng-Robinson EOS, showing that the entire relevant super-critical realm (blue area) for CO_2 is accessible with LB simulations.

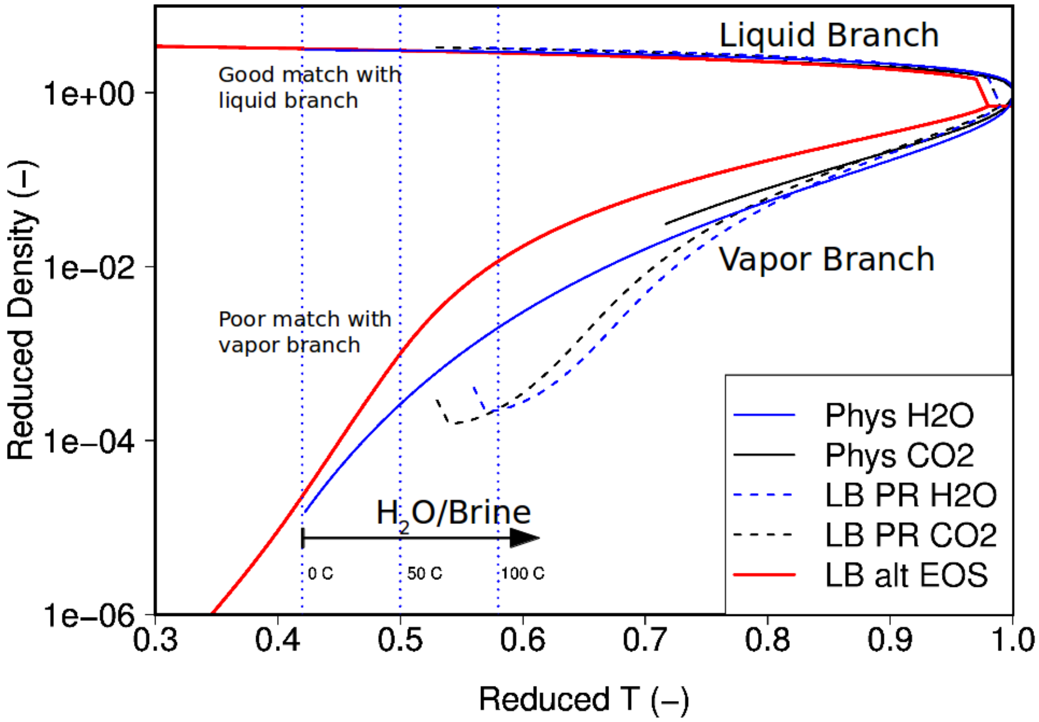

Figure 2. Modified van der Waals EOS (“LB alt EOS) with suitable liquid densities and numerical stability for earth surface and reservoir conditions (0 °C and greater).

Poster 15

Integrated X-ray, neutron and electron microscopic crystal chemical investigation of uranium contamination

David C. Elbert and David R. Veblen
Department of Earth and Planetary Sciences, Johns Hopkins University, Baltimore, MD 21218

This project involves multidisciplinary investigation of crystal chemical relations important in uranium-contaminated soils. Work on uranium-contaminated soils from numerous locations highlights the importance of uranyl phosphates, uranyl silicates, and uranium oxide minerals in groundwater zones at DOE sites and in weathered ore deposits.

In situ X-ray and neutron scattering experiments show dehydration reactions in autunite-group minerals are sensitive to both temperature and a_{H_2O}. The studied dehydration reactions are reversible and although reaction kinetics are difficult to quantify, complete reversal takes only minutes to hours in the lab setting.

Neutron scattering experiments on powders have been used to constrain the structure of interlayer hydration environments in the Cu uranyl-phosphate, metatornernite and it's lesser hydrates. Structural solution from powder experiments require peak indexing that is complicated by significant peak overlap. We have used electron diffraction and inferences from X-ray work to constrain the indexing and allow preliminary structure solution using charge flipping and simulated annealing techniques.

The environmental geochemistry of uranium is redox sensitive with dominant species being U(IV) or U(VI). Transmission Electron Microscope (TEM) based electron energy-loss spectroscopy (EELS) has been used by several workers to provide insight into uranium valence at the sub-micron scale. Previous work centered on use of $O_{4,5}$ and $M_{4,5}$ absorption edge structure to probe details of bonding and valence state in U. These methods are problematic for two reasons: 1) $M_{4,5}$ edges have extremely small scattering cross sections and require impractical electron fluences that damage samples rapidly. 2) $O_{4,5}$ edges are completely hidden beneath the giant resonance. Our work now focuses on $N_{4,5}$ and $N_{6,7}$ edges to provide uranium valence information.

Poster 16

The influence of water on the deformation behavior of mantle rocks

S. Mei[1], D. L. Kohlstedt[1], N.A. Dixon[2], and W. B. Durham[2]
[1]*University of Minnesota, Minneapolis, MN 55455*
[2]*Massachusetts Institute of Technology, Cambridge, MA 02129*

The effect of water on the rheological properties of mantle rocks (e.g., olivine and garnet, both are major mantle minerals) were investigated with triaxial compressive creep experiments at high pressures ($2 \leq P \leq 7$ GPa) using a deformation-DIA apparatus. In our experiments, a sample column composed of a sample and alumina pistons was assembled with a talc sleeve and graphite resistance heater into a 6.2-mm edge length cubic pressure medium. Experiments were carried out at the National Synchrotron Light Source at Brookhaven National Laboratory. In each run, differential stress and sample displacement were monitored *in-situ* using synchrotron x-ray diffraction and radiography, respectively. Experimental results reveal a significant influence of water on the rheological response of both olivine and garnet. For example, the Peierls stress of olivine under hydrous conditions (~4.5 GPa) is much lower than it under anhydrous conditions (>6 GPa). At a given stress, garnet deforms ~2 orders of magnitude faster under hydrous conditions than that under anhydrous conditions. The deformation behavior of both olivine and garnet under hydrous conditions has been quantitatively described in the form of a flow law that establishes the dependence of deformation rate on stress, temperature, pressure, and water fugacity. The flow laws for olivine and garnet quantified in this study provide critical constraints for modeling the dynamic activities occurring within Earth's interior.

Poster 17

Structure and Dynamics of Aqueous Solutions and Mineral-Solution Interfaces

David J. Wesolowski, Ariel A. Chialvo, Andrew G. Stack, Lukas Vlcek, Miroslaw S. Gruszkiewicz, Eugene Mamontov, Paul.R.C. Kent (ORNL), Peter.T. Cummings (Vanderbilt), Jorge.O. Sofo, James.D. Kubicki, A.C.T. van Duin (Penn State), Michael L. Machesky (Illinois), Paul.A. Fenter, Francesco Belluci (ANL), Franz Geiger (Northwestern)

The fundamental understanding and consequent description of geochemical environments and processes depend on our ability to capture accurately the relevant physicochemical phenomena taking place at the mineral-fluid interfaces, where the latter relies on our atomic-level interpretation of the interplay between the nature of the minerals, their porosity, fluid composition, and state conditions. Typically, interfacial fluids exhibit microstructural, dynamical, and thermophysical behaviors that differ significantly from the bulk counterparts, as a manifestation of the molecular asymmetry between fluid-fluid and solid-fluid interactions, whose immediate consequence is an inherent inadequacy of classical macroscopic modeling approaches to describe interfacial fluids. The starting point in the development of a fundamental and predictive understanding of fluid-rock interactions is the nature of the interface, at the atomic to nanoscale. This interfacial region is characterized by mineral surface atom relaxation, surface oxygen protonation, ion adsorption, and the strong ordering and hindered mobilities of interfacial fluids and solutes within a few nanometers of the interface. Since this is precisely the region in which surface reactions occur, it is vital to understand in detail the relationships between altered interfacial fluid and substrate structures, transport dynamics and bonding strengths and geometries. However, at this scale, neither atomic-nanoscale experimental probes (*e.g.*, X-ray and neutron scattering, nonlinear optical spectroscopies, *etc*.), nor computational methodologies (*e.g.*, static and dynamic *ab initio* calculations, classical and reactive molecular simulation) alone are sufficient to capture the quantitative details of interfacial phenomena needed to build predictive models of interfacial equilibria and reaction rates and mechanisms. The experimental and computational approaches mentioned above have been fully integrated in our studies of the structure and dynamics of water and aqueous electrolytes at model mineral surfaces that exhibit a range of bulk substrate polarizability (quartz, cassiterite, rutile) and covalent vs. ionic bonding (quartz, barite). Recent progress includes predictive understanding of the temperature dependence of ion sorption and interfacial transport properties of aqueous electrolytes at the rutile (110) surface, the influence of substrate polarizability on the degree of water dissociation and the hydrophobicity of rutile versus cassiterite (110) surfaces driven by unusually strong hydrogen bonding, and the influence of dissolved ions on the H-bonding at quartz (101)-solution interfaces that is the first step in the dissolution of the surface. These observations have enabled us to test and challenge the ability of current *ab initio* approaches to adequately describe the bonding and dynamics of interfacial water and the stabilities of nanoparticles in the environment. Our studies emphasize the crucial need for physically sound molecular models for simulation purposes to gain understanding of the fluid behavior and their physicochemical interactions with mineral. However, the complexity of such models makes their force-field optimization extremely challenging. To address that challenge while avoiding significant computational expenses from either matrix search or gradient-based methods, we have developed an alternative approach that takes advantage of underlying statistical mechanical links between the system's particle interactions and the observable thermodynamic, structural, and dynamic properties.

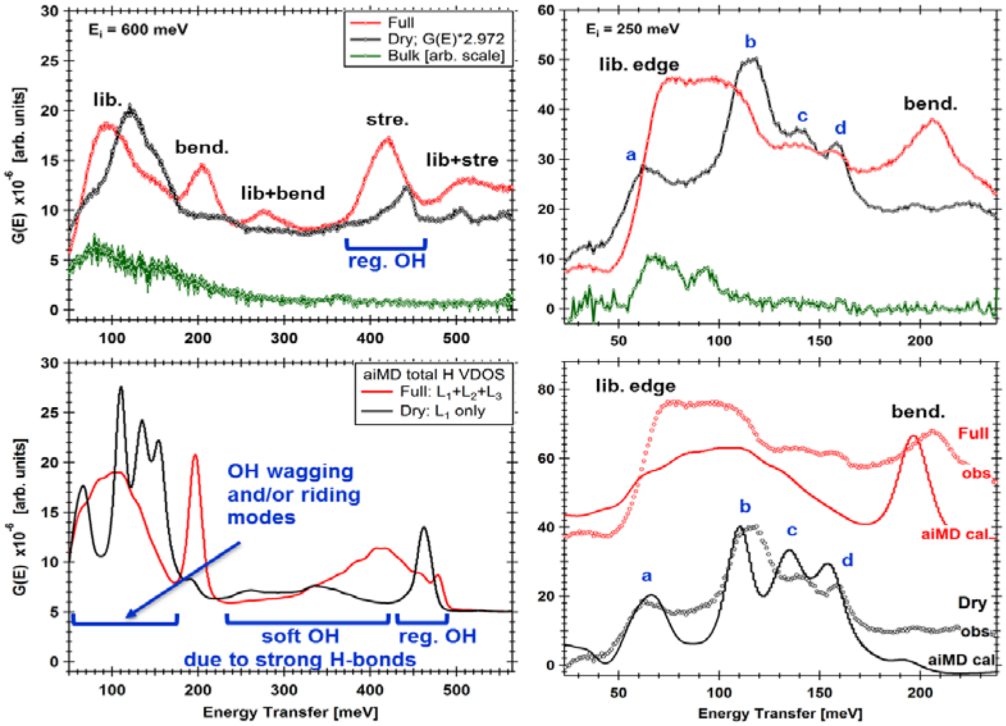

Dynamic properties of water on hydrated cassiterite (SnO$_2$) nanoparticles as a function of surface coverage, by Inelastic Neutron Scattering (top) and *ab initio* Molecular Dynamics (Wang *et al*., 2014).

Recent Publications:

Dellostritto, M.; Kubicki, J.; Sofo, J. Density Functional Theory Simulation of Hydrogen-Bonding Structure and Vibrational Densities of States at the Quartz (101)-Water Interface and its Relation to Dissolution as a Function of Solution pH and Ionic Strength. *J. Phys.: Condens. Matter* **2014** (in press)**.**

Kumar, K., Kent, P.R.C., Wesolowski, D.J., Kubicki, J.D., Modeling water adsorption on rutile (110) using van der Walls density functional and DFT plus U methods, *J. Phys. Chem. C* **2013**, *117*, 23638-23644.

Mamontov, E.; O'Neill, H.; Zhang, Q.; Wang, W.; Wesolowski, D.J. Common Features in the Macroscopic Dynamics of Hydration Water on Organic and Inorganic Surfaces. *J. Phys.: Condens. Matter* **2012,** *24*, 064104.

Parez, S.; Predota, M.; Machesky, M. The Dielectric Properties of Water at Rutile and Graphite Surfaces: Effect of Molecular Structure. *J. Phys. Chem. C* **2014** (in press)**.**

Predota, M., Machesky, M.L., Wesolowski, D.J., Cummings, P.T., Electric double layer at rutile (110) surface. 4. Effect of temperature and pH on the adsorption and dynamics of ions. *J. Phys. Chem. C.*, **2013**, *117*, 22852-22866.

Raju, M.; Kim, S-Y.; Van Duin, A.; Fichthorn, K. ReaxFF Reactive Force Field Study of the Dissociation of Water on Titania Surfaces. *J. Phys. Chem. C.* **2013**, *117*, 10558-10572.

Wang, H.-W.; Wesolowski, D.; Proffen, T.; Vlcek, L.; Wang, W.; Allard, l.; Kolesnikov, A.; Feygenson, M.; Anovitz, L.; Paul, R. Structure and Stability of SnO$_2$ Nanocrystals and Surface-Bound. *J. Am. Chem Soc.* **2013**, *18*, 6885-6895.

Wang, H.-W., DelloStritto, M.J., Kumar, N.K., Kolesnikov, A.I., Kent, P.R.C., Kubicki, J.D., Wesolowski, D.J., Sofo, J.O., Vibrational density of states of strongly H-bonded interfacial water: Insights from Inelastic Neutron Scattering and theory, *J. Phy. Chem. C* **2014** (in press)

Poster 18

Gas and melt migration in the crust and mantle: new clues from mafic veins

Dr. Mark D. Kurz and Joshua Curtice
Marine Chemistry and Geochemistry, Woods Hole Oceanographic Institution, Woods Hole, MA

In an effort to constrain noble gas behavior during melting and melt migration in the crust and mantle, we have measured helium concentrations and isotopic compositions in transects through two centimeter-scale veins, with millimeter resolution, in two different tectonic settings. One is a clinopyroxenite vein in the Josephine Ophiolite (Oregon, USA), hosted by harzburgite. The vein has ^{4}He concentrations up to 10 times higher than the host harzburgite. Because pyroxenite veins are thought to form through mantle melt percolation, the enrichment confirms that helium behaves as an extremely incompatible element. There is a sharp helium concentration contrast at the vein/host interface, suggesting that the concentration variations were produced during vein emplacement, and that clinopyroxene has higher helium solubility and storage capacity. Total ^{3}He/^{4}He in the host harzburgite ranges from 6.5 to 7.1 times atmosphere (Ra), in agreement with previous measurements (Recanati et al., 2012). The bulk ^{3}He/^{4}He in the vein varies between 4.5 and 5.3Ra, significantly lower than the harzburgite, reflecting radiogenic production since vein emplacement or slab related fluxes. A second transect was measured across an amphibole diorite vein hosted by granoblastic basalt in 15 Ma ocean crust, formed at the superfast spreading East Pacific Rise (recovered near 1500 meters depth in ODP Hole 1256D). The amphibole and plagioclase at the vein center have 5-10 times higher abundances of He, Ne, and Ar, and slightly higher ^{3}He/^{4}He and ^{40}Ar/^{36}Ar, compared to the host basalt. These two studies show that isotopic and concentration variations have been preserved since emplacment at~ 15 Ma and ~ 157 Ma, and that mantle helium isotopic compositions are retained over these time scales. The isotopic variations suggest that it may be possible to determine Th-U-He vein emplacement ages, if the Th and U heterogeneities can be understood; preliminary ICP-MS studies suggest that there are huge Th and U variations within the vein material. The short length scale isotopic variations place some time limits for diffusion and post-emplacement cooling below the closure temperature. These preliminary data are not necessarily representative of the crust or mantle, as they are the first studies of this kind, and represent such different tectonic settings, but they highlight the importance of melting and melt migration. The ocean crustal vein data demonstrates the potential importance of amphibole in determining crustal noble gas inventories, with implications for subduction zone fluxes and crust-melt interactions at mid-ocean ridges. These data may also provide important constraints on mantle models, suggesting that preferential melting of these vein types would yield lower ^{3}He/^{4}He than host mantle, and that vein melting cannot explain unradiogenic noble gas isotopic signatures, found at some hotspots.

Poster 19

1st Principles Simulation of Interface Processes: Methods Development, Application and Analysis of Observations

John H. Weare[1]and Eric Bylaska[2]
University of California, San Diego and PNNL

The structure and electronic properties of aqueous fluids at the mineral/surface interface influence many chemical processes such as mineral growth and dissolution, natural oxidation-reduction reactions and biochemical respiration. The metal oxide minerals that are key to processes present a difficult electronic structure problem since their properties are heavily dependent on the properties of the strongly localized d electrons and the complex hydration processes of the ions in the interface region. The disorder of the surface/solution interface, the interaction of the solution phase with the highly charged mineral surface and aqueous ions, and the need to dynamically sample the structure of the interface phase further increases the difficulty of simulation. Ab initio molecular dynamics methods have provided a means to simulate dynamics from molecules to nanoscale systems. However, these methods have been limited to relatively small particle numbers and short time-scales. To treat the more complex problems of the surface/fluid interface we have developed highly parallel gradient corrected DFT calculations and have used these algorithms to calculate the surface structure and reactions of mineral surfaces with absorbed layers containing reactive solutes. These calculations done using many processors can describe limited (10s of ps) interface dynamics for very large systems (see figure). However, to obtain even qualitative agreement with the spin localization in these systems it is necessary to include some level of exchange. To treat these problems we have developed highly parallel algorithms that implement hybrid exchange functionals (inclusion of “exact exchange”). For even higher levels of electronic structure calculations we have developed novel parallel in time algorithms. These methods compute the time dimension of a dynamical simulation in a parallel fashion and can efficiently spread high-level electronic structure methods (MP2) over many processors. Because of the complexity of these problems direct simulation of cannot be carried to sufficiently long time scale to meaningfully sample phase space. To meet this challenge we are developing methods to more efficiently sample interface structure and reactions and to provide first principle free energy estimates of structural changes. Parameter free first principle simulation of XAFS measurements of uranium incorporated into iron oxides by Ilton and Barger with the help of S. Kersit for simulations, and crystal truncation rod measurements of hydrated goethite interface structure will also be presented.

The hydration structure and the changes in ion hydration structure in the interface region is another target of our research program. Applications of our newly developed 1st principle methods directly computing EXAFS and XRD scattering intensities will be presented. These include analysis of new XAFS and XRD measurements for recent experiments for the environmentally important Al^{3+} (aq) (AlCl3(aq)) ion system by J.F. Fulton. This data set is of unprecedented precision and for the 1st time includes high resolution XRD measurements and EXAFS of the Al^{3+}, O, and Cl^- species. The remarkable agreement that we are obtaining from these calculations suggests that we will for the first time to be able to probe structural features of important ion associations with both EXAFS and XRD calculations with parameter free simulations.

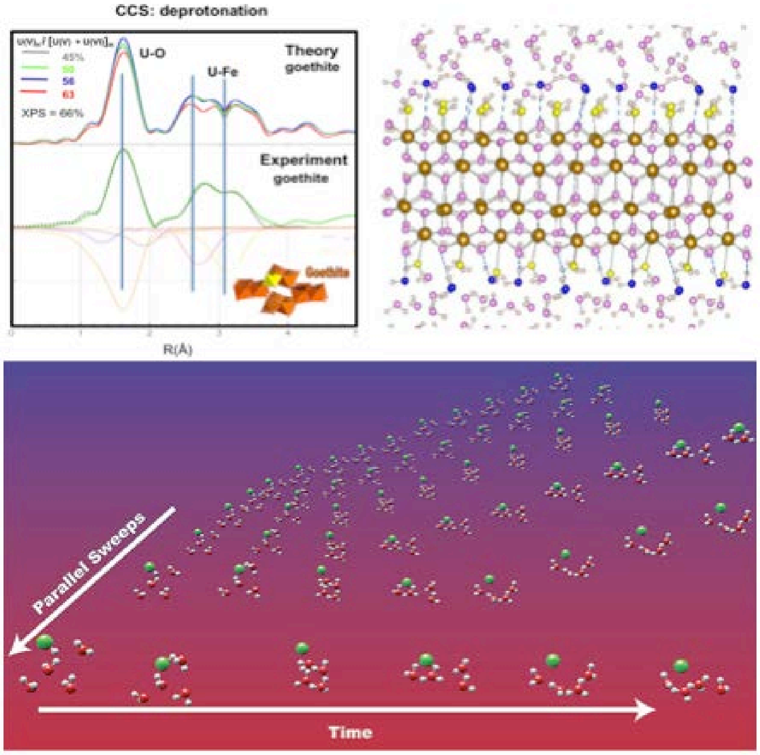

Figure: (top left) EXAFS analysis of uranium in goethite (Kersit, Bylaska, Ilton in prep.). (top right) Hydrated goethite interface structure (Chen, Bylaska, Weare et al. in prep.). (bottom) New parallel in time algorithms speed up high-level molecular dynamics simulations to enable predictions involving the properties of complex materials (Bylaska, Weare, et al. 2013. "Extending molecular simulation time scales: Parallel in time integrations for high-level quantum chemistry and complex force representations." *Journal of Chemical Physics* 139(7):074114).

Poster 20

Three-Dimensional Inverse Modeling of Damped Elastic Wave Propagation in the Fourier Domain

Petr Petrov and Greg Newman
Lawrence Berkeley National Laboratory

Three-dimensional (3D) full waveform inversion (FWI) of seismic wavefields is routinely implemented with explicit time-stepping simulators. A clear advantage of explicit time stepping is the avoidance of solving large-scale implicit linear systems that arise with frequency domain formulations. However, FWI using explicit time stepping requires a very fine time step and (as a consequence) significant computational resources and run times. If the computational challenges of wavefield simulation can be effectively handled, an FWI scheme implemented within the frequency domain, offers a cost effective alternative to FWI in the time domain. This advantage comes by utilizing only a few frequencies, which are all that are necessary for imaging the seismic attributes.

We have therefore implemented a 3D FWI scheme for elastic wave propagation in the Fourier domain. To overcome the computational bottleneck in the wavefield simulation, we have exploited an efficient Krylov iterative solver for the elastic wave equations approximated with second and fourth order finite differences. The solver does not exploit multi-level preconditioning for wavefield simulation, but is coupled efficiently to the inversion iteration workflow to reduce computational cost. The workflow is best described as a series of sequential inversion experiments where the data have been laddered such that we first image highly damped data, followed by data where damping is systemically reduced.

The key to our modeling approach is its ability to take advantage of solver efficiency when the elastic wavefields are damped. As the inversion experiment progresses, damping is significantly reduced, effectively simulating nondamped wavefields in the Fourier domain. While the cost of the forward simulation increases as damping is reduced, this is counterbalanced by the cost of the outer inversion iteration, which is reduced because of a better starting model obtained from the larger damped wavefield used in the previous inversion experiment. For cross-well data, it is also possible to launch a successful inversion experiment without laddering the damping constants. With this type of acquisition geometry, the solver is still quite effective using a small fixed damping constant. To avoid cycle skipping, we also employ a multiscale imaging approach, in which frequency content of the data is also laddered (with the data now including both reflection and cross-well data acquisition geometries). Thus the inversion process is launched using low frequency data to first recover the long spatial wavelength of the image. With this image as a new starting model, adding higher frequency data refines and enhances the resolution of the image. FWI using laddered frequencies with an efficient damping schemed enables reconstructing elastic attributes of the subsurface at a resolution that approaches half the smallest wavelength utilized to image the subsurface.

Poster 21

Computational Studies of Interfacial Processes in Carbonate Mineral Geochemistry

David A. Dixon, *The University of Alabama* (Virgil Jackson, Graduate student, PhD completed, 08/2013, K. Sahan Thanthirwatte, Postdoctoral Fellow), Sebastien Kerisit and Anne Chaka, *Pacific Northwest National Laboratory*

The prediction of the long-term stability and safety of geologic sequestration of greenhouse gases requires a detailed understanding of subsurface transport and chemical interactions between the disposed greenhouse gases and the geologic media. We are particularly interested in modeling the interactions of CO_2 and H_2O with mineral surfaces to develop molecular mechanisms of mineral formation and dissolution, especially for carbonates.

$(MO)_n$ and $(MCO_3)_n$ (M = Mg, Ca) nanoclusters and their interactions with H_2O and CO_2 have been studied. The initial geometries for the low energy clusters were generated by using our tree growth-hybrid genetic algorithm using semi-empirical molecular orbital theory followed by density functional theory and coupled cluster CCSD(T) calculations. For $(MgO)_n$, $n > 3$, the low energy 3-D structures are mainly cuboids, tubes, and polyhedrons, or their derivatives. The relative stability of these isomers changes as *n* increases, and also depends on whether *n* is a prime number. The average Mg-O bond distance and coordination number (CN) increase as *n* increases (Figure 1) and are slowly converging to the bulk values (r= 2.106 Å, CN = 6) as the cubic structures start to become dominant. Portions of the potential energy surfaces for solvent (aqueous) displacement reactions involving the metal ions Mg^{2+} and Ca^{2+} with CO_2 and HCO_3^- have been calculated and show different inner/outer ion pair formation. Studies of the reactions of CO_2 and H_2O with MO the nanoclusters have been performed and show carbonate and hydroxide formation. $(MCO_3)_n$ clusters with $n > 7$ show the elimination of CO_2 with the formation of a O^{2-} center.

Divalent cation-rich silicate minerals such as olivines have a high potential for undergoing carbonation reactions, a process that can lead to long-term storage of carbon as carbonate minerals. Studies published to date on olivine carbonation in H_2O-bearing supercritical CO_2 fluids (WBSF) have highlighted the strong dependence of the extent and rate of carbonation on the water content of the WBSF. A suite of computational techniques including static electronic structure calculations, *ab initio* molecular dynamics (MD) simulations, and classical MD simulations were employed to (1) evaluate the energetics of CO_2/H_2O competitive adsorption at the surface of olivine minerals (M_2SiO_4, M=Ca, Mg, Fe, Mn, etc) as a function of surface coverage; and (2) quantify the partition of water between the WBSF and a model Mg_2SiO_4 surface as a function of water content.

An *ab initio* thermodynamic framework for predicting properties of hydrated magnesium carbonate minerals has been developed using density-functional theory linked to macroscopic thermodynamics through the experimental chemical potentials for MgO, H_2O, and CO_2. The model was benchmarked for brucite, magnesite, nesquehonite, and hydromagnesite. The model shows that small differences in experimental conditions determine whether nesquehonite, hydromagnesite, or magnesite is formed from the carbonation of brucite, and what transformations are expected to occur on geological time scales. Applications of this approach include an independent means to evaluate differences in thermodynamic data for lansfordite, predicting the properties of Mg analogs of the Ca-based hydrated carbonates monohydrocalcite and ikaite which have not been observed in nature, and an estimation of the thermodynamics of barringtonite from the stoichiometry and a single experimental observation.

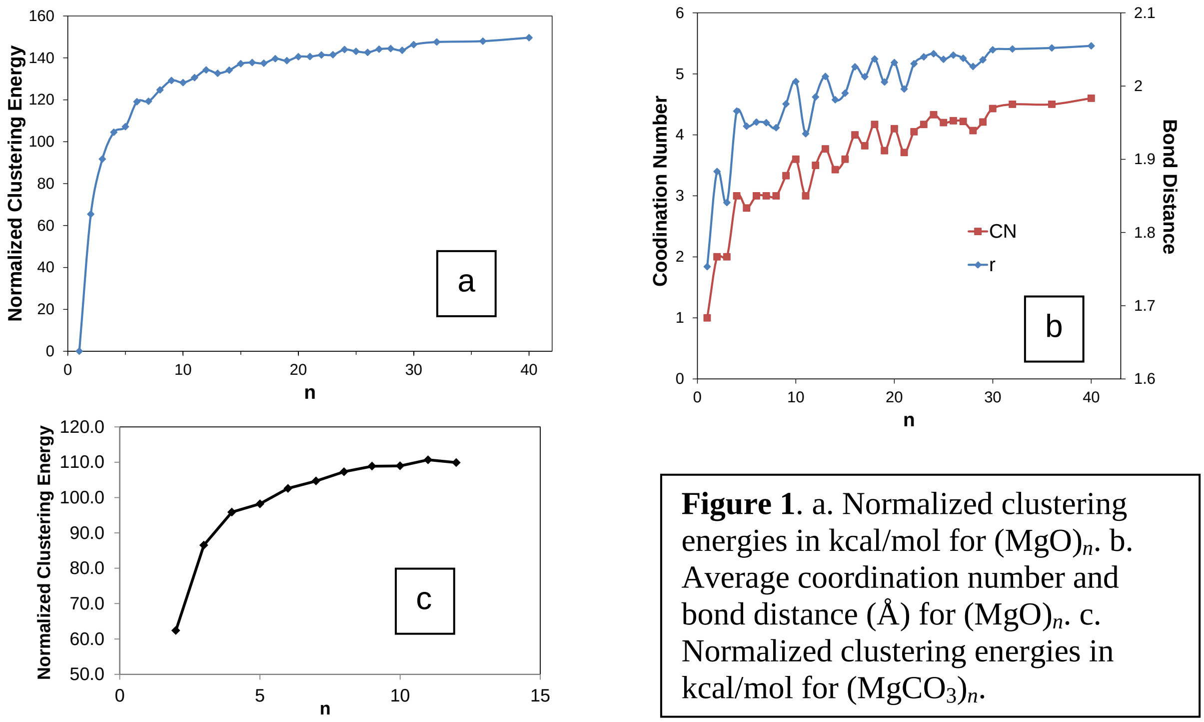

Figure 1. a. Normalized clustering energies in kcal/mol for $(MgO)_n$. b. Average coordination number and bond distance (Å) for $(MgO)_n$. c. Normalized clustering energies in kcal/mol for $(MgCO_3)_n$.

Publications

"*Ab initio* Thermodynamic Model for Magnesium Carbonates and Hydrates" A. Chaka and A. Felmy, J. Phys. Chem. A, accepted March 2014.

"Near-Infrared Spectroscopic Investigation of Water in Supercritical CO_2 and the Effect of $CaCl_2$," Z. Wang, A. R. Felmy, C. J. Thompson, J. S. Loring, A. G. Joly, K. M. Rosso, H. T. Schaef, and D. A. Dixon, *Fluid Phase Equilibria*, **2013**, *338*, 155-163.

"Water and Carbon Dioxide Adsorption at Olivine Surfaces" S. Kerisit, E.J. Bylaska, and A.R. Felmy, *Chemical Geology*, **2013**, *359*, 81-89.

"Structure and Dynamics of Forsterite-scCO_2/H_2O Interfaces as a Function of Water Content" S. Kerisit, John H. Weare, A.R. Felmy, *Geochimica et Cosmochimica Acta*, **2012**, *84*, 137-151.

"High Level ab initio Predictions of the Energetics of $m CO_2 \cdot (H_2O)_n$ ($n = 1 - 3$, $m = 1 - 12$) Clusters" K. S. Thanthiriwatte, J. R. Duke, V. E. Jackson, A. R. Felmy, and D. A. Dixon, *J. Phys. Chem. A*, **2012**, *116*, 9718-9729

"Thermochemical Properties of Selenium Fluorides, Oxides and Oxofluorides," V. E. Jackson, D. A. Dixon, and K. O. Christe, *Inorg. Chem.* **2012**, *51*, 2472-2485

Poster 22

Poroelastic Interactions between Seismic Waves and Fluid-Filled Fractures at Low (<1 kHz) Frequencies: Theory and Laboratory Measurements

Seiji Nakagawa[1], Valeri Korneev[1], Steven Pride[1], Jim Berryman[1], Don Vasco[1], and Shinichiro Nakashima[1,2]
[1]*Lawrence Berkeley National Laboratory,* [2]*Yamaguchi University, Japan*

This research is conducted as part of the LBNL's overarching effort to develop an advanced time-lapse geophysical monitoring methodology for reservoir fluid-invasion processes. Our immediate objective is to establish quantitative rock-physics relationships between the poroelastic properties of rock and fractures, and the resulting seismic properties—including frequency-dependent velocity (dispersion), attenuation, and anisotropy—through a combination of laboratory experiments and poroelastic modeling of fractures. This ongoing study examines interactions between single fractures containing fluid and propagating seismic waves at frequencies much lower than conventional ultrasonic tests, and this presentation will include: (1) quasi-static measurements of fracture compliance related to the fracture-normal seismic wave propagation, and (2) guided wave measurements focused on intrafracture fluid-pressure wave propagation (fracture-parallel wave propagation).

Fractures in low-permeability rock have a dominant impact on the rock's mechanical and hydrological properties. During injection of fluid in a reservoir, induced fluid pressure can create new fractures and/or alter the properties of new fractures, which are monitored via time-lapse seismic measurements. The relationships between fracture properties and their effect on the seismic wave propagation under a range of stress and pore pressures have been studied, but most of the laboratory experiments to date have been conducted at ultrasonic frequencies (hundreds of kHz to several MHz). The large differences in the frequencies between the laboratory and the field—where typically employed wave frequencies are several Hz up to a few tens of kHz—can results in very different seismic velocity and attenuation, particularly when poroelastic interactions between the waves and the rock (including fractures) are present.

Although the mechanical compliance of fractures can have a large impact on estimation of reservoir stress state and fluid content, only a limited number of fracture compliance measurements are available, particularly in the subkilohertz frequency range relevant to field seismic measurements. Also, most laboratory measurements are for the normal fracture compliance, and measurements for the shear fracture compliance are rather rare. For this reason, a special laboratory device has been under development over the past several years (e.g., Nakagawa, 2013), which allows us to measure both normal and shear compliances of an interface (fracture) simultaneously, in the frequency range of <1 Hz–~100 Hz. Using this device, dynamic fracture compliances of a sheared, water-saturated, and drained fracture were measured, under small fracture-normal stress. For the saturated fracture, the normal fracture compliance was clearly frequency dependent, with the relaxation frequency at 10~20 Hz. This result, however, did not agree well with a theoretical model, which predicted much larger compliance changes and a higher relaxation frequency than the experiment. Observed normal to shear fracture compliance ratio ranged from 1.8 to 2.8 for the saturated fracture and 1.7 to 1.9 for the drained fracture, both decreasing with increasing normal stress on the fracture.

In contrast to the fracture compliance measurements related to the fracture-normal wave propagation, the second part of this presentation focuses on seismic wave propagation along and within a fracture. A fluid-saturated flat channel between solids (i.e., a fracture) is known to support guided waves—sometimes called Krauklis waves (e.g., Korneev, 2008). At the high-frequency limit, these are the acoustic waves trapped in a fracture; at the low-frequency limit, they become diffusing pressure through a fluid channel. Krauklis waves propagate primarily along the fluid part of a fracture, can have very low velocity and large attenuation, and are very dispersive at low frequencies. We conducted laboratory measurements of the velocity and attenuation of Krauklis waves at the frequency rage of <10 Hz up to ~1 kHz, using analogue fracture models. As far as we know, laboratory measurements of the Krauklis waves at such low frequencies have never been made before. Measured waves were strongly dispersive and had low velocity and high attenuation. Further, the behavior of the waves varied as a function of the fracture compliance and permeability. The experimental results were then compared to theoretical predictions by dispersion equations derived using the Schoenberg’s Linear-Slip-Interface Model (1980), which was extended for poroelastic fractures with fracture-parallel fluid flow. Although the mechanical compliance (or stiffness) of the fracture was used as a fitting parameter, the model showed good agreement with the experiment.

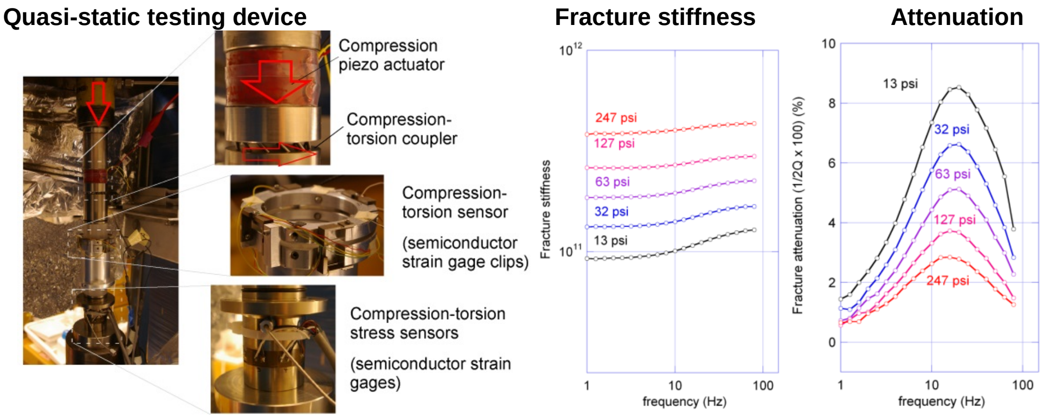

Fig. 1 Experimental setup for quasi-static mechanical deformation and stress measurements of a fracture. Currently, the experiment is conducted exclusively without confining pressure. Apparent specific normal fracture stiffness (1/compliance) and its attenuation were measured as a function of the effective normal stress on the fracture, indicating strongly frequency-dependent behavior.

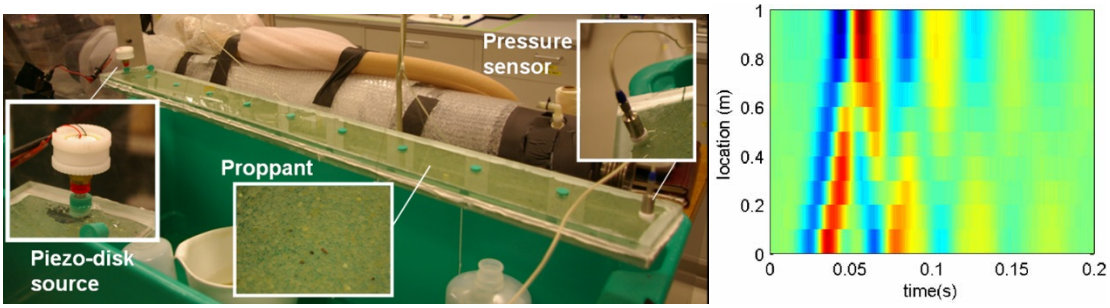

Fig. 2 Experimental setup (a “tri-layer” model) for measurements of guided wave propagation within a fluid-filled fracture. Propagating pressure pulses are measured along the length of the model, as well as the vibration (resonance) within the entire fluid-filled fracture. The density plot shows an example of measured waves for an open fracture (dominant frequency ~20 Hz; velocity ~50 m/s)

Poster 23

Insights into the Geochemistry of U-bearing Phases: Theory and Experiment

Paul S. Bagus[1] and Eugene S. Ilton[2]

[1]*Chemistry Department, University of North Texas, Denton, Texas;* [2]*Pacific Northwest National Laboratory, Richland, Washington*

The overall objective of this project is to develop a predictive thermodynamic model for oxidation states of uranium incorporated in trace to minor concentrations in minerals where the emphasis has thus far has been on Fe (hydr)oxides. Important milestones for achieving this goal include developing techniques for determining the oxidation state and local bonding or coordination environment of trace to minor concentrations of uranium in minerals such as hematite and goethite. XPS and XAS have been the traditional tools for investigating these systems, and we have achieved experimental and theoretical success using them. In order to obtain unambiguous and necessary detailed information, such as local charge compensation schemes (CCS), we have been coupling spectroscopy with *ab initio* modeling. Here, we highlight recent advances in *ab initio* simulations of 1.) the U4f XPS of U(VI, V, and IV) in octahedral coordination and 2.) the XAS NEXAFS (or XANES) L_{III}-edge for U(VI, V, and IV) in octahedral coordination. The XPS studies focus on the establishing the nature of the losses from the main peaks to the satellites and on establishing the electronic character of the satellites. This work shows that the positions of the satellites, relative to the main peaks, depend on the nominal U oxidation state. For the XAS, the different covalent character in the various U oxidation states makes it possible to use the width of the L_{III}-edge XAS peak as a fingerprint of the nominal oxidation state. For both XPS and XAS, we have developed and applied novel theoretical methods to determine the covalent character of the U-O interaction. Our combination of theory and experiment permits these core-level spectroscopies to be used as robust measures of the nominal U oxidation state. We also present initial results from *ab initio* MD modeling of U(IV, V, and VI) substituting for Fe(III) in goethite as a function of different CCS. These dynamical structural models were input into FEFF to yield simulated EXAFS which were then compared to experimental systems where U was incorporated into goethite during reductive transformation of ferrihydrite. Close comparison suggests that both U(V) and U(VI) substitute in regular octahedral sites of goethite with deprotonation serving to neutralize charge. This brings us closer to developing the correct half-cell reactions to couple redox reactions for U incorporated in Fe (oxy)hydroxides to solution parameters.

Poster 24

Elastic Network Models and the Resonance Behavior of Berea Sandstone

Timothy W. Darling[1], Will Struble[1], James A. TenCate[2] and Paul A. Johnson[2]

[1] University of Nevada, Reno, NV 89557; [2] Los Alamos National Laboratory, Los Alamos NM 87545

The response of Berea sandstone to applied stress has been shown to be significantly nonlinear at resulting strains as low as 10^{-6}. The local stress and strain is expected to concentrate in the small cross-section grain-bonding regions which dominate the mechanical response. These complex regions are susceptible to influences from chemical (water, CO_2, e.g.) migration, fracturing, plastic effects, and thermal effects – or combinations of these. We have measured the moisture content and temperature dependence of the nonlinear response of a lab core sample of Berea sandstone with the goal of using a network elastic structure in the COMSOL finite-element code to understand the effects of these influences. We examine the response through the driven resonances and acoustic response of the sample at vacuum and high temperature using vacuum furnace apparatus from LANL. Much of the measurement has been at UHV conditions, very unusual conditions for a sandstone sample. The removal of all free water and of at least some of the water from the hydrated clays and feldspars produced an unusual attenuation at higher temperatures, but did not reduce the degree of nonlinearity. CO_2 gas and water were added independently to the dried sample, but also did not alter the character of the nonlinear response. The assumption of elastic isotropy in polycrystal porous samples is difficult to study since experiments usually ignore the shear components of the strain. These components are critical, since elastic properties such as very small, zero or negative Poisson ratios are related to rotation of grains. We have concentrated effort on modeling porous materials using a finite-element model in COMSOL that includes all available distortions of a sample. The vibration spectrum of an object has components from the entire apparent elastic tensor, although dominated by shear at low frequencies and varying with large scale inhomogeneities. We have created a geometrical model in COMSOL of the form of an nxnxn array of rectangular prism "grains" bonded by smaller cross-section prisms. The bonds are randomly placed on the grain faces to introduce a randomization and to transmit torques to the grains. The ability to reproduce the vibrational spectrum of the network with a continuum model is the question we are investigating – a continuum model with no structure cannot reproduce a negative Poisson ratio, for example. At the 4x4x4 level, grains with 4 or less bonds dominate the model, and no isotropic elastic constants reproduce the spectrum. A cubic model fits better, but does not have the low Poisson ratio expected. As we progress to larger arrays we hope to approach the solution to modeling a network at large scales where the introduction of nonlinearity to the bonds and the inclusion of surface energy in the free energy can shed light on the influence of chemistry on nonlinear mechanical responses.

Poster 25

Adsorption of metals and oxyanions to mineral surfaces

Lynn E. Katz,[1] Kevin Leung,[2] Heather C. Allen,[3] and Louise J. Criscenti[4]

[1]Department of Civil, Architectural and Environmental Engineering, College of Engineering, The University of Texas at Austin, 1 University Station C1700, Austin, TX 78712; [2]Nanostructure Physics Department, Sandia National Laboratories, P.O. Box 5800, MS 1415, Albuquerque, NM 87185; [3]Department of Chemistry and Biogeochemistry, The Ohio State University, 100 West 18th Avenue, Columbus, OH 43210, [4]Geochemistry Department, Sandia National Laboratories, P.O. Box 5800, MS 0754, Albuquerque, NM 87185

The need to predict trace metal and oxyanion adsorption to mineral surfaces in geochemistry is critical to many DOE missions including providing adequate geochemical, flow, and transport assessments for potential nuclear waste repository and carbon sequestration sites. Surface complexation models used to describe equilibrium between adsorbed and aqueous species rely on the selection of surface complexes that are both consistent with available molecular-scale spectroscopic observations and simulations, and successfully describe bulk experimental adsorption data within a surface complexation model framework.

Our research has been driven by a balance between acquiring a fundamental understanding of reactivity at mineral-water interfaces and the need for practical application. Surface acidity constants for silica and goethite surface sites have been calculated using density functional methods and compared to those determined from surface titration experiments and crystal bond-valence methods. Potential of mean force calculations of cation-anion pairs in solution have been performed to evaluate if energetic trends in ion pairing calculated with modern-day force fields can reproduce equilibrium constants used in aqueous speciation and adsorption calculations. Raman spectroscopy on aqueous systems of the same ion pairs has been performed as a precursor to examining the properties of the same aqueous solutions at mineral interfaces using total reflection (TIR)-Raman spectroscopy.

TIR-Raman spectroscopy has been used to examine the adsorption of oxyanions such as sulfate and selenite to hematite and silica. The study on sulfate adsorption to hematite showed that inner-sphere sulfate adsorption proceeds in a bidentate fashion. Research on selenite adsorption to silica is underway. In the meantime, a surface complexation model has been developed that can account for the simultaneous adsorption of trace metals and oxyanions. Spectroscopic and molecular simulation research is underway to explore, support, and/or disprove the surface complexes proposed by this model.

Sandia National Laboratories is a multi-program laboratory operated by Sandia Corporation, a wholly owned subsidiary of Lockheed Martin Corporation, for the United States Department of Energy's National Nuclear Security Agency Administration under contract DE-AC04-94AL85000.

Poster 26

Modified Invasion Percolation Model for Hydrofracture and other Applications

J. Quinn Norris[1], Donald L Turcotte[2], John B Rundle[1,2]

[1] *Department of Physics, UC Davis, One Shields Ave, Davis, CA USA*
[2] *Department of Geology, UC Davis, One Shields Ave, Davis, CA USA*

Recent developments in hydraulic fracturing (fracking) have enabled the recovery of large quantities of natural gas and oil from old, low-permeability shales. These developments include a change from low-volume, high-viscosity fluid injection to high-volume, low-viscosity injection. The injected fluid introduces distributed damage that provides fracture permeability for the extraction of the gas and oil. In order to model this process, we utilize a loopless nontrapping invasion percolation previously introduced to model optimal polymers in a strongly disordered medium and for determining minimum energy spanning trees on a lattice. We performed numerical simulations on a two-dimensional square lattice and find significant differences from other percolation models. Additionally, we find that the growing fracture network satisfies both Horton-Strahler and Tokunaga network statistics. As with other invasion percolation models, our model displays burst dynamics, in which the cluster extends rapidly into a connected region. We introduce an alternative definition of bursts to be a consecutive series of opened bonds whose strengths are all below a specified value. Using this definition of bursts, we find good agreement with a power-law frequency-area distribution. These results are generally consistent with the observed distribution of microseismicity observed during a high-volume frack.

Poster 27

The Unique Properties of Magnesium and its Role in the Environment

Louise J. Criscenti,[1] Heather C. Allen,[2] and Lynn E. Katz[3]

[1] Geochemistry Department, Sandia National Laboratories, Albuquerque, NM 87185
[2]Department of Chemistry & Biochemistry, The Ohio State University, Columbus, OH 43210
[3] Department of Civil, Architectural and Environmental Engineering, College of Engineering, The University of Texas at Austin, Austin, TX 87185

The aqueous magnesium cation exhibits different solvation and complexation properties than the other alkaline earth metal cations. These unique properties contribute to magnesium's importance in human and plant nutrition, algal metabolism, and soil properties. Magnesium is responsible for hundreds of biochemical reactions in the human body. In plants, magnesium is the central atom of the porphyrin ring of the chlorophyll molecule, and is essential for the conversion of CO_2 to oxygen, specifically for the light harvesting reaction of photosystem I. In algal species, magnesium is not only a key component of algae, but it is also required for molecular phosphate transfer in energy production. The presence or lack of magnesium also has dramatic effects on the properties of soils. The ratio of calcium to magnesium in a soil determines the tightness of a soil. Higher calcium levels provide a looser soil; the more magnesium, the tighter a soil. The importance of Mg in all of these natural systems is dependent on the unique properties of Mg^{2+} in aquatic systems. While previous research has highlighted the role that bulk physical chemical properties of Mg play in these processes, few studies have focused on the unique solvation and molecular bonding characteristics of Mg that facilitate its role in adsorption, coagulation, precipitation, and ion exchange processes in environmental systems.

In this research, Mg^{2+} solvation and complexation are examined at air-water and mineral/water interfaces using molecular dynamics simulations, Raman spectroscopy, and bulk reactor experiments. Results confirm that trends in contact ion pair formation which decrease with decreasing cation size and increasing cation charge density are related to the metal hydration free energies. In turn, the amount of thermal energy required to remove the waters of hydration from the metal cation and the ratio of outer-sphere to inner-sphere complexation at the surface of oxide minerals decreases from Mg^{2+} to Ba^{2+} which has significant implications for fate and transport of these ions in the environment. Several examples are presented to illustrate these points including molecular dynamics profiles that reveal that pairing in aqueous $Mg(NO_3)_2$ is thermodynamically unfavorable, whereas in $Ca(NO_3)_2$ and $Sr(NO_3)_2$ solutions, the formation of contact ion pairs is preferred over solvent-shared and solvent-separated ion pairing. Moreover, the constancy of the $Mg^{2+}–OH_2$ Raman peak as a function of concentration and the presence of a linear correlation between $Mg(NO_3)_2$ concentration and peak intensity of the $Mg^{2+}–OH_2$ band confirms that there is no replacement of Mg^{2+} hydration water molecules by nitrate anions in our concentration range. Adsorption studies and molecular dynamics simulations of Mg^{2+} on oxide minerals confirm that Mg^{2+} does not lose its waters of hydration upon adsorption to the mineral/water interface for temperatures ranging from 22 to 277 °C. Other examples of ion pairing of alkaline earth metals with chloride and carbonate are also presented to illustrate the unique properties of Mg^{2+}.

Sandia National Laboratories is a multi-program laboratory operated by Sandia Corporation, a wholly owned subsidiary of Lockheed Martin Corporation, for the United States Department of Energy's National Nuclear Security Administration under contract DE-AC04-94AL85000.

Poster 28

Nucleation and Fracture in Complex Geo - Systems

W. Klein
Department of Physics, Boston University

Collaborators: J. B. Rundle, H. Gould and T. Keyes

Many processes in geological systems are initiated by a nucleation event. Examples include fracture, cloud formation and the formation of clathrates. Understanding the nature of the initiating or nucleation event can lead to prediction and control. The standard, or classical, theory of nucleation has proven to be incomplete and does not describe several processes in systems with long range interactions such water and systems with elastic interactions. Over the past several years we have formulated a theory of nucleation that incorporates the effects generated by the long range interactions common in geological materials. In this presentation we describe this non classical theory and discuss its application to both fracture and the nucleation of clathrate hydrides.

1. W. Klein, “The Instability of Alexander-McTague Crystals and its Implication for Nucleation” Phys. Rev. E, 64, 056110 (2001)
2. W. Klein, T. Lookman, A. Saxena and D. Hatch, “Nucleation in Systems with Elastic Forces” Phys. Rev. Lett. 88, 085701 (2002)
3. F. J. Cherne, M. I. Baskes, R. B. Schwarz, S. G. Srinivasan, and W. Klein “Non-classical Nucleation in Supercooled Nickel” Modelling and Simulation in Material Science and Engineering 12 1063-1068 (2004)
4. K. Barros and W. Klein, “Liquid to Solid Nucleation via Onion Structure Droplets” Journal of Chemical Physics 139, 174505 (2013)
5. J. B. Rundle and W. Klein, “Non-Classical Nucleation and Growth of Cohesive Tensile Cracks,” Phys. Rev. Lett. 63, 171 (1989)

Poster 29

Geochemical Studies of Natural Geological and Environmental Materials using High-Energy X-ray Probes

Lanzirotti A., Newville, M., Sutton S. R., Rivers M. L., Stubbs, J. E., Eng, P. J., and Wirick S.
University of Chicago and GSECARS

Development of hard X-ray microprobe techniques that can be applied to geochemical problems has provided the earth and environmental science research community with new capabilities in microfocused X-ray absorption spectroscopy, XRF microprobe analysis, microdiffraction, and elemental computed microtomography. The research conducted at GSECARS sector 13 at the Advanced Photon Source and at beamlines X26A and X27A at the National Synchrotron Light Source continue to advance our knowledge of the composition, structure and properties of earth materials, the processes that produce them and the processes they control. The unique capabilities of these beamlines have fostered groundbreaking experiments relevant to the DOE-Geosciences programs including hydrothermal fluid chemistry, mineral-water interface reactions, igneous petrology, and biogeochemistry. Specific examples of research by our group and collaborators include speciation of metals in hydrothermal fluids, environmental behavior of actinide-bearing compounds, redox dynamics of multivalent trace elements in soils, the geochemistry of toxic metals and metalloids in contaminated sediments, tailings, airborne particulates, and well-waters, and valence state partitioning in igneous minerals. Studies have also evaluated the efficiencies of various contaminant remediation strategies.

The recently commissioned GSECARS 13-ID-E microprobe at the Advanced Photon Source provides exciting new capabilities now, including a tunable energy range from 2.4 keV (sulfur K edge) to 28 keV, the use of KB mirrors to achieve beams with spatial resolution of 500 nm, and an innovative, state-of-the-art, direct-drive rotary stage monochromator that not only provides exceptional stability for sub-micrometer spectroscopy, but also allows rapid “fly-scan” X-ray absorption spectroscopy opening new scientific opportunities for geochemists. Coupled with high-speed area detectors that are now available, the high focused beam intensity of the beamline also allows coupled “fly-scan” microfocused X-ray diffraction and fluorescence experiments at scan rates up to 30 Hz. This provides earth scientists with the ability to characterize both the elemental composition and mineralogy in heterogeneous samples in an imaging mode at micrometer and sub-micrometer spatial resolutions. The recently upgraded 13-ID-C/D beamline offers enhanced opportunities for surface and interface science, such as the partitioning of metals between mineral surfaces and biofilms, corrosion of substrate minerals containing heavy metals and radionuclides, and surface speciation of metal and metalloid sorbates.

New beamlines that are now in the planning stages at NSLS-II, such as the SRX and XFM beamlines, promise to routinely provide both sub-micrometer XRF and microfocused Extended X-ray Absorption Fine Structure (μEXAFS) spectroscopy capabilities for geoscience research.

Poster 30

Geofluid Dynamics of Faulted Sedimentary Basins

Grant Garven, *Earth & Ocean Sciences, Tufts University, Medford, Massachusetts*
Byeongju Jung, *Earth Sciences, Uppsala University, Sweden*
James R. Boles, *Geological Sciences, University of California at Santa Barbara*

Faults are known to affect basin-scale groundwater flow, and exert a profound control on petroleum migration/accumulation, the PVT-history of hydrothermal fluids, and the natural (submarine) seepage from offshore reservoirs. For example, in the Santa Barbara basin, measured gas flow data from a natural submarine seep area in the Santa Barbara Channel helps constrain fault permeability k ~ 30 millidarcys for the large-scale upward migration of methane-bearing formation fluids along one of the major fault zones. At another offshore site near Platform Holly, pressure-transducer time-series data from a 1.5 km deep exploration well in the South Ellwood Field demonstrate a strong ocean tidal component, due to vertical fault connectivity to the seafloor. Analytical solutions to the poroelastic flow equation can be used to extract both fault permeability and compressibility parameters, based on tidal-signal amplitude attenuation and phase shift at depth. For the South Ellwood Fault, we estimate permeability k ~ 40 millidarcys (hydraulic conductivity $K \sim 4 \times 10^{-7}$ m/s) and specific storage coefficient $S_s \sim 3 \times 10^{-6}\ m^{-1}$. The tidal-derived hydraulic properties also suggest a low effective porosity for the fault zone, n ~ 1 to 3%.

In a similar vein, our studies of faults in the Los Angeles basin, suggest an important role for the natural retention of fluids along the Newport-Inglewood fault zone. Based on the estimates of fault permeability derived above, we have also constructed new two-dimensional numerical simulations to characterize large-scale multiphase flow in complex heterogeneous and anisotropic geologic profiles, such as the Los Angeles basin. The numerical model was developed in our lab at Tufts from scratch, and based on an IMPES-type algorithm for a finite element/volume mesh. This numerical approach allowed us model large differentials in fluid saturation and relative permeability, caused by complex geological heterogeneities associated with sedimentation and faulting. Our two-phase flow models also replicated the formation-scale patterns of petroleum accumulation associated with the basin margin, where deep faults resulted in stacked petroleum reservoirs along the Newport-Inglewood Fault, as deep geofluids migrated out of the basin to the Palo Verde Peninsula. Recent isotope data collected by Boles et al. (see this volume) also verify fault connectivity at the deep crustal scale.

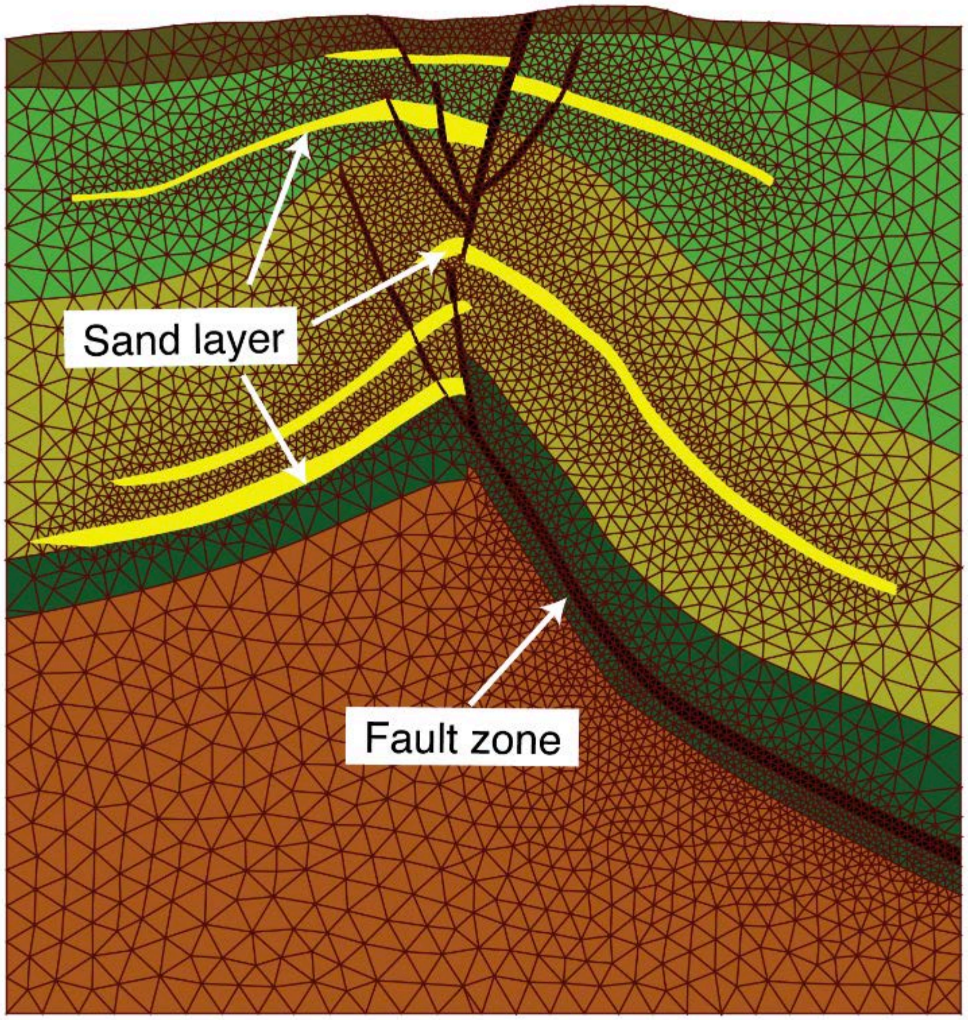

FIGURE 1. Numerical mesh used to study fault-controlled geofluid dynamics in the Inglewood field, Los Angeles basin.

Recent Publications Supported by DE-FG02-07ER15900:

Jung, B., 2013, *Geohydrology of Multiphase Flow and Petroleum Migration in the Los Angeles Basin*, Ph.D. Dissertation, Department of Civil & Environmental Engineering, Tufts University, Medford, Massachusetts.

Jung, B., Garven, G., and J.R. Boles, 2013, Effects of episodic fluid flow on hydrocarbon migration in the Newport-Inglewood Fault Zone, southern California. Geofluids, doi:10.1111/gfl.12070.

Jung, B., Garven, G., and J.R. Boles, 2014, The geohydrology of faults and petroleum migration in the Los Angeles basin, California: *American Journal of Science* (accepted with revisions).

Poster 31

Development of a Tender-Energy Microprobe for Geosciences at NSLS and NSLS-II: First Measurements

Paul A. Northrup
Stony Brook University and Brookhaven National Laboratory

A new tender-energy (1-8 keV) X-ray microprobe is currently being commissioned at Beamline X15B at the National Synchrotron Light Source (NSLS). This offers both X-ray fluorescence (XRF) imaging and microbeam X-ray absorption spectroscopy (XAS), at tunable spatial resolution from ~50 microns down to ~5 microns. This facility operating in the tender energy range, in a non-vacuum (helium) sample environment, provides unique access to lighter elements (Mg through Ca) for studies of their distribution, chemical speciation and local structure in heterogeneous crystalline or noncrystalline materials. Initial measurements demonstrate the applicability of this facility for a variety of Geoscience research. This instrument will operate at the NSLS until that facility shuts down at the end of September 2014, then move to the TES (Tender Energy Spatially Resolved and *in-situ* X-ray Absorption Spectroscopy) beamline at NSLS-II with expected operation beginning in October 2015.

Poster 32

Comparison of Helium isotopes in Tertiary Basins of Southern California: Evidence of Fault-Related Mantle Helium

James Boles[1], John E. Lupton[2], Hilario Camacho[3], and Grant Garven[4]

[1]Dept. Earth Science, Univ. of California, Santa Barbara, CA 93106; [2]Hatfield Marine Center, Newport, Oregon 97365; [3]Occidental Oil and Gas Corporation, Bakersfield, CA 93311; [4]Dept. of Earth and Ocean Sciences, Tufts Univ, Medford, MA 02155

Our objective is to quantify fault permeability in southern California basins. Cenozoic sedimentary basins in Europe formed by crustal loading have relatively low ^{3}He/^{4}He ratios (R/Ra <1), whereas basins in Europe and Japan formed by extension, in which mantle-derived igneous activity intrudes the basin, have R/Ra >1 (Oxburgh et al., 1986). A study of the Sacramento basin gas fields (Poreda et al., 1986) also shows that the highest high R/Ra values (1.97 to 2.75) are found in gas fields associated with buried Plio-Pleistocene igneous intrusive rocks. Other fields in the area typically have R/Ra values close to or less than 1.0. In the southern San Joaquin basin, R/Ra values are consistently low (R/Ra 0.015 to 0.64; average = 0.21), presumably due to the thick sedimentary section (> 7 km) and absence of an igneous connection to the mantle in the lower part of the basin.

Our new helium isotopic results acquired from August 2012 through March 2014, demonstrate a strong mantle signature along the Newport-Inglewood fault in the Los Angeles basin. Examples are the Dominguez, Huntington Beach, Inglewood, Long Beach, and Long Beach Airport oil fields, where corrected R/Ra values are between 1.53 and 5.31 (mean = 2.92). Many of these fields have igneous intrusions in the deep part of the sequence that result from early-mid Miocene extension. In contrast, the central, western, and northern part of the Los Angeles basin (e.g. Santa Fe Springs, Sawtelle, Sansinena fields) have relatively low mantle signatures with R/Ra values between 0.18 and 0.32 (mean = 0.25). The Sawtelle and Sansinena fields are associated with major faults, but these faults are apparently not deeply rooted. In contrast, the Newport-Inglewood fault appears to be a major deep-seated structural feature that is unique in the basin.

Poster 33

***Panorama*, A New Gas Source, Electron Impact, Double-Focusing, Multi-Collector Mass Spectrometer for the Measurement of Isotopologues in Geochemistry**

E. D. Young[1], P. Freedman[2], D. Rumble[3], and E. Schauble[1,]
[1]University of California, Los Angeles, [2]Nu Instruments Ltd., [3]Geophysical Laboratory

Panorama is a high-Mass Resolving Power gas-source multiple-collector mass spectrometer designed for measuring rare isotopologues of atmospheric and geochemical gases. The instrument, the largest of its kind in the world, has been constructed and is undergoing final testing at the factory of Nu Instruments (Wrexham, Wales, UK). The magnetic sector has a radius of 800 mm that, when combined with typical slit widths of 40 microns and aberrations of ~ 0.017 mm, yields a nominal MRP of ~37,000. Sensitivity is provided by a Daly detector on the central collection channel. With this instrument we should be able to measure $\Delta^{13}CDH_3$ and $\Delta^{12}CD_2H_2$ with virtually no mass spectrometric interferences.

Measurements of the combined ratio of the clumped isotopologues $^{13}CDH_3$ and $^{12}CD_2H_2$ to $^{12}CH_4$ in methane gas samples have been reported by Stolper et al. (GCA, **126**, 169-191, 2014). It was not possible to resolve the two clumped isotopologues for independent analysis because of the trade-off between high mass resolution and transmission in the ***Ultra*** mass spectrometer used in the investigation: mass resolution sufficiently high to resolve the isotopologues did not yield ion beams of sufficient intensity for accurate measurement. The failure to resolve the two clumped isotopologues imposes a constraint in the interpretation of the data. The constraint can be understood by visualizing the mixing of two methane gas samples each having high temperature, stochastic abundances of clumped isotopologues but each differing by 45 per mil in bulk $\delta^{13}C$ and by 250 per mil in δD. The resulting mixtures have excesses in $^{12}CD_2H_2$ compared to thermodynamically equilibrated methane gas. Physical mixing of gas samples does not reorder clumped isotopologue abundances, thus, for a given bulk $\delta^{13}C$ and given δD, a sample of mixed gases does not have a distribution of clumped isotopologues appropriate to its temperature of formation. The interpretative constraint can only be removed by measuring separately the individual ratios of $^{13}CDH_3$ to $^{12}CH_4$ and of $^{12}CD_2H_2$ to $^{12}CH_4$. ***Panorama*** has already achieved a mass resolution of 40,000 in factory tests with adequate ion beam intensity for measurement of the individual ratios.

Tuning and adjustment of ***Panorama*** in the factory continues as this is written with the current objective of improving the stability of ion beam intensities.

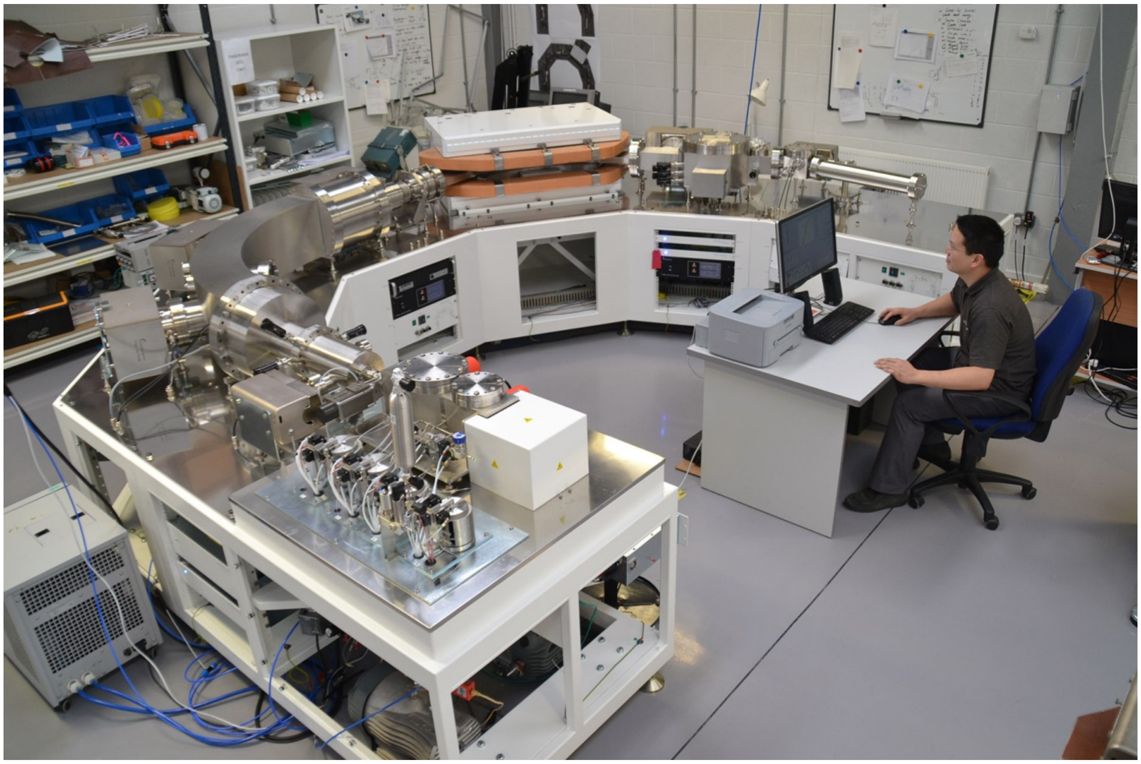

Panorama Mass Spectrometer, Nu Instruments Ltd. Wrexham, Wales, UK. March 2014.

Poster 34

Frequency-dependent attenuation and elasticity in unconsolidated earth materials

Hernan A. Makse[1] and David L. Johnson[2]
[1]*Levich Institute and Physics Department, City College of New York, New York, NY 10031*
[2]*Schlumberger-Doll Research, One Hampshire, Cambridge, MA 02139*

We develop a theoretical understanding of sound propagation, elasticity and dissipation in granular materials. The topic is relevant for the efficient production of hydrocarbon and for identifying and characterizing the underground formation for storage of either CO2 or nuclear waste material. We employ a set of experimental and theoretical concepts including the dynamic effective mass of granular media, normal modes analysis, and numerical simulations based on Discrete Element Methods to study acoustics and dissipation in granular media. We have analyzed the acoustic response of loose granular material and derived theoretical expressions of the effective mass in terms of the complex valued normal modes of the confined granular medium. The theory accurately predicts the frequencies, widths, and relative amplitudes of the various resonance modes [1,2]. A set of computer simulations has been performed to test the theory and finds agreement with theoretical and experimental results. We extract the low-frequency (<15 kHz) normal modes and investigate the corresponding effect of different damping and stress [3,4]. We demonstrate that, as damping increases, the normal modes exhibit roughly circular trajectories in the complex frequency plane. The complex valued normal modes characterize the dissipative and elastic properties of the granular material. Thus, our findings can be applied to interpret sonic logging data of near wellbore structures.

Furthermore, we have studied the structural properties determining the elastic response of granular media using a statistical mechanics volume ensemble approach. A theory has been developed to determine the microstructure of granular packing composed of any object shape to find equations of state relating the porosity, stress and coordination number [5,6]. The theory allows us to describe the equations of state of granular materials relating porosity, stress and coordination number with the goal of describing sound propagation and elasticity in earth formations.

[1] J.J. Valenza, C.-J. Hsu, R. Ingale, N. Gland, H.A. Makse, D.L. Johnson, *Dynamic effective mass of granular media and the attenuation of structure borne sound*, Phys. Rev. E **80**, 051304 (2009).
[2] J.J. Valenza, C.-J. Hsu, D.L. Johnson, *Effect of granular media on the vibrational response of a resonant structure: theory and experiment,* J. Acoust. Soc. Am. **128**, 2768 (2010).
[3] Y. Hu, D.L. Johnson, J.J. Valenza, F. Santibáñez, H.A. Makse, *Stress-dependent normal mode frequencies from the effective mass of granular matter*, Phys. Rev E (2014).
[4] Y. Hu, H.A. Makse, J.J. Valenza, D.L. Johnson, *Frequency-dependent attenuation and elasticity in unconsolidated earth materials: effect of damping,* Geophysics (2014).
[5] A. Baule, R. Mari, L. Bo. L. Portal, H. A. Makse, *Mean-field theory for random close packings of axisymmetric particles,* Nature Comm. **4**, 2194 (2013).
[6] A. Baule, H.A. Makse, Fundamental challenges in packing problems: from spherical to non-spherical particles. Soft Matter**,** DOI: 10.1039/c3sm52783b (2014).

Poster 35

Particulate Suspension Flow in Fractures

Joel Koplik
City College of New York

Background: Fluids recovery from subsurface reservoirs is complicated by the presence of suspended solid particles which can reduce throughput and contaminate the efflux, and may even accumulate locally to form a jammed or clogged structure which blocks the flow. Transport via connected fracture networks provides the most effective means of fluids recovery in practice, but fracture flow is typically dominated by channeling into a limited number of flow paths and is particularly sensitive to clogging. A detailed understanding of the conditions under which jams form, their response to controlled perturbations in the flow, and their global effects on transport will enhance our understanding of the dynamics and improve our ability to extract subsurface fluids.

Flow in single tight fractures: When the fracture aperture is much larger than the particle diameter a suspension will flow steadily and nearly rectilinearly, even at high solids fraction and even when density contrast cause the particles to accumulate near walls. However, in narrower apertures surface roughness of the fracture walls leads to strong variations in the local velocity field, as well as regions where particles may be excluded or else flow only to points where they become trapped. We have investigated this situation using lattice-Boltzmann numerical simulations of rigid non-colloidal particles suspended in a Newtonian liquid flowing in a synthetic (but realistic) fracture joint with self-affine surface roughness. The results are consistent with experimental observations of “flow channeling,” whereby significant fluid fow and particle transport is highly heterogeneous and occurs only in distinct well-defined paths which span the fracture. The quantitative results indicate that these preferred flow channels are quite distinct from the high aperture sub-regions of the fracture, a somewhat expected result since significant flow requires a connected path spanning the fracture, in addition to high local permeability. Furthermore, the behavior is not ``self-averaging’’, in that different initial conditions and different statistical realizations of the fracture geometry produce entirely different transport paths. An example is shown in Fig. 1 below. An additional complication is that the preferred particle paths have only a rough correspondence to the preferred pure-fluid paths. In order to model these phenomena without resort to computationally-costly direct numerical simulation, we have examined several widely-used methods which take account of connectivity as well as heterogeneity in transport, such as invasion percolation and critical path analysis, with limited success to date.

Flow in fracture junctions: going beyond individual fracture joints, we have begun simulations of fluid and suspension flow in systems where two fractures intersect, as illustrated in Fig. 2. The goal here is understand the degree to which the flows in the two fractures interfere with each other and either enhance or reduce the motion of fluid and particles. Further specific questions include the effects of gravity, the possibility of particle accumulation at junctions, and the degree of mixing within the two streams.

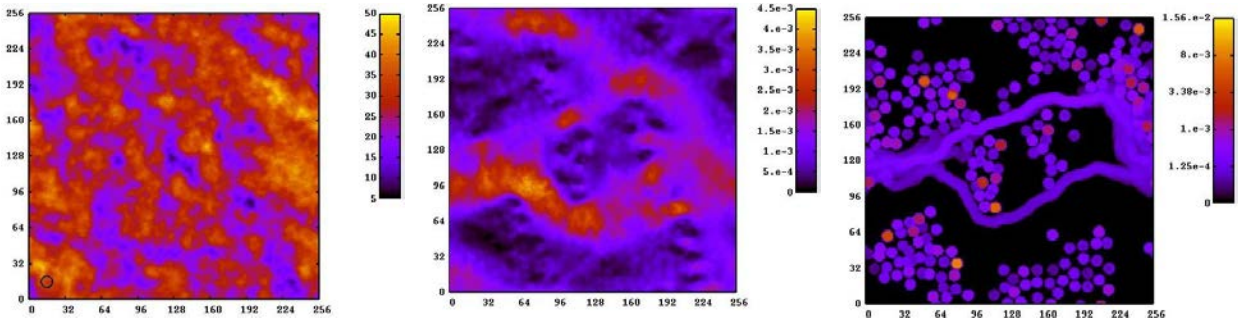

Figure 1: Aperture map of a simulated fracture (left), contour plot of fluid flow speed in the fracture when a pressure gradient is applied from left to right (middle), and contour plot of suspended particle speed in the fracture.

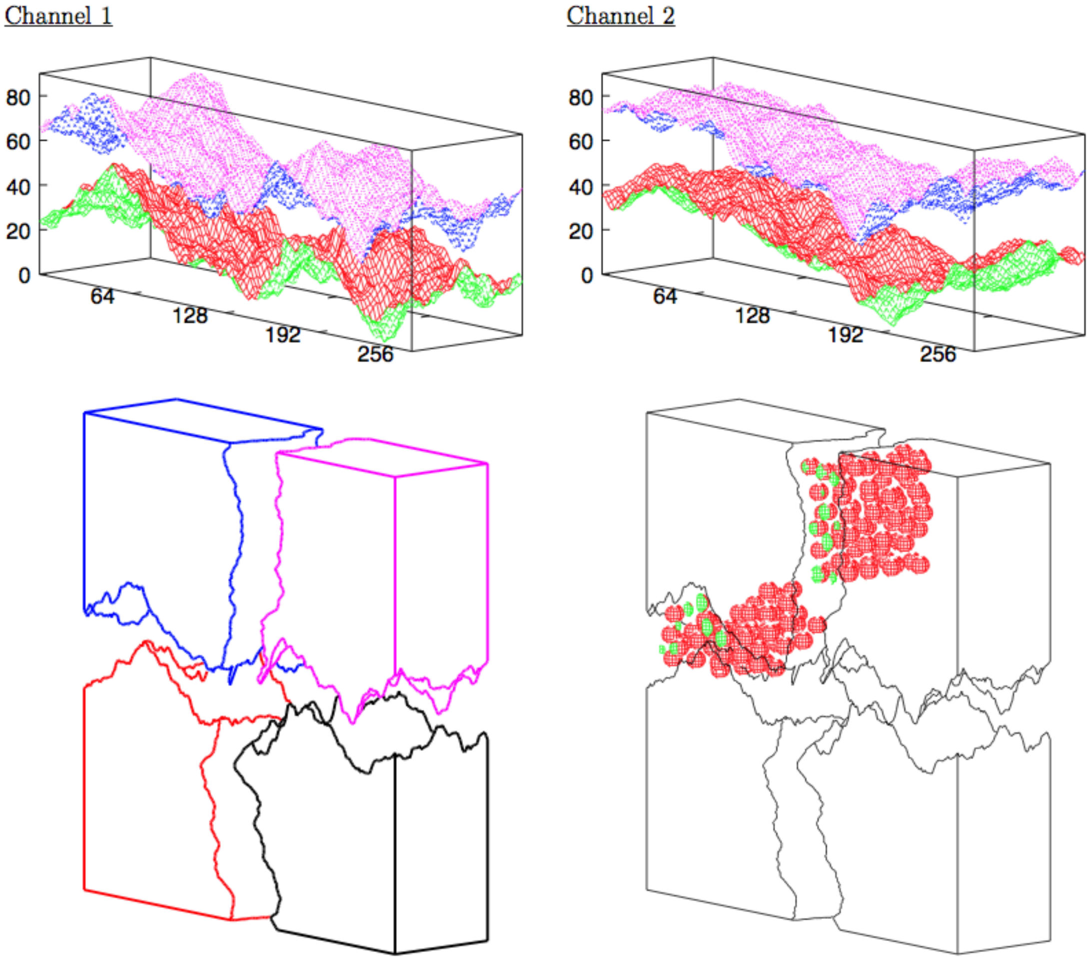

Figure 2: Geometry for an intersecting fracture simulation. The bounding surfaces of the individual fractures are labeled Channel 1,2 and they are combined as indicated at the lower left of the figure. Initial particle positions are shown in the lower right frame.

Participants:

Larry Anovitz, Oak Ridge National Laboratory, anovitzlm@ornl.gov
Paul Bagus, University of North Texas, bagus@unt.edu
James Boles, University of California, Santa Barbara, boles@geol.ucsb.edu
Ronaldo Borja, Stanford University, borja@stanford.edu
Geoffrey Bowers, Alfred University, bowers@alfred.edu
Susan L. Brantley, Pennsylvania State University, sxb7@psu.edu
Bill Casey, University of California, Davis, whcasey@ucdavis.edu
Ariel Chialvo, Oak Ridge National Laboratory, chialvoaa@ornl.gov
David Cole, Ohio State University, cole.618@osu.edu
Louise Criscenti, Sandia National Laboratory, Albuquerque, ljcrisc@sandia.gov
Timothy W. Darling, University of Nevada, Reno, darling@unr.edu
Akhil Datta-Gupta, Texas A&M University, datta-gupta@pe.tamu.edu
Don DePaolo, Lawrence Berkeley National Laboratory, djdepaolo@lbl.gov
Tom Dewers, Sandia National Laboratory, tdewers@sandia.gov
David Dixon, University of Alabama, dadixon@bama.ua.edu
Nathaniel Dixon, Massachusetts Institute of Technology, dixonn@mit.edu
William Durham, Massachusetts Institute of Technology, wbdurham@mit.edu
Elizabeth Eide, National Research Council, eeide@nas.edu
Dave Elbert, Johns Hopkins University, elbert@jhu.edu
Brian Evans, Massachusetts Institute of Technology, brievans@MIT.EDU
Andrew Felmy, Pacific Northwest National Laboratory, ar.felmy@pnl.gov
Paul Fenter, Argonne National Laboratory, Fenter@anl.gov
Grant Garvin, Tufts University, Grant.Garven@tufts.edu
Siddarth Gautam, Ohio State University, gautam.25@osu.edu
Ben Gilbert, Lawrence Berkeley National Laboratory, bgilbert@lbl.gov
Pupa Gilbert, University of Wisconsin, pupa@physics.wisc.edu
Anthony Giuffre, Virginia Tech, giuffre@vt.edu
Steve Goldstein, Los Alamos National Laboratory, sgoldstein@lanl.gov
Jeff Greathouse, Sandia National Laboratory, jagreat@sandia.gov
Anastasia Ilgen, Sandia National Laboratory, agilgen@sandia.gov
Kathleen Issen, Clarkson University, issenka@clarkson.edu
Hope Jahren, University of Hawaii, jahren@hawaii.edu
Paul Johnson, Los Alamos National Laboratory, paj@lanl.gov
Ruben Juanes, Massachusetts Institute of Technology, juanes@MIT.EDU
Zuleima Karpyn, Pennsylvania State University, ZKarpyn@psu.edu
Lynn E. Katz, University of Texas, Austin, lynnkatz@mail.utexas.edu
Abby Kavner, University of California, Los Angeles, akavner@ucla.edu
R. James Kirkpatrick, Michigan State University, rjkirk@cns.msu.edu
William Klein, Boston University, klein@bu.edu
David Kohlstedt, University of Minnesota, dlkohl@umn.edu
Joel Koplik, City College of New York, koplik@sci.ccny.cuny.edu
Arshad Kudrolli, Clark University, akudrolli@clarku.edu
Mark Kurz, Woods Hole Oceanographic Institute, mkurz@whoi.edu

Anthony Ladd, University of Florida, ladd@che.ufl.edu
Antonio Lanzirotti, University of Chicago, lanzirotti@uchicago.edu
Steve Laubach, Bureau of Economic Geology, UT, Austin, steve.laubach@beg.texas.edu
Sang Soo Lee, Argonne National Laboratory, sslee@anl.gov
Hernan Makse, City College of New York, hmakse@lev.ccny.cuny.edu
Maria Mastalerz, Indiana University, mmastale@indiana.edu
Gary Mavko, Stanford University, mavko@stanford.edu
Shenghua Mei, University of Minnesota, meixx002@umn.edu
Sebastian Mergelsberg, Virginia Tech, merges@vt.edu
Cass Miller, University of North Carolina, casey-miller@unc.edu
Claudia Mora, Los Alamos National Laboratory, cmora@lanl.gov
Seiji Nakagawa, Lawrence Berkeley National Laboratory, snakagawa@lbl.gov
Paul Northrup, Stony Brook University, northrup@bnl.gov
Jon Olson, University of Texas, Austin, jolson@mail.utexas.edu
Brian Phillips, Stony Brook University, bphillips@stonybrook.edu
David D. Pollard, Stanford University, dpollard@stanford.edu
Steve Pride, Lawrence Berkeley National Laboratory, srpride@lbl.gov
Laura Pyrak-Nolte, Purdue University, ljpn@physics.purdue.edu
Frank Richter, University of Chicago, richter@geosci.uchicago.edu
Kevin Rosso, Pacific Northwest National Laboratory, kevin.rosso@pnl.gov
Gernot Rother, Oak Ridge National Laboratory, rotherg@ornl.gov
Dan Rothman, Massachusetts Institute of Technology, dhr@MIT.EDU
Douglas Rumble, Carnegie Institution of Washington, rumble@gl.ciw.edu
John Rundle, University of California, Davis, rundle@cse.ucdavis.edu
John Scales, Colorado School of Mines, jscales@mines.edu
Marcel Schaap, University of Arizona, mschaap@cals.arizona.edu
Michele Scherer, University of Iowa, schererm@engineering.uiowa.edu
Arndt Schimmelmann, Indiana University, aschimme@indiana.edu
Brian Shubert, University of Louisiana, Lafayette, Schubert@louisiana.edu
Steve Singer, LBNL, SWSinger@lbl.gov
Andrew Stack**,** Oak Ridge National Laboratory, stackag@ornl.gov
Gary Stinchcomb, Penn State University, ges@psu.edu
Neil Sturchio, University of Illinois, Chicago, Sturchio@uic.edu
Steve Sutton, University of Chicago, sutton@cars.uchicago.edu
Dimitri Sverjensky, Johns Hopkins University, sver@jhu.edu
Alexis Templeton, University of Colorado, alexis.templeton@COLORADO.EDU
Tetsu Tokunaga, Lawrence Berkeley National Laboratory, tktokunaga@lbl.gov
Aradhna Tripati, Univiersity of California, Los Angeles, aradhna.tripati@gmail.com
John Valley, University of Wisconsin, valley@geology.wisc.edu
Bruce Watson, Rensselaer Polytechnic Institute, watsoe@rpi.edu
John Weare, University of California, San Diego, jweare@ucsd.edu
Hans-Rudolf Wenk, University of California, Berkeley, wenk@berkeley.edu
David Wesolowski, Oak Ridge National Laboratory, wesolowskid@ornl.gov
Dorthe Wildenschild, dorthe@engr.orst.edu
Jie Xu, Virginia Tech, jie7@vt.edu
Hongkyu Yoon, Sandia National Laboratory, hyoon@sandia.gov

Guests:
Joanne Fredrich, BP, Joanne.Fredrich@bp.com
Michael Manga, University of California at Berkeley, manga@seismo.berkeley.edu
Thomas Torgerson, National Science Foundation, ttorgers@nsf.gov

DOE Staff:

Diane Marceau, Office of Basic Energy Sciences, Diane.Marceau@science.doe.gov
Nicholas B. Woodward, Office of Basic Energy Sciences, nick.woodward@science.doe.gov